ECONSTOR
Make Your Publications Visible.

A Service of

ZBW Leibniz-Informationszentrum Wirtschaft
Leibniz Information Centre for Economics

Gondauri, Davit

Working Paper

Regional Economic Birch-Swinnerton-Dyer Modelling: A Local-to-Global Framework for Structural Rank Formation, Corridor Stress and World-Economy Calibration

Suggested Citation: Gondauri, Davit (2026) : Regional Economic Birch-Swinnerton-Dyer Modelling: A Local-to-Global Framework for Structural Rank Formation, Corridor Stress and World-Economy Calibration, ZBW - Leibniz Information Centre for Economics, Kiel, Hamburg

This Version is available at:
https://hdl.handle.net/10419/341570

Standard-Nutzungsbedingungen:

Die Dokumente auf EconStor dürfen zu eigenen wissenschaftlichen Zwecken und zum Privatgebrauch gespeichert und kopiert werden.

Sie dürfen die Dokumente nicht für öffentliche oder kommerzielle Zwecke vervielfältigen, öffentlich ausstellen, öffentlich zugänglich machen, vertreiben oder anderweitig nutzen.

Sofern die Verfasser die Dokumente unter Open-Content-Lizenzen (insbesondere CC-Lizenzen) zur Verfügung gestellt haben sollten, gelten abweichend von diesen Nutzungsbedingungen die in der dort genannten Lizenz gewährten Nutzungsrechte.

Terms of use:

Documents in EconStor may be saved and copied for your personal and scholarly purposes.

You are not to copy documents for public or commercial purposes, to exhibit the documents publicly, to make them publicly available on the internet, or to distribute or otherwise use the documents in public.

If the documents have been made available under an Open Content Licence (especially Creative Commons Licences), you may exercise further usage rights as specified in the indicated licence.

WWW.ECONSTOR.EU

Mitglied der Leibniz-Gemeinschaft

Regional Economic Birch-Swinnerton-Dyer Modelling: A Local-to-Global Framework for Structural Rank Formation, Corridor Stress and World-Economy Calibration

Davit Gondauri

ORCID: https://orcid.org/0000-0002-9611-3688
PhD, Professor, Business & Technology University, Georgia
Corresponding author: Davit Gondauri, Dgondauri@gmail.com

Abstract

This study develops a regional economic Birch-Swinnerton-Dyer-inspired framework for measuring the world economy as a local-to-global structural system rather than as a set of isolated GDP aggregates. The framework does not claim to prove, test or replicate the classical Birch-Swinnerton-Dyer conjecture. Instead, it translates its local-to-global measurement logic into a transparent economic analogue in which public macro-regional anchors are transformed into systemic-stress components, weighted regional-network structure, economic curve coefficients, discriminant diagnostics, finite-state trace analogues, Euler-factor analogues, a constructed economic L-function and an L-order measure. The empirical universe consists of a World normalization anchor and ten macro-regional/corridor nodes, with an N = 150 regional-year closure layer used for calibration, robustness diagnostics and claim discipline. The central result is that local regional reductions, represented by finite-state regimes rather than literal arithmetic reductions over finite fields, contain measurable information about structural economic rank formation. Structural rank is constructed from productive, Hodge-flow, network and agentic components and is compared with the L-order analogue through rank gaps, agreement diagnostics, sensitivity checks and placebo logic. The model further introduces regulator, Tamagawa-type friction, torsion, BridgeStress, scenario-threshold and action-concentration diagnostics to distinguish output mass, absorption capacity, locked capacity, corridor leverage and systemic transmission exposure. Results support a strong calibrated measurement claim: local regional signals and Euler-factor information are informative about global structural rank under a disciplined analogue architecture. At the same time, robust-inference and external-proxy layers are interpreted conservatively; weak p-values, small regional clusters, circularity risk and directional external screening are not upgraded into causal or theorem-level confirmation. The contribution is therefore methodological and empirical: a reproducible regional BSD-inspired measurement architecture for structural rank, corridor stress and local-to-global macroeconomic calibration.

Keywords

Birch-Swinnerton-Dyer analogue; regional macroeconomics; local-to-global measurement; structural rank; economic L-function; finite-state reductions; Hodge-flow rank; systemic stress; corridor economics; BridgeStress; Middle Corridor; regional networks; panel calibration; robust inference; external-proxy screening

JEL Classification

C02; C43; C51; C58; C63; C67; F14; F15; F17; O18; O47; R11; R12; R41

Claim Boundary Statement

The proposed BSD-inspired framework is a calibrated regional economic measurement architecture. It is not a proof of the classical BSD conjecture, not a causal law and not a claim of strong external econometric validation where robust-inference and external-proxy evidence remain diagnostic or directional.

Data and Replication Package Statement

All data-package and replication materials associated with this manuscript version are archived on Zenodo and should be cited as: Gondauri, D. (2026). Regional Economic Birch-Swinnerton-Dyer Modelling: Data and Replication Package for a Local-to-Global Framework of Structural Rank Formation, Corridor Stress and World-Economy Calibration [Data set]. Zenodo. https://doi.org/10.5281/zenodo.20796984. The package is the external audit companion to the manuscript and documents the extracted tables, core result files, formulas, algorithms, source ledger, metadata, checksums and reproducibility scripts used to support the reported regional BSD-inspired measurement architecture.

1. Introduction

1.1. General Research Context and Problem Statement

The contemporary world economy is increasingly difficult to interpret through isolated national or regional aggregates alone. Output mass, income depth, growth pressure, corridor exposure, technological capacity, resilience and network position operate jointly. A large region may dominate global GDP but remain comparatively insulated from corridor stress; a smaller region may have modest output mass but become systemically relevant because it lies at a strategic transmission interface. This study is positioned within that analytical problem: how can regional economic structure be measured when local signals, corridor pressure and global rank formation are interdependent rather than separable?

The problem is not merely descriptive. Standard macroeconomic comparison usually begins with GDP, GDP per capita, growth and trade shares. These indicators are indispensable, but they do not by themselves explain how regional stress, finite-state local conditions, network curvature, transmission channels and structural rank combine inside a world-system setting. The methodological challenge is therefore to design a model that is simultaneously mathematical, econometric and interpretable: mathematical because the local-to-global mechanism must be formally specified; econometric because the constructed objects require empirical closure and validation discipline; and interpretable because the results must distinguish measurement, calibration, screening and statistical confirmation.

The study responds to this problem through a regional economic analogue of the Birch-Swinnerton-Dyer local-to-global architecture. The classical BSD conjecture links local reductions and the behavior of an L-function to algebraic rank on an elliptic curve. This research does not claim to prove, test or replicate the classical conjecture. Instead, it uses the conceptual architecture of BSD as a disciplined measurement grammar: regional public-data anchors are transformed into economic curve coefficients, local finite-state traces, Euler-factor analogues, a constructed economic L-function, an L-order measure and a structural-rank object. The central analytical question is whether local regional information, when formalized through this framework, contains measurable information about global structural rank formation.

The resulting research problem can be stated as follows: existing regional macroeconomic diagnostics insufficiently capture the local-to-global formation of structural economic rank under corridor-sensitive world-system conditions. A high-level methodology is required to connect public macroeconomic anchors, regional stress, finite-state local reductions, network structure, corridor transmission and structural-rank calibration without overstating the evidence as classical BSD proof, causal law or strong external validation where the empirical diagnostics do not support such claims.

1.2. Research Object, Boundaries and Data Status

The research object is a World-normalized regional economic system interpreted through a BSD-inspired local-to-global measurement framework. The empirical universe consists of the World anchor and ten macro-regional or corridor-sensitive nodes: East Asia and Pacific, North America, Europe, Latin America and Caribbean, South Asia, Middle East and North Africa, Sub-Saharan Africa, Oceania, Central Asia and the Caucasus. The World row is used only as a normalization anchor; it is not treated as a competing regional node. This boundary is crucial because the study is not a country-ranking exercise. Its purpose is to measure regional rank formation at the macro-regional and corridor-system level.

The data status is deliberately conservative. The public-data anchor layer uses source-family logic associated with World Bank WDI/DataBank indicators for GDP and GDP per capita and IMF World Economic Outlook source-family logic for regional growth projections. These inputs are then transformed through author-calculated regional aggregation, transition-GDP calculation, normalization, stress construction, corridor coding, coefficient mapping, local trace construction and rank calibration. The study therefore separates public anchors from derived analytical objects. This distinction is essential for transparency: variables generated from common inputs may support calibration and internal diagnostics, but they cannot automatically be treated as independent causal validation evidence.

The calibration and robustness layer is specified as an N = 150 regional-year panel, built from ten regional nodes over fifteen years. The N = 150 structure is used for closure diagnostics, not to transform the BSD-inspired analogue into a causal econometric law. Fixed-effects screening, robust inference, negative controls, anti-circularity tests, sensitivity checks, external-proxy screening, equivalence tests, out-of-sample validation and permutation logic operate as evidence gates. The model therefore has two empirical levels: a substantive regional/corridor benchmark and a panel-based closure architecture.

The study is bounded by four principles. First, it is regional, not country-level. Second, it is a calibrated analogue, not a proof of the classical Birch-Swinnerton-Dyer conjecture. Third, its strongest claim is internal local-to-global measurement consistency, not causal confirmation. Fourth, external observable-proxy evidence is treated as directional screening unless sign, p-value, variable lineage and robustness jointly support a stronger interpretation.

Table 1.1 summarizes the core boundary conditions of the study. It clarifies what the research measures, what it deliberately excludes and how each empirical layer should be interpreted.

Table 1.1. Research design boundary and evidence-status matrix

Design component	Operational definition	Analytical role	Claim boundary
World anchor	Global GDP, growth and income-depth reference used for normalization.	Fixes the scale against which regions are compared.	Not a competing observation in the rank hierarchy.
Regional node set	Ten macro-regional/corridor nodes: EAP, NAM, EUR, LAC, SAS, MENA, SSA, OCE, CAS and CAU.	Defines the substantive regional universe.	Not a country-level panel and not a geopolitical ranking.
BSD-inspired analogue	Economic curves, finite-state traces, Euler factors, L-function analogue and LOrder.	Creates the local-to-global measurement architecture.	Not a proof or empirical test of the classical BSD conjecture.
Structural rank	Composite rank built from productive, Hodge-flow, network and agentic components.	Provides the global rank object against which LOrder is calibrated.	A constructed measurement object, not a welfare or political index.
N = 150 closure layer	Ten regions over fifteen years with diagnostic econometric tests.	Audits calibration, robustness, external screening and falsification.	Supports claim discipline; does not establish causal law.
External proxy layer	Inflation pressure, trade openness, logistics proxy, growth revision and related observable proxies.	Provides directional external screening.	Not strong statistical confirmation when p-values are weak or signs are mixed.

Source: *Author synthesis based on the methodological, results and interpretation chapters.*

1.3. Research Aim

The aim of the study is to develop and empirically audit a regional economic Birch-Swinnerton-Dyer-inspired local-to-global framework for measuring how regional public-data anchors, systemic stress, corridor exposure, finite-state local reductions and network structure combine into structural economic rank formation in the world economy.

More specifically, the study aims to demonstrate that a disciplined mathematical analogue can convert regional macroeconomic information into a transparent measurement sequence: World-normalized inputs -> systemic stress -> regional network structure -> economic curve coefficients -> discriminant audit -> finite-state local traces -> Euler factors -> economic L-function behavior -> L-order analogue -> structural-rank calibration -> corridor and scenario diagnostics -> econometric closure. The aim is not to replace standard macroeconomics with mathematical metaphor. It is to build a reproducible bridge between regional macroeconomic measurement and a formal local-to-global architecture.

The final aim is evidentiary as much as technical: the research seeks to show where the BSD-inspired construction is strong, where it is diagnostic, and where academic caution is required. This is why the framework includes negative controls, robust-inference warnings, circularity safeguards, external-proxy demotion rules and decision-gate logic.

1.4. Research Objectives

The study pursues the following objectives:

1. To construct a World-normalized regional public-data anchor panel that defines the empirical coordinate system for the analysis.
2. To transform regional macroeconomic inputs into a multi-component systemic-stress layer that distinguishes output mass from growth pressure, income fragility, transition momentum and corridor exposure.
3. To build a connected weighted regional/corridor graph and verify its adequacy for local-to-global analysis through density, connectedness, degree, transitivity and clustering diagnostics.
4. To map regional economic conditions into economic curve coefficients a and b and audit the resulting curve objects through discriminant and non-degeneracy criteria.
5. To operationalize BSD-inspired finite-state local reductions through q-bases, regional trace analogues, aggregate traces, Euler-factor analogues and a constructed economic L-function around s = 1.
6. To define a multi-component structural-rank object that combines productive, Hodge-flow, network and agentic dimensions without collapsing into GDP size.
7. To test the calibrated correspondence between the L-order analogue and structural rank through rank gaps, visual diagonal alignment, equivalence logic and agreement diagnostics.
8. To construct economic analogues of regulator, Tamagawa-type friction and torsion in order to interpret absorption capacity, local friction and locked capacity across regions.
9. To estimate BridgeStress and corridor-rank leverage for the Caucasus, Central Asia, the Black Sea interface, the Caspian interface and related regional transmission channels.
10. To run scenario, spectral-threshold and triangular-action diagnostics in order to interpret how regional-corridor shocks compress the transition boundary of the system.
11. To implement an N = 150 closure layer that includes high-R2 decomposition, fixed-effects screening, robust inference, external-proxy screening, negative controls, circularity safeguards, out-of-sample validation, sensitivity tests and placebo distributions.
12. To formulate a scientifically cautious claim hierarchy that distinguishes strong internal calibration from diagnostic external screening and from non-causal methodological interpretation.

1.5. Research Questions and Hypothetical Framework

The study is organized around research questions that connect the macro-regional data layer with the BSD-inspired mathematical layer and the econometric closure layer. The questions are not framed as theorem-level propositions. They are formulated as empirical and methodological questions about measurement, calibration and interpretability.

Table 1.2 presents the research questions and their associated hypothesis-level expectations. The hypotheses are intentionally stated as calibration and diagnostic expectations, not as causal laws.

Table 1.2. Research questions and hypothesis-level expectations

Research question	Hypothesis-level expectation	Methodological test	Expected evidentiary status
RQ1. Can regional public-data anchors be converted into a coherent local-to-global measurement system?	H1. World-normalized regional anchors provide a stable coordinate system for the BSD-inspired construction.	Regional anchor panel, transformation rules and source ledger.	Foundational design condition.
RQ2. Does systemic stress reveal regional pressure not captured by GDP mass alone?	H2. Stress rankings differ from GDP rankings because growth pressure, income fragility and corridor exposure alter regional position.	Systemic-stress composite and raw-to-normalized audit.	Substantive measurement evidence.
RQ3. Can regional states be represented through non-degenerate economic curve objects?	H3. The constructed coefficient pairs generate heterogeneous and non-degenerate economic discriminants.	Coefficient mapping, elliptic-cubic visualization and discriminant audit.	Mathematical-analogue admissibility.
RQ4. Are local trace signals stable across finite-state q-bases?	H4. Protective and stress-bearing regional signs remain stable across q = 2, 3, 5, 7 and 11.	Finite-state trace matrix and trace heatmap.	Local-reduction consistency.
RQ5. Does the L-order analogue approximate structural rank?	H5. LOrder and structural rank remain close within the declared calibration tolerance band.	Rank gaps, diagonal scatter, MAE/RMSE, equivalence and agreement audits.	Core internal calibration evidence.
RQ6. Do corridor-sensitive nodes become visible through BridgeStress?	H6. The Caucasus and Central Asia display high BridgeStress because corridor role and fragility compensate for low GDP mass.	BridgeStress ranking, corridor-function table and corridor-coding sensitivity.	Corridor-mechanism evidence.
RQ7. Do econometric and external-proxy diagnostics support overclaiming?	H7. Robust inference and external proxies should be interpreted conservatively when p-values are weak or signs are mixed.	TWFE, robust p-values, external-proxy screening, negative controls and decision gates.	Claim-discipline evidence.

Source: *Author synthesis based on the research architecture and claim-boundary logic of Chapters 3-5.*

The core hypothetical framework can be expressed compactly as LOrder_{r,t} approximately corresponds to StructuralRank_{r,t} within a calibrated rank-scale tolerance band. This expression is not an equality theorem. It is the central empirical analogue: finite-state local reductions and Euler-factor information should be informative about the independently defined structural-rank object. Where the correspondence is close, the local-to-global measurement

logic is supported. Where external-proxy or robust-inference diagnostics are weak, the claim remains a calibrated measurement result rather than a statistically confirmed causal mechanism.

1.6. Scientific Novelty of the Research

The scientific novelty of the study consists in the construction of a regional economic BSD-inspired framework that is neither a metaphorical borrowing nor a direct claim about number theory. Its innovation lies in converting a deep local-to-global mathematical logic into an auditable economic measurement architecture. The model does not state that economies are elliptic curves. It states that regional economic systems can be measured through a structured analogue in which local finite-state signals, Euler-factor products and order-of-behavior measures are compared with independently constructed structural rank.

The first element of novelty is the replacement of country-level ranking with a World-normalized regional/corridor benchmark. This allows the model to capture the difference between output mass and systemic relevance. For example, large output regions define the mass layer of the world economy, while smaller transition-sensitive regions such as the Caucasus and Central Asia can become analytically important through corridor exposure, fragility, curvature participation and BridgeStress.

The second element of novelty is the construction of economic curve coefficients a_{r,t} and b_{r,t} from regional macroeconomic and corridor variables. This gives the model a formal coefficient space in which discriminants, non-degeneracy, traces and L-function analogues become interpretable measurement objects. The discriminant audit is especially important because it prevents the model from proceeding with degenerate or nearly singular constructed objects.

The third element of novelty is the finite-state local-reduction design. Instead of treating q-bases as literal prime fields, the study uses q = 2, 3, 5, 7 and 11 as finite-state grids for regional economic states. This preserves the BSD-inspired local-to-global architecture while maintaining conceptual honesty: the trace analogue measures economic state behavior under controlled discretization, not point counts over finite fields.

The fourth element of novelty is the explicit linkage between LOrder and structural rank. Structural rank is not defined as GDP size. It is a composite of productive depth, Hodge-flow structure, network rank and agentic capacity. The L-order analogue is then evaluated against this rank object through gaps, visual alignment, equivalence, Bland-Altman logic, leave-out validation, q-base sensitivity and placebo distributions.

The fifth element of novelty is the built-in claim-discipline architecture. The research does not hide weak external-proxy evidence, small-cluster limitations or circularity risk. Instead, it classifies external validation as directional screening where appropriate, treats robust inference as diagnostic when p-values are weak, and uses negative controls, residualization, variable-lineage checks, sensitivity tests and decision gates to prevent overinterpretation.

1.7. Theoretical, Methodological and Practical Significance

The theoretical significance of the study is that it expands the analytical language of regional economics by introducing a disciplined local-to-global rank-formation framework. It brings together concepts from elliptic-curve-inspired measurement, network economics, Hodge-flow interpretation, systemic-stress diagnostics, corridor economics and panel-econometric caution. This is not a claim that economic theory should be reduced to number theory. Rather, it is a claim that formal mathematical architectures can help define new measurement grammars for complex economic systems.

The methodological significance is substantial. The study provides a full transformation chain from public macroeconomic anchors to stress scores, coefficient maps, discriminants, traces, Euler factors, L-function behavior, LOrder, structural rank, regulator analogues, Tamagawa-type frictions, torsion, BridgeStress, scenario thresholds and action concentration. Each component has a methodological role and a claim boundary. The model thereby avoids the common weakness of constructed-index research: producing a complex index without sufficient lineage, falsification, sensitivity analysis or external audit discipline.

The practical significance lies in regional diagnostics. The framework can help analysts distinguish between output-mass power, structural rank, stress exposure, corridor leverage, absorption capacity and locked capacity. It is particularly useful for interpreting corridor-sensitive regions such as the Caucasus, Central Asia, the Black Sea interface and the Caspian connection. In this setting, the study provides a way to explain why a small-output region can still be structurally relevant to global stress transmission.

The policy and strategic relevance is therefore indirect but meaningful. The model does not prescribe policy mechanically. It provides a diagnostic architecture for identifying where regional shocks may compress systemic thresholds, where action concentration may occur, where corridor-stress exposure is high, and where resilience and agentic capacity raise structural rank. Such information can support research on logistics, regional resilience, infrastructure prioritization, macrofinancial stress monitoring and corridor-risk evaluation.

1.8. Research Limitations and Principle of Academic Caution

The study is intentionally built around academic caution. Its first limitation is conceptual: the BSD framework is used as an analogue, not as a theorem applied to the economy. The economic curve, trace, Euler factor, L-function and L-order objects are constructed measurement analogues. They should not be interpreted as literal elliptic curves, arithmetic local reductions or analytic ranks in the classical mathematical sense.

The second limitation is empirical. The regional/corridor structure reduces the complexity of the world economy to ten macro-regional nodes and a World anchor. This is appropriate for the research aim, but it necessarily abstracts from country-level heterogeneity, sectoral composition and micro-level institutional details. The N = 150 panel strengthens the closure layer, but ten regional clusters remain a small-cluster setting. Robust-inference results must therefore be interpreted with care.

The third limitation concerns external validation. External observable-proxy models provide directional screening rather than strong independent confirmation when p-values are weak or signs are mixed. The study therefore does not claim that the external layer statistically proves the BSD-inspired mechanism. It uses this layer to evaluate whether the constructed rank signal behaves plausibly against observable proxies.

The fourth limitation is circularity risk. Because several variables are author-calculated from overlapping inputs, the study uses variable-lineage screens, residualized LOrder and external-only diagnostics. Even with these safeguards, the strongest claim remains calibrated internal local-to-global consistency, not independent causal validation.

The fifth limitation concerns reproducibility and version control. The manuscript records source-family logic, transformation rules, formulas, algorithms and output interpretation, and the associated data and replication materials for this manuscript version are archived on Zenodo under DOI 10.5281/zenodo.20796984. The Zenodo package functions as the external replication artifact for the reported tables, formulas, algorithms, figure catalogues, source ledger, metadata, checksums and reproducibility scripts. The manuscript therefore treats replication closure as a cited companion record rather than as an unresolved archival requirement (Gondauri, 2026).

The principle of academic caution can therefore be summarized as follows: the study supports a strong calibrated measurement claim inside a regional economic BSD analogue; it does not prove BSD, does not establish causal law, does not turn weak external-proxy results into confirmation, and does not treat constructed variables with overlapping lineage as independent validation evidence.

1.9. Structure of the Research Logic

The research is organized as an integrated architecture. Chapter 3 defines the methodology, including the classical BSD reference logic, economic analogue, regional panel design, transformations, curve coefficients, discriminants, trace analogues, Euler factors, L-function, structural rank, corridor model, scenario layer and econometric closure procedures. Chapter 4 reports the results through the World-regional anchor panel, systemic-stress results, curve and L-function diagnostics, rank-order correspondence, corridor leverage, scenario threshold compression and the N = 150 closure architecture. Chapter 5 interprets the results, showing how each empirical object contributes to the final claim level. Chapter 6 concludes by returning to the aim, research questions, novelty, significance and limitations stated in the introduction.

2. Literature Review

2.1. Scope and Review Strategy

This chapter reviews the literature required to position the regional BSD-inspired framework as a formal local-to-global economic measurement architecture. The review is not limited to one discipline because the model itself is

deliberately interdisciplinary: it combines the local-to-global logic of elliptic-curve L-functions, network and Hodge-style decomposition, regional and corridor economics, economic complexity, systemic-risk propagation, and conservative panel-econometric validation. The literature is therefore organized around the analytical chain used in the study: public macro-regional anchors, stress and corridor exposure, network structure, curve-coefficient construction, finite-state local traces, Euler-factor analogues, L-function behavior, structural rank, calibration, robustness and claim discipline.

The review uses 157 academic journal references with DOI links. Each reference is included because it supports one of five methodological needs: the mathematical local-to-global analogy, the measurement of complex economic structure, regional and corridor transmission, network/systemic-risk propagation, or econometric validation and falsification. The central criterion is relevance to the present framework rather than disciplinary proximity alone.

2.2. Literature Coverage Map

Table 2.1 summarizes how the reviewed literature is allocated across the core research blocks. The table also clarifies that the present study does not borrow mathematical terminology loosely; each literature block corresponds to a specific methodological or interpretive function in Chapters 3-5.

Literature block	Number of references	Function in this study	Relation to Chapters 3-5
BSD and elliptic-curve local-to-global mathematics	8	Defines the formal local-to-global grammar: curves, discriminants, local traces, Euler factors and L-functions.	Supports the analogue design in Methodology Sections 3.2 and 3.7-3.12.
Network science and graph structure	28	Provides the graph, centrality, clustering, community, multilayer and higher-order network basis.	Supports regional graph adequacy, structural rank, Hodge-flow and visual diagnostics.
Hodge, topology and higher-order structure	7	Justifies decomposition of flows, cycle structure, simplicial/Laplacian reasoning and topological audits.	Supports Hodge-flow rank, triangular action and higher-order local-to-global interpretation.
Economic complexity, productivity and growth	18	Provides the theory of productive capabilities, structural development, growth, institutions and complexity.	Supports structural-rank construction and the distinction between GDP size and capability depth.
Regional economics, trade and corridor transmission	29	Explains geography, trade cost, market access, supply chains, infrastructure and corridor mechanisms.	Supports the Caucasus/Central Asia/Black Sea/Caspian BridgeStress interpretation.
Network macroeconomics and systemic risk	25	Explains shock propagation, systemic fragility, contagion, financial networks and macro-network risk.	Supports stress, scenario, threshold and action-concentration interpretations.
Econometric identification, robust	34	Defines panel inference, fixed effects, robust standard errors, dynamic	Supports N = 150 closure and the non-causal

inference and panel diagnostics		diagnostics and small-cluster caution.	interpretation of weak robust-inference results.
Calibration, falsification and validation discipline	8	Supports equivalence, agreement, negative controls, placebo logic and sensitivity discipline.	Supports the decision-gate architecture and claim-boundary discipline.

Source: Author synthesis of the 157 reviewed academic journal references.

2.3. Local-to-Global Mathematical Foundations: BSD, Elliptic Curves and L-Functions

The mathematical foundation of the present study is the local-to-global architecture associated with elliptic curves and L-functions. In the classical setting, the Birch-Swinnerton-Dyer conjecture relates information obtained from local reductions of an elliptic curve to the analytic behavior of its L-function and the algebraic rank of rational points. The origin of this logic is not a loose analogy but a highly structured number-theoretic programme in which curve coefficients, discriminants, local factors and rank are linked through explicit mathematical objects (Birch & Swinnerton-Dyer, 1965; Coates & Wiles, 1977; Gross & Zagier, 1986; Wiles, 1995; Taylor & Wiles, 1995; Lenstra, 1987; Schoof, 1985; Atkin & Morain, 1993).

For the present research, the decisive lesson from this literature is not that economies are elliptic curves. The lesson is methodological: a complex global object may be studied through disciplined local reductions when the transformation chain is explicit and the claim boundary is maintained. This is why Chapter 3 distinguishes classical finite-field point counts from economic finite-state reductions and why Chapter 4 interprets the constructed L-function as a measurement analogue rather than as a proof of analytic continuation or a number-theoretic theorem. The literature also justifies the use of non-degeneracy audits: before a curve-like object can support local traces or Euler-type factors, its coefficient space must avoid singular collapse.

2.4. From Mathematical Analogy to Economic Measurement Grammar

The movement from BSD mathematics to economic measurement requires a careful epistemic translation. The reviewed literature shows that formal structure can be productive when it organizes observable variables, but it becomes misleading if mathematical terms are treated as literal economic facts. The present study therefore uses BSD as a measurement grammar: economic curve coefficients summarize regional state variables; finite-state grids replace prime-field reductions; trace analogues measure protective versus stress-bearing state behavior; Euler factors combine local information; and the L-order analogue is evaluated against a separately constructed structural-rank object.

This translation follows the conservative principle embedded in the mathematical and econometric literature: the validity of a constructed object depends on explicit mapping, non-degeneracy, robustness and claim discipline. The economic BSD analogue is therefore closer to a calibrated measurement framework than to a metaphor. It is also distinct from pure index construction because each step has a corresponding local-to-global role, and each role is later subjected to closure tests.

2.5. Economic Complexity, Productive Capabilities and Structural Rank

The structural-rank component of the study is grounded in the economic-complexity and growth literature. Capability-based approaches show that development cannot be reduced to output size alone: productive knowledge, diversification, revealed comparative advantage, institutional quality, technological direction and growth dynamics jointly determine a region's structural position (Hidalgo et al., 2007; Hidalgo & Hausmann, 2009; Hausmann & Hidalgo, 2011; Caldarelli et al., 2012; Tacchella et al., 2012; Cristelli et al., 2013; Balassa, 1965; Solow, 1956; Romer, 1986; Lucas, 1988; Barro, 1991; Mankiw et al., 1992; Aghion & Howitt, 1992; Grossman & Helpman, 1991; Acemoglu, 2002; Acemoglu et al., 2001; Rodrik et al., 2004; Frankel & Romer, 1999).

This literature is directly relevant to the study's refusal to equate GDP mass with structural rank. Classical growth models explain the role of capital, technology and human-capital accumulation; endogenous-growth models add innovation, creative destruction and directed technical change; institutional-growth studies add the deep conditions that shape long-run development. Economic-complexity studies then move further by treating productive capability as a networked and compositional phenomenon rather than as a single scalar variable. In the present framework, this supports the construction of structural rank from productive, Hodge-flow, network and agentic components rather than from GDP alone.

The main unresolved issue in this literature is that complexity and capability measures often explain productive structure but do not by themselves define a formal local-to-global mechanism. They can rank economies, identify capabilities or explain diversification, but they do not specify how local regional state reductions become informative about a global rank object. The present study fills this gap by connecting structural rank to finite-state local traces and an L-order analogue.

2.6. Network Science, Centrality, Clustering and Higher-Order Structure

Network science supplies the second foundation of the model. The world economy is not a collection of independent observations; it is a weighted relational system in which nodes, edges, centrality, clustering, community structure and multilayer connections govern transmission and vulnerability. The reviewed network literature establishes the concepts required to treat regional economic nodes as connected objects rather than as isolated entries in a table (Watts & Strogatz, 1998; Barabasi & Albert, 1999; Albert et al., 2000; Strogatz, 2001; Newman, 2003; Boccaletti et al., 2006; Freeman, 1978; Bonacich, 1987; Borgatti, 2005; Opsahl et al., 2010; Barrat et al., 2004; Onnela et al., 2005; Girvan & Newman, 2002; Newman & Girvan, 2004; Newman, 2006; Rosvall & Bergstrom, 2008; Fortunato, 2010; Brin & Page, 1998; Kleinberg, 2000; Barabasi, 2009; Newman, 2003b; Clauset et al., 2004; Radicchi et al., 2004; Blondel et al., 2008; Mucha et al., 2010; Kivela et al., 2014; De Domenico et al., 2013; Battiston et al., 2020).

Centrality and flow concepts justify the regional network adequacy block in Chapter 4. A local-to-global interpretation is credible only if the graph is connected and has enough structure for flows, cycles and higher-order interactions to be meaningful. Density, weighted degree, clustering and community logic allow the study to interpret why high-output nodes and corridor-sensitive nodes play different roles. The network literature also supports the distinction between position and size: a node may be economically large but weakly exposed to a given transmission channel, while a smaller node may have high corridor leverage.

Higher-order network and topological methods sharpen this argument. Hodge-style decomposition, simplicial Laplacians and persistent-topology studies show that pairwise edges alone do not exhaust the structure of a system; cycles, curl, harmonic components and higher-order interactions may carry information that ordinary node rankings miss (Horak & Jost, 2013; Jiang et al., 2011; Ghrist, 2008; Edelsbrunner et al., 2002; Zomorodian & Carlsson, 2005; Carlsson, 2009; Otter et al., 2017). This is the basis for treating Hodge-flow rank, triangular-cycle action and discriminant basins as structural diagnostics rather than decorative mathematics.

2.7. Regional Economics, Trade Costs, Corridors and Global Value Chains

The regional and corridor layer of the study draws on trade, geography, infrastructure, supply-chain and market-access literature. The central finding across this field is that distance, transport costs, border frictions, infrastructure, market access and production fragmentation shape economic outcomes in ways that GDP totals cannot fully capture (Krugman, 1991; Glaeser et al., 1992; Henderson et al., 1995; Redding & Sturm, 2008; Combes et al., 2008; Duranton & Puga, 2001; Anderson & van Wincoop, 2003; Eaton & Kortum, 2002; Melitz, 2003; Helpman et al., 2008; Chaney, 2008; Donaldson, 2018; Donaldson & Hornbeck, 2016; Limao & Venables, 2001; Djankov et al., 2010; Hummels & Schaur, 2013; Portugal-Perez & Wilson, 2012; Martincus et al., 2017; Rauch, 1999; Nunn, 2007; Chor, 2010; Antras & Chor, 2013; Johnson & Noguera, 2012; Koopman et al., 2014; Yi, 2003; Costinot et al., 2013; Fally, 2015; Antras & de Gortari, 2020; Carvalho et al., 2021).

For the present study, this literature justifies the separate treatment of corridor exposure and BridgeStress. Gravity models and trade-cost studies explain why geography and frictions matter; market-access studies show that transport infrastructure alters the spatial distribution of gains; global value-chain research explains why intermediate inputs and production stages transmit shocks across regions; and logistics studies show that time itself becomes a trade barrier. These findings support the interpretation that the Caucasus, Central Asia, the Black Sea interface and the Caspian crossing can be systemically relevant despite modest output shares.

The unresolved limitation in much regional trade literature is that corridor relevance is often treated through bilateral flows, infrastructure measures or trade-cost effects, while the broader system-level rank implication remains implicit. The present study extends this literature by linking corridor role, fragility and curvature participation to BridgeStress and by embedding this corridor measure inside the same local-to-global BSD-inspired architecture used for structural rank.

2.8. Network Macroeconomics, Systemic Risk and Shock Propagation

Network macroeconomics and systemic-risk research provide the conceptual bridge between regional structure and systemic stress. Production-network studies show that micro or sectoral shocks can aggregate through input-output linkages; granular macroeconomics shows that large units can generate aggregate volatility; financial-network studies show that contagion and systemic risk depend on topology, exposure, leverage and resilience (Acemoglu et al., 2012; Acemoglu et al., 2015; Carvalho, 2014; Gabaix, 2011; Foerster et al., 2011; Carvalho & Gabaix, 2013; Allen & Gale, 2000; Elliott et al., 2014; Battiston et al., 2012; Haldane & May, 2011; Brunnermeier, 2009; Adrian & Brunnermeier, 2016; Acharya et al., 2017; Billio et al., 2012; Diebold & Yilmaz, 2014; Forbes & Rigobon, 2002; Bisias et al., 2012; Battiston et al., 2016; Acemoglu et al., 2016; Glasserman & Young, 2015; May et al., 2008; Gai & Kapadia, 2010; Nier et al., 2007; Eisenberg & Noe, 2001; Rogers & Veraart, 2013).

This literature supports the systemic-stress and scenario layers of the study. Stress is not treated as a simple output-weighted statistic; it is decomposed into mass exposure, growth pressure, income fragility, transition momentum and corridor exposure. Similarly, the scenario layer interprets threshold compression as a network phenomenon: shocks change edge weights, spectral modes, threshold ratios and triangular action concentration. The systemic-risk literature also warns that connectivity is ambiguous: it can distribute risk under moderate shocks but amplify contagion when exposures are concentrated or resilience is weak.

The present framework adds a rank-formation perspective to this literature. It asks not only whether shocks propagate, but whether local finite-state stress and protection signals are informative about structural rank. This makes the study broader than a contagion model and more formal than a descriptive regional risk map.

2.9. Econometric Validation, Robust Inference and Claim Discipline

The econometric literature is essential because the study constructs several author-calculated variables. Without robust diagnostic rules, a high-dimensional measurement framework could easily overclaim. Panel-econometric research on fixed effects, dynamic panels, robust covariance estimation, cross-sectional dependence, small-cluster problems and heterogeneous treatment effects establishes the standards that the present study applies to the N = 150 closure layer (White, 1980; Newey & West, 1987; MacKinnon & White, 1985; Arellano & Bond, 1991; Arellano & Bover, 1995; Blundell & Bond, 1998; Hausman, 1978; Mundlak, 1978; Nickell, 1981; Pesaran, 2006; Pesaran, 2015; Driscoll & Kraay, 1998; Bertrand et al., 2004; Cameron et al., 2008; Wooldridge, 2005; Angrist & Pischke, 2010; Imbens & Wooldridge, 2009; Conley, 1999; Beck & Katz, 1995; Stock & Watson, 2008; Hansen, 1999; Bai, 2009; Ibragimov & Muller, 2010; Bell & McCaffrey, 2002; Roodman, 2009; Windmeijer, 2005; Imbens & Kolesar, 2016; Abadie et al., 2023; Sun & Abraham, 2021; Callaway & Sant'Anna, 2021; de Chaisemartin & D'Haultfoeuille, 2020; Heckman, 1979; Manski, 1993; Athey & Imbens, 2017).

This literature explains why the study separates internal calibration from econometric confirmation. Two-way fixed effects, high overall R2 and positive coefficients may be useful diagnostics, but they do not automatically establish causal law. Robust inference must consider heteroskedasticity, serial correlation, cross-sectional dependence, common shocks, small-cluster bias and dynamic-panel limitations. This is why the methodology reports classical, HC3, clustered, HAC/Driscoll-Kraay and related diagnostics, and why a positive LOrder coefficient with weak p-values is interpreted only as a consistency signal.

The external-proxy layer is treated with the same caution. If an external proxy has the expected sign but weak statistical support, the status is directional watch. If the sign is opposite or unstable, the result remains diagnostic only. This logic follows the broader credibility-revolution literature: design, identification, robustness and falsification matter more than attractive model fit.

2.10. Calibration, Agreement, Falsification and Reproducibility

The calibration literature is particularly important for this study because the core empirical claim is practical correspondence, not exact equality. Agreement methods, equivalence testing, sensitivity analysis, negative controls and mediation/falsification logic provide the tools for evaluating whether two constructed objects agree within a declared tolerance band and whether that agreement is likely to be mechanical (Bland & Altman, 1986; Lin, 1989; Schuirmann, 1987; Rosenbaum, 1987; Lipsitch et al., 2010; Imai et al., 2010; Pearl, 1995; Rubin, 1974).

This literature supports the rank-gap, MAE, RMSE, equivalence, Bland-Altman, negative-control, residualization and permutation-placebo layers of Chapters 3 and 4. The point is not to make the model appear stronger than it is. The

point is to prevent internal calibration from being misread as independent causal validation. Negative controls test whether the LOrder measure explains outcomes it should not explain. Residualization and variable-lineage audits test whether overlap among constructed variables creates circularity. Equivalence and agreement tests evaluate practical closeness on the 0-5 rank scale. Placebo logic tests whether the observed correspondence is better than randomized alternatives.

2.11. Research Gap and Positioning of the Present Study

The reviewed literature resolves many components of the problem but not the complete problem addressed here. Number theory provides a rigorous local-to-global architecture, but it does not provide an economic measurement model. Economic-complexity research measures capabilities and productive structure, but it does not formalize BSD-style local reductions, traces and Euler factors. Network science explains structure, centrality and higher-order interaction, but it does not by itself create a calibrated L-order-to-rank analogue. Regional trade and corridor studies explain market access, transport costs and supply-chain transmission, but they often stop short of defining structural rank formation. Systemic-risk literature explains contagion and shock propagation, but it is usually not framed as a local-to-global rank problem. Econometric literature provides diagnostic discipline, but it does not supply the conceptual architecture of the BSD analogue.

The present study integrates these strands into one framework. Its contribution is not a claim that each field has missed its own problem. Rather, the contribution is architectural: it creates a transparent route from public regional macro-data to stress, network structure, economic curve coefficients, non-degeneracy, finite-state traces, Euler factors, an economic L-function, LOrder, structural rank, corridor leverage, scenario thresholds and N = 150 closure diagnostics. It then assigns claim levels so that strong internal calibration is not confused with theorem-level proof or causal econometric confirmation.

2.12. What Researchers Have Attempted, What They Have Resolved, What Remains Unresolved, and What the Present Study Contributes

Researchers have tried to solve four related problems. First, mathematicians formalized a powerful local-to-global programme through elliptic curves, local reductions, L-functions and rank, culminating in the BSD framework and related modularity results. This solved the problem of a rigorous mathematical language for connecting local arithmetic data to global rank, but it did not solve the problem of measuring regional economic systems. Second, economists and complexity researchers developed ways to measure productive capabilities, growth, institutions and economic structure. This solved the problem of moving beyond GDP-only interpretation, but it did not supply a formal local-to-global transformation chain. Third, network, trade, geography and systemic-risk researchers showed that connectivity, corridor exposure, supply chains and network topology shape propagation and vulnerability. This solved the problem of identifying transmission channels, but it did not connect those channels to BSD-style rank correspondence. Fourth, econometric and validation researchers developed robust inference, panel diagnostics, agreement tests, negative controls, sensitivity checks and claim discipline. This solved the problem of how to avoid overclaiming, but it did not define the substantive regional BSD-inspired object.

What remains unresolved in the literature is therefore the integrated measurement problem: how to determine whether local regional states, represented through stress, corridor exposure, finite-state reductions and network structure, contain measurable information about global structural economic rank. The present study addresses precisely this unresolved space. It constructs a BSD-inspired regional economic analogue, tests the internal correspondence between LOrder and structural rank, interprets corridor-sensitive nodes through BridgeStress, and then restricts the claim through robust-inference, external-proxy, placebo, circularity and reproducibility gates. The final contribution is a strong but disciplined one: the framework supports calibrated local-to-global consistency in a regional economic measurement system, while explicitly refusing to claim proof of BSD, causal law or strong external validation where the evidence does not justify it.

3. Methodology

This chapter defines the mathematical, computational and econometric methodology used to generate the regional BSD-inspired results reported in Chapter 4. The methodology is deliberately built as an analogue framework: it imports the local-to-global logic of the Birch-Swinnerton-Dyer conjecture into a transparent regional macroeconomic measurement system, but it does not claim to prove, test or replicate the classical number-theoretic conjecture. The empirical object is a calibrated regional-year benchmark in which public macroeconomic anchors, corridor exposure, finite-state reductions, curve coefficients, local traces, Euler-factor analogues, L-function behavior and structural-rank measures are linked through auditable transformations.

The methodological design has three layers. The first layer constructs the regional economic universe: a World anchor, ten macro-regional/corridor nodes, regional stress variables, network structure, curve coefficients and corridor-leverage indicators. The second layer builds the BSD-inspired mathematical analogue: economic cubic curves, non-degeneracy audits, finite-state local traces, Euler factors, an economic L-function and an L-order indicator. The third layer provides empirical closure: N = 150 regional-year calibration, fixed-effects screening, robust-inference diagnostics, external-proxy screening, negative controls, circularity safeguards, equivalence tests, out-of-sample validation, sensitivity checks and decision-gate logic.

3.1. Methodological Correspondence with the Results Chapter

The methodology is organized so that every substantive and closure subsection of Chapter 4 has a direct methodological source. Table 3.1 provides a compact crosswalk between the results architecture and the methodological operations required to reproduce it.

Table 3.1. Methodological correspondence between the results chapter and Chapter 3 methodology

Results section	Results object	Methodological operation	Methodology location
4.1	World and Regional Public-Data Anchor Panel	regional anchor panel; World normalization; regional/corridor node definition	Sections 3.3-3.4
4.2	Regional Systemic-Stress Results	multi-component stress construction	Section 3.5
4.3	Raw-to-Normalized Stress Audit	min-max audit and interval anchoring	Section 3.5
4.4	Regional Network Adequacy	weighted graph diagnostics	Section 3.6
4.5	Economic Elliptic-Cubic Surface	geometric curve visualization	Sections 3.7 and 3.16
4.6	Curve Coefficients a and b	coefficient mapping from economic variables	Section 3.7
4.7	Discriminant and Non-Degeneracy	economic discriminant audit	Section 3.8
4.8	Discriminant Visualization	coefficient-space visual audit	Section 3.16
4.9	Local Trace Analogues	finite-state local reductions	Section 3.9
4.10	Trace Heatmap	q-base stability visualization	Sections 3.9 and 3.16
4.11	Economic Euler Factors	aggregate trace and Euler-factor construction	Section 3.10
4.12	Economic L-Function	L-function product and local behavior near s = 1	Section 3.10

4.13	Regional Structural Rank	rank object and component decomposition	Section 3.11
4.14	Structural-Rank Visualization	rank hierarchy plot	Sections 3.11 and 3.16
4.15	Order-of-Behavior Analogue	LOrder vs structural rank comparison	Sections 3.10-3.12
4.16	Rank-Order Scatter	calibration scatter and diagonal check	Sections 3.12 and 3.16
4.17	Economic Regulator	rank-support and absorption-capacity analogue	Section 3.13
4.18	Tamagawa-Type Frictions	local friction factors	Section 3.13
4.19	Economic Torsion	locked capacity and circularity analogue	Section 3.13
4.20	Structural-Rank Surface	response surface over agentic capacity and resilience	Section 3.14
4.21	BridgeStress	corridor-rank leverage model	Section 3.15
4.22	BridgeStress Visualization	corridor hierarchy plot	Sections 3.15 and 3.16
4.23	Middle Corridor Interpretation	qualitative corridor-function mapping	Section 3.15
4.24	Scenario Output	shock-amplitude, spectral threshold and action	Section 3.17
4.25	Threshold Compression Figure	scenario path visualization	Sections 3.17 and 3.16
4.26	Action Concentration	triangular-cycle stress energy	Section 3.17
4.27	Cubic Discriminant Basin	coefficient-space discriminant surface	Sections 3.8 and 3.16
4.28	N=150 Closure Checklist	results architecture and claim-boundary gate	Section 3.18
4.29	High-R2 Closure	model-fit decomposition and FE caution	Section 3.19
4.30	External Proxy Screening	directional observable-proxy panel and models	Section 3.20
4.31	Negative Controls	placebo, randomized and temporal falsification tests	Section 3.21
4.32	Dependence and Robust Inference	CD, serial dependence, HAC and small-cluster corrections	Section 3.22
4.33	Dynamic and Threshold Diagnostics	persistence and regime checks with claim boundaries	Section 3.23
4.34	Circularity Safeguards	variable lineage and residualized LOrder	Section 3.24
4.35	Calibration and Agreement	equivalence, MAE/RMSE and Bland-Altman audits	Section 3.25

4.36	Leave-Out and OOS Validation	block deletion and held-out validation	Section 3.26
4.37	Weight, q and Corridor Sensitivity	perturbation, q-base and coding robustness	Section 3.27
4.38	Decision Criteria and Placebo Distribution	claim gates and permutation inference	Section 3.28
4.39	Source and Reproducibility	source ledger, seeds and output hashes	Section 3.29
4.40	Evidence Map and Reviewer Risk	evidence classification and risk-response logic	Section 3.30
4.41	Final Results Synthesis	integrated claim level and limitation discipline	Section 3.31

Source: Author methodological design based on the Chapter 4 regional BSD-inspired results architecture.

3.2. Mathematical Foundation: Classical BSD Logic and Economic Analogue

The classical Birch-Swinnerton-Dyer conjecture concerns elliptic curves over the rational numbers and the relationship between the analytic behavior of an L-function and the algebraic rank of rational points on the curve. In its classical form, an elliptic curve can be represented by a non-singular cubic equation. The present study uses this mathematical architecture as an analogue: regional economic objects are mapped into curve coefficients, local reductions, Euler factors and an order-of-behavior indicator, while the interpretation remains economic and empirical rather than number-theoretic.

(3.1) Classical elliptic curve: E : y^2 = x^3 + a x + b, with a, b in Q or R depending on the field of interpretation.

(3.2) Classical discriminant: Delta(E) = -16(4a^3 + 27b^2). Non-singularity requires Delta(E) != 0.

(3.3) Finite-field point count: N_p = #E(F_p), where F_p is the finite field with p elements.

(3.4) Classical local trace: a_p = p + 1 - N_p.

(3.5) Classical local Euler factor: L_p(E,s) = (1 - a_p p^{-s} + p^{1-2s})^{-1}.

(3.6) Classical Hasse-Weil L-function: L(E,s) = product over p of L_p(E,s), subject to the usual arithmetic conditions.

(3.7) Classical analytic rank: r_an(E) = ord_{s=1} L(E,s).

(3.8) BSD rank statement: r_an(E) = rank E(Q).

(3.9) Classical leading-term structure: L^{(r)}(E,1)/r! is proportional to (Omega_E * Reg_E * |Sha_E| * product_p c_p) / |E(Q)_tors|^2.

In this study, q-bases such as 2, 3, 5, 7 and 11 are not interpreted as literal primes over which regional economies are reduced. They are finite-state grids used to discretize regional economic states. The economic trace analogue therefore does not count points on a true elliptic curve over a finite field; it measures how a regional state behaves under controlled finite-state reductions.

(3.10) Economic curve analogue: E_{r,t}^{econ}: y^2 = x^3 + a_{r,t} x + b_{r,t}, where r indexes region and t indexes year.

(3.11) Economic BSD correspondence: LOrder_{r,t} approximately corresponds to StructuralRank_{r,t} within a calibrated rank-scale tolerance band, not by theorem-level equality.

(3.12) Claim boundary: Economic BSD analogue = calibrated measurement framework, not a proof of BSD and not a causal econometric law.

3.3. Unit of Analysis, Regional Sets and Panel Structure

The unit of analysis has two levels. The substantive BSD-inspired construction is reported at the regional/corridor-node level, while the calibration and robustness layer uses a regional-year panel with 10 regions over 15 years, producing N = 150 observations. Countries are deliberately excluded from the reported results so that the analysis remains aligned with a macro-regional world-system framework.

(3.13) Regional node set: R = {EAP, NAM, EUR, LAC, SAS, MENA, SSA, OCE, CAS, CAU}, with |R| = 10.

(3.14) World anchor: WLD is used as a normalization anchor and is not treated as a competing regional node.

(3.15) Panel universe: P = R x T, where |R| = 10, |T| = 15 and N = |P| = 150.

(3.16) Observation vector: X_{r,t} = (GDP_{r,t}, share_{r,t}, transitionGDP_{r,t}, growth_{r,t}, GDPpc_{r,t}, corridor_{r,t}, ...).

The World row fixes the global reference scale. Regional observations are interpreted relative to this anchor through output mass, world-output share, transition GDP, projected growth and income depth. This design prevents the regional benchmark from becoming a disguised country ranking.

3.4. Public-Data Anchor Panel and Transformation Rules

The public-data layer supplies the empirical coordinate system for the entire methodology. It contains macro-regional GDP mass, world-output share, transition GDP, projected growth and GDP per capita. These variables are interpreted as public anchor variables before any BSD-inspired transformation is applied.

(3.17) World-output share: m_{r,t} = GDP_{r,t} / GDP_{WLD,t}.

(3.18) Projected transition GDP: TGDP_{r,t+h} = GDP_{r,t} * (1 + g_{r,t+h})^h, where h is the transition horizon.

(3.19) Income depth: ID_{r,t} = GDPpc_{r,t}.

(3.20) Share-normalized mass exposure: M_{r,t} = 100 * (m_{r,t} - min_R m_{r,t}) / (max_R m_{r,t} - min_R m_{r,t}).

(3.21) General min-max normalization: N(x_{r,t}) = 100 * (x_{r,t} - min_R x_{r,t}) / (max_R x_{r,t} - min_R x_{r,t}).

(3.22) Inverse-fragility normalization: F(x_{r,t}) = 100 - N(x_{r,t}), applied when lower raw values imply higher vulnerability.

All transformed variables retain a clear lineage: public-source inputs are separated from author-calculated transformations. This separation is essential because later validation models must not treat variables with deterministic overlap as independent external evidence.

Algorithm 3.1. Construct the regional public-data anchor panel

1. Load the World anchor and the ten regional/corridor nodes.
2. Extract or aggregate GDP, world-output share, transition GDP, projected growth and GDP per capita.
3. Tag WLD as the normalization anchor and all other entries as regional/corridor nodes.
4. Apply the same regional aggregation rules across the substantive and N = 150 panel layers.
5. Preserve a source ledger that records public input families, transformations and output variables.

3.5. Systemic-Stress Construction and Raw-to-Normalized Audit

The systemic-stress layer converts macro-regional inputs into a multi-channel pressure measure. It is not a GDP ranking. It combines mass exposure, growth-gap pressure, income-fragility pressure, transition momentum and corridor exposure so that both large output regions and smaller corridor-sensitive regions can be represented.

(3.23) Growth-gap pressure: GGP_{r,t} = N(g_{r,t} - median_R(g_{r,t})), with orientation chosen so that higher values indicate stronger transition pressure.

(3.24) Income-fragility pressure: IFP_{r,t} = 100 - N(GDPpc_{r,t}).

(3.25) Transition-momentum pressure: TMP_{r,t} = N(TGDP_{r,t+h} - GDP_{r,t}).

(3.26) Corridor exposure: CE_{r,t} = N(corridor score_{r,t}).

(3.27) Raw stress composite: sigma^*_{r,t} = w_M M_{r,t} + w_G GGP_{r,t} + w_I IFP_{r,t} + w_T TMP_{r,t} + w_C CE_{r,t}, with sum of weights = 1.

(3.28) Normalized stress score: Stress_{r,t} = 100 * (sigma^*_{r,t} - min_R sigma^*_{r,t}) / (max_R sigma^*_{r,t} - min_R sigma^*_{r,t}).

(3.29) Stress audit interval: I_sigma = [min_R sigma^*_{r,t}, max_R sigma^*_{r,t}].

The raw-to-normalized audit ensures that the 0-100 stress score is anchored by the observed regional interval. It also makes corridor cases such as the Caucasus and Central Asia visible even when their output mass is small, because corridor exposure and fragility are retained as separate stress channels.

Algorithm 3.2. Build systemic stress and audit the normalization interval

1. Normalize each stress component on the same regional universe.
2. Orient each component so that larger values consistently mean higher pressure.
3. Aggregate components into the raw composite sigma* using declared weights.
4. Convert sigma* into a 0-100 stress score using min-max scaling.
5. Report the minimum, maximum and normalized position of each region as an audit table.

3.6. Regional Network Construction and Adequacy Diagnostics

The local-to-global logic requires a connected regional system. The methodology therefore represents the regional benchmark as a weighted graph whose nodes are regional/corridor units and whose edges encode corridor-sensitive regional connections. The graph is not an arbitrary visualization; it supplies the structure for centrality, Hodge-flow, triangular-action and scenario calculations.

(3.30) Weighted regional graph: G = (R, E, W), where R is the node set, E is the set of weighted regional edges and W = [w_{ij}] is the weighted adjacency matrix.

(3.31) Edge-weight rule: w_{ij} = Phi(output proximity_{ij}, corridor link_{ij}, stress interaction_{ij}, regional adjacency_{ij}).

(3.32) Graph density: D = 2|E| / (|R|(|R|-1)).

(3.33) Weighted degree: deg_i^w = sum_j w_{ij}.

(3.34) Weighted centrality index: C_i = N(centrality_i), where centrality_i may combine degree, eigenvector or betweenness information.

(3.35) Global transitivity: T_G = 3 * number of closed triangles / number of connected triples.

(3.36) Weighted clustering: Clust_i^w = geometric mean of triangle edge weights around node i, normalized to the regional graph.

A connected graph with sufficient density and non-trivial clustering is a necessary condition for interpreting local regional states as part of a global structure. Without this network adequacy step, the later Hodge-flow, cycle and local-to-global claims would be under-identified.

Algorithm 3.3. Construct the weighted regional graph

1. Define the ten regional/corridor nodes and exclude the World anchor from competitive node calculations.
2. Construct a weighted adjacency matrix using corridor-sensitive connections and regional interaction logic.
3. Compute density, connected components, average degree, average edge weight, transitivity and weighted clustering.
4. Retain the graph only if it is connected and sufficiently dense for triangular and Hodge-based diagnostics.
5. Use the same graph in centrality, structural-rank, BridgeStress and scenario layers.

3.7. Economic Curve Coefficients and the Elliptic-Cubic Surface

The coefficient layer maps regional economic conditions into the coefficient pair (a, b) of an economic cubic curve. The a coefficient is interpreted as a structural-protection and productive-depth coordinate, while the b coefficient captures asymmetry, corridor stress and deformation in the regional object. The mapping is author-calculated but auditable because each input component is explicitly defined.

(3.37) Coefficient vector: z_{r,t} = (ID_{r,t}, C_{r,t}, Res_{r,t}, AC_{r,t}, Stress_{r,t}, CE_{r,t}, Frag_{r,t}).

(3.38) Economic a coefficient: a_{r,t} = alpha_0 + alpha_1 ID_{r,t} + alpha_2 C_{r,t} + alpha_3 Res_{r,t} + alpha_4 AC_{r,t} - alpha_5 Stress_{r,t} - alpha_6 Frag_{r,t}.

(3.39) Economic b coefficient: b_{r,t} = beta_0 + beta_1 CE_{r,t} + beta_2 Curv_{r,t} + beta_3 BridgeStress_{r,t} - beta_4 Res_{r,t} - beta_5 C_{r,t}.

(3.40) Average coefficient surface: S(x,y) = x^3 + mean_R(a_{r,t}) x + mean_R(b_{r,t}) - y^2.

The elliptic-cubic surface is used as a geometric diagnostic. It does not claim that an economy is literally an elliptic curve. It shows how a high-dimensional regional economic state can be compressed into a curve-like coefficient space that later supports discriminant, trace and L-function analogues.

3.8. Economic Discriminant and Non-Degeneracy Audit

The discriminant audit verifies that constructed regional curve objects do not collapse into singular or numerically degenerate cases. A non-zero discriminant is required before the coefficient pair can be retained for local trace and Euler-factor calculations.

(3.41) Economic discriminant: $\Delta^{econ}_{r,t} = -16(4a_{r,t}^3 + 27b_{r,t}^2)$.

(3.42) Non-degeneracy condition: $|\Delta^{econ}_{r,t}| > \varepsilon_D$, where ε_D is a small numerical tolerance.

(3.43) Discriminant basin: $B_D(a,b) = -16(4a^3 + 27b^2)$, evaluated over the displayed coefficient grid.

The sign and magnitude of the discriminant are not used as welfare labels. They are used to confirm coefficient-space heterogeneity and to support the interpretation that regional objects differ meaningfully before local reduction is applied.

3.9. Finite-State Local Reductions and Trace Analogues

The local trace layer is the first explicitly BSD-inspired step. In classical arithmetic, local traces summarize finite-field reductions of the curve. In this economic analogue, q-bases define finite-state grids over regional states. The trace analogue is a signed signal: positive values indicate locally protective structural capacity, while negative values indicate stress-bearing, fragile or corridor-compressed local states.

(3.44) Finite-state base set: $Q = \{2, 3, 5, 7, 11\}$.

(3.45) Finite-state discretization: $d_q(x_{r,t}) = \text{floor}(q * N(x_{r,t})/100)$, with $d_q \in \{0, 1, ..., q-1\}$.

(3.46) Protective-state score: $P_{r,t} = \omega_A AC_{r,t} + \omega_R Res_{r,t} + \omega_C C_{r,t} + \omega_I ID_{r,t}$.

(3.47) Stress-state score: $U_{r,t} = \omega_S Stress_{r,t} + \omega_B BridgeStress_{r,t} + \omega_F Frag_{r,t} + \omega_K Curv_{r,t}$.

(3.48) Regional trace analogue: $A_{r,q,t} = \lambda_q * (P_{r,t} - U_{r,t}) / \kappa_A$, where λ_q allows trace magnitude to scale with q.

(3.49) Aggregate trace: $A_{q,t} = \sum_{r \in R} m_{r,t} A_{r,q,t}$.

The key methodological requirement is q-stability. If trace signs and relative ordering change arbitrarily across q, the local-reduction layer is weak. If they remain stable, the finite-state reduction provides a credible local-state signal for constructing Euler factors.

Algorithm 3.4. Compute local traces across finite-state bases

1. Standardize all variables entering the protective and stress-state scores.
2. Discretize regional states under each q-base in $Q = \{2, 3, 5, 7, 11\}$.
3. Compute protective-state and stress-state scores for each region and year.
4. Calculate signed regional trace analogues $A_{r,q,t}$.
5. Aggregate traces with world-output share weights and inspect q-base sign stability.

3.10. Economic Euler Factors, L-Function and L-Order Analogue

The economic Euler factors aggregate local trace information into a product object around $s = 1$. This step is the methodological bridge between local finite-state reductions and global order-of-behavior measurement. The construction follows the formal architecture of an L-function but remains a calibrated economic analogue.

(3.50) Economic Euler factor: $F_q(s) = (1 - A_{q,t} q^{-s} + q^{1-2s})^{-1}$.

(3.51) q-weighted economic L-function: $L_{econ,t}(s) = \prod_{q \in Q} F_q(s)^{\nu_q}$, with $\sum_q \nu_q = 1$ or product weights declared.

(3.52) Log L-function: $\log L_{econ,t}(s) = \sum_{q \in Q} \nu_q \log F_q(s)$.

(3.53) Regional local L-object: $L_{r,t}(s) = \prod_{q \in Q} (1 - A_{r,q,t} q^{-s} + q^{1-2s})^{-\nu_q}$.

(3.54) Order-of-behavior score: $o_{r,t} = -[d/ds \log L_{r,t}(s)]$ evaluated at $s = 1$.

(3.55) L-order analogue: $LOrder_{r,t} = 5 * (o_{r,t} - \min_R o_{r,t}) / (\max_R o_{r,t} - \min_R o_{r,t})$.

The L-order analogue is not a classical order of vanishing. It is a normalized order-of-behavior measure extracted from the local trace and Euler-factor structure. It is later compared with structural rank under calibration and equivalence rules rather than exact equality.

3.11. Structural Rank Construction: Productive, Hodge-Flow, Network and Agentic Components

Structural economic rank is defined as a composite measure that combines productive depth, flow structure, network position and agentic capacity. This construction prevents the rank object from collapsing into GDP size. It also creates an independently specified target for the L-order analogue.

(3.56) Standardized component matrix: $Z_{r,t} = \text{standardize}(\text{Productive, Flow, Network, Agentic variables})$.

(3.57) PCA/productive rank: $R^P_{r,t} = Z^P_{r,t}\, v_1$, where v_1 is the first principal-component loading vector.

(3.58) Incidence representation: B_1 is the node-edge incidence matrix and B_2 is the edge-triangle incidence matrix.

(3.59) Hodge flow decomposition: $f = B_1^T \phi + B_2 \psi + h$, where $B_1 h = 0$ and $B_2^T h = 0$.

(3.60) Hodge-flow rank: $R^H_{r,t} = N(\phi_{r,t})$ or an equivalent normalized potential-based flow rank.

(3.61) Network rank: $R^N_{r,t} = N(\theta_1 \text{degree}_{r,t} + \theta_2 \text{centrality}_{r,t} + \theta_3 \text{clustering}_{r,t})$.

(3.62) Agentic rank: $R^A_{r,t} = N(\text{agentic capacity}_{r,t})$.

(3.63) Structural rank: $\text{Rank}_{r,t} = \pi_P R^P_{r,t} + \pi_H R^H_{r,t} + \pi_N R^N_{r,t} + \pi_A R^A_{r,t}$, with $\sum \pi = 1$.

This rank construction is the empirical counterpart of the algebraic rank concept in the classical BSD analogy. The correspondence claim is therefore not that economies have rational points, but that local finite-state economic reductions carry measurable information about a structured rank object.

Algorithm 3.5. Construct structural rank

1. Standardize the productive, Hodge-flow, network and agentic components.
2. Estimate the productive component using PCA or an equivalent productive-depth index.
3. Compute Hodge-flow potential from the regional network flow field.
4. Compute network and agentic sub-ranks from centrality, clustering, resilience and agentic variables.
5. Aggregate components to the 0-5 structural-rank scale with declared weights.

3.12. Rank-Order Correspondence and Calibration Logic

The core BSD-inspired empirical claim is evaluated by comparing the L-order analogue with structural rank. The comparison is not framed as exact equality. It is framed as calibrated local-to-global consistency: local reductions and Euler factors should approximate the independently defined structural rank within a small rank-scale error.

(3.64) Rank gap: $e_{r,t} = \text{Rank}_{r,t} - \text{LOrder}_{r,t}$.

(3.65) Absolute gap: $|e_{r,t}| = |\text{Rank}_{r,t} - \text{LOrder}_{r,t}|$.

(3.66) Rank-scale MAE: $\text{MAE} = (1/N) \sum_{r,t} |\text{Rank}_{r,t} - \text{LOrder}_{r,t}|$.

(3.67) Rank-scale RMSE: $\text{RMSE} = \sqrt{(1/N) \sum_{r,t} (\text{Rank}_{r,t} - \text{LOrder}_{r,t})^2}$.

(3.68) Rank-order stability: $\rho_S = \text{Spearman}(\text{LOrder}_{r,t}, \text{Rank}_{r,t})$.

A strong methodology requires that the correspondence survive not only in a full-sample scatter plot but also under block deletion, out-of-sample validation, q-base changes and permutation placebo tests. These are specified in later methodological sections.

3.13. Regulator, Tamagawa-Type Friction and Torsion Analogues

The BSD analogy is extended beyond rank correspondence by constructing economic analogues of regulator, Tamagawa factors and torsion. These variables are not imported as literal arithmetic invariants. They serve as structured economic diagnostics that help explain why rank, local friction and locked capacity differ across regions.

(3.69) Economic regulator: $\text{Reg}_{r,t}^{\text{econ}} = \text{Rank}_{r,t}^{\gamma_1} * (1 + C_{r,t}/100)^{\gamma_2} * (1 + \text{Res}_{r,t}/100)^{\gamma_3}$.

(3.70) Tamagawa-type friction: $\text{Tam}_{r,t}^{\text{econ}} = 1 + \tau_S \text{Stress}_{r,t} + \tau_C \text{CE}_{r,t} + \tau_F \text{Frag}_{r,t}$, after scaling components to [0,1].

(3.71) Locked-capacity torsion: $\text{Tor}_{r,t}^{\text{econ}} = \tau_0 + \tau_1 \text{Frag}_{r,t} + \tau_2 \text{Curv}_{r,t} + \tau_3 (100 - C_{r,t})$, rescaled to the reported torsion interval.

(3.72) Absorption-capacity condition: High Rank and high Reg^{econ} require positive centrality and resilience support, not only output mass.

The regulator captures rank supported by centrality and resilience. Tamagawa-type frictions capture local obstacles arising from stress, fragility and corridor exposure. Torsion captures capacity that is present but locked in non-productive circularity due to fragility, curvature or weak centrality.

3.14. Structural-Rank Response Surface

The structural-rank surface is a visual and analytical response function over agentic capacity and resilience. It shows whether the rank object increases in a systematic way when productive coordination and shock absorption rise together.

(3.73) Rank response surface: Rank(AC,Res) = beta_0 + beta_1 AC + beta_2 Res + beta_3(AC * Res) + beta_4 AC^2 + beta_5 Res^2.

(3.74) Interaction effect: partial^2 Rank / partial AC partial Res = beta_3.

A positive interaction term means that agentic capacity and resilience reinforce each other. This supports the methodological choice to build structural rank as a composite object rather than a one-dimensional GDP-size measure.

3.15. Corridor-Rank Leverage, BridgeStress and Middle Corridor Interpretation

The corridor methodology separates strategic transmission exposure from internal output mass. BridgeStress is designed to identify regions whose global relevance arises through corridor role, fragility and curvature participation. This is central for the Caucasus, Central Asia, the Black Sea interface and the Caspian crossing logic.

(3.75) Corridor-role vector: CR_{r,t} = (CE_{r,t}, Role_{r,t}, Frag_{r,t}, Curv^+_{r,t}).

(3.76) Raw BridgeStress: BS^*_{r,t} = lambda_1 CE_{r,t} + lambda_2 Role_{r,t} + lambda_3 Frag_{r,t} + lambda_4 Curv^+_{r,t}.

(3.77) Normalized BridgeStress: BridgeStress_{r,t} = 100 * (BS^*_{r,t} - min_R BS^*_{r,t}) / (max_R BS^*_{r,t} - min_R BS^*_{r,t}).

(3.78) Corridor robustness requirement: rank(BridgeStress_{CAU}) = 1 and rank(BridgeStress_{CAS}) = 2 should remain stable under alternative corridor-coding schemes, if the Middle Corridor claim is robust.

The qualitative corridor-function table is treated as an interpretation layer, not as a separate statistical model. It explains why the Caucasus and Central Asia can be high BridgeStress nodes despite low GDP share.

Algorithm 3.6. Estimate BridgeStress and corridor interpretation

1. Assign corridor exposure and corridor-role scores to each regional/corridor node.
2. Combine corridor role with fragility and positive curvature participation.
3. Normalize the raw BridgeStress score to 0-100.
4. Rank regions by BridgeStress and compare the order under alternative corridor-coding schemes.
5. Use the qualitative corridor-function table to interpret, not inflate, the numerical corridor result.

3.16. Visual Diagnostics and Figure Construction Rules

Visual diagnostics are used to reveal structure that is difficult to communicate through tables alone. Each figure is tied to a specific methodological object: curve surface, discriminant distribution, trace heatmap, L-function behavior, structural-rank hierarchy, rank-order correspondence, rank response surface, BridgeStress hierarchy, threshold compression and discriminant basin.

(3.79) Figure admissibility rule: Each visual V_k must be generated from a declared table or formula object O_k and must not introduce an unreported hidden variable.

(3.80) Caption consistency rule: Figure internal title number = Figure caption number = figure reference number in the manuscript.

The visual layer is descriptive and diagnostic. It does not create new statistical evidence unless linked to a reported quantitative table or formula.

3.17. Scenario Simulation, Spectral Threshold and Action Concentration

The scenario layer evaluates how regional-corridor shocks compress the local-to-global transition boundary. Shock amplitude modifies the regional stress network, after which the first positive eigenvalue, spectral radius, normalized threshold and action are recalculated.

(3.81) Scenario-amended stress: Stress_{r,t}^{(h)} = Stress_{r,t} + h * ShockLoad_{r,t}, where h is the shock amplitude.

(3.82) Scenario-amended adjacency: W^{(h)} = W o (1 + h * Xi), where o denotes elementwise multiplication and Xi is the shock-exposure matrix.

(3.83) Graph Laplacian under shock: L^{(h)} = D^{(h)} - W^{(h)}.

(3.84) First positive spectral mode: lambda_1^{(h)} = min{lambda > 0 : lambda is an eigenvalue of L^{(h)}}.

(3.85) Spectral radius: rho^{(h)} = max_j |lambda_j(W^{(h)})|.

(3.86) Normalized threshold: Theta^{(h)} = lambda_1^{(h)} / rho^{(h)}.

(3.87) Triangular cycle action: Action^{(h)} = sum_{triangles ijk} omega_{ijk} (curl_{ijk}^{(h)})^2.

(3.88) Top-five action share: Share_5 = 100 * (sum of five largest triangle actions) / (total action).

A falling threshold indicates that smaller disturbances can become systemically transmissible. A high top-five action share indicates that stress energy is concentrated in a limited number of regional channels rather than distributed uniformly across the global regional system.

Algorithm 3.7. Run regional-corridor scenario simulations

1. Choose scenario amplitudes and shock channels such as price pressure, financial spread stress, logistics disruption and geopolitical energy shock.
2. Update stress scores and edge weights according to the shock-exposure matrix.
3. Recompute spectral modes, spectral radius and normalized threshold.
4. Recompute triangular-cycle action and action concentration.
5. Classify threshold compression as a scenario diagnostic, not as causal proof.

3.18. N = 150 Econometric Closure Architecture

The N = 150 closure layer is not used to turn the BSD analogue into a causal law. It is used to audit calibration, robustness, external-proxy screening, falsification, anti-circularity, sensitivity and reproducibility. The key methodological rule is claim discipline: if a diagnostic is weak, it remains a diagnostic and is not upgraded into confirmation.

(3.89) Panel observation: y_{r,t}, LOrder_{r,t}, Rank_{r,t}, Z_{r,t}, for r in R and t in T.

(3.90) Two-way fixed-effects baseline: y_{r,t} = alpha + beta LOrder_{r,t} + Z_{r,t}^{prime} gamma + mu_r + tau_t + epsilon_{r,t}.

(3.91) Within-transformed model: y~_{r,t} = beta LOrder~_{r,t} + Z~_{r,t}^{prime} gamma + epsilon~_{r,t}.

(3.92) Claim-gate rule: Statistical confirmation requires sign stability, admissible variable lineage, robust inference support and external-outcome consistency; otherwise the claim remains calibration or screening.

This architecture separates substantive BSD-analogue construction from empirical screening. It also protects the manuscript against overclaiming when robust p-values or external-proxy results are weak.

3.19. High-R2 Decomposition and Model-Fit Interpretation

High R2 is treated as a diagnostic risk rather than automatic evidence. In regional panels, persistent cross-regional heterogeneity can generate extremely high model fit under fixed effects. The methodology therefore decomposes fit into overall, within, between, fixed-effect-only, incremental and partial components.

(3.93) Overall R2: R2_overall = 1 - sum(y_{r,t} - yhat_{r,t})^2 / sum(y_{r,t} - ybar)^2.

(3.94) Within R2: R2_within = 1 - sum(y~_{r,t} - yhat~_{r,t})^2 / sum(y~_{r,t})^2.

(3.95) Incremental R2 of LOrder: Delta R2_L = R2(full model) - R2(model without LOrder).

(3.96) Partial R2 of LOrder: R2_partial = (SSR_reduced - SSR_full) / SSR_reduced.

The interpretation is conservative: high overall R2 can support internal fit, but it cannot by itself establish causality, theorem-level confirmation or strong external validity.

3.20. External Observable-Proxy Screening

External observable-proxy variables are used only for directional screening. They are source-based or proxy-transformed observables such as inflation pressure, trade openness, logistics proxy, growth revision, external stress and external resilience. The methodology explicitly prevents this layer from being described as strong external econometric validation when p-values are weak or signs are mixed.

(3.97) Outcome-specific external-proxy model: Y^k_{r,t} = alpha_k + beta_k LOrder_{r,t} + Z_{r,t}^{prime} gamma_k + mu_r + tau_t + epsilon^k_{r,t}.

(3.98) Directional sign screen: sign(beta_k) = expected sign_k, otherwise classify as opposite-sign diagnostic.

(3.99) External screening decision: Status_k = {directional watch, diagnostic only, caution}, based on sign, p-value and variable lineage.

A non-significant but expected-sign coefficient is retained as directional watch evidence only. A non-significant opposite-sign coefficient is retained as diagnostic-only evidence. Neither case is treated as independent confirmation of the BSD-inspired mechanism.

3.21. Negative Controls, Falsification and Placebo Outcomes

A constructed index is not credible if it explains everything. Negative controls test whether LOrder fails to explain deliberately unrelated, randomized or temporally destroyed outcomes. This layer is essential for distinguishing structured calibration from mechanical overfitting.

(3.100) Negative-control model: NC_{r,t} = alpha + beta_NC LOrder_{r,t} + mu_r + tau_t + u_{r,t}.

(3.101) Falsification pass condition: beta_NC is statistically weak and substantively near zero for unrelated or randomized outcomes.

(3.102) Future-shuffle control: Y^{future-shuffled}_{r,t} = random permutation of Y_{r,t+k} across region-year cells.

(3.103) Reversed-year control: Y^{rev}_{r,t} = Y_{r,T-t+1}.

The model passes the falsification logic when randomized and temporally broken outcomes do not produce meaningful LOrder effects.

3.22. Dependence Diagnostics, Robust Inference and Small-Cluster Correction

The N = 150 panel has only ten regional clusters and likely cross-regional common shocks. Classical standard errors are therefore insufficient as the only inference method. The methodology reports cross-sectional dependence, serial-dependence risk, HC3, clustered, wild-cluster, Satterthwaite-style and Driscoll-Kraay/HAC-compatible inference.

(3.104) Pesaran CD statistic: CD = sqrt(2T/(N_R(N_R-1))) * sum_{i<j} corr(e_i, e_j).

(3.105) Serial-dependence screen: e_{r,t} = rho_e e_{r,t-1} + v_{r,t}.

(3.106) HC3 variance: V_HC3 = (X^prime X)^{-1} X^prime diag(e_i^2/(1-h_i)^2) X (X^prime X)^{-1}.

(3.107) Cluster-robust variance: V_CR = (X^prime X)^{-1} [sum_g X_g^prime e_g e_g^prime X_g] (X^prime X)^{-1}.

(3.108) Driscoll-Kraay/HAC logic: V_DK = Gamma_0 + sum_{l=1}^L k(l,L)(Gamma_l + Gamma_l^prime), with declared lag length L.

(3.109) Robust-inference interpretation rule: positive beta with weak p-values = consistency signal only, not econometric confirmation.

This methodology preserves the positive sign of LOrder as a consistency signal where present, but it does not convert weak p-values into strong empirical proof. Small-cluster caveats remain part of the reported claim boundary.

3.23. Dynamic and Threshold Diagnostics with Claim Boundaries

Dynamic and threshold specifications are retained as diagnostics. The short time dimension and small regional cross-section make structural dynamic-panel claims risky. Threshold models are used to test whether high BridgeStress regimes change the rank-stress relationship, but they do not become the primary evidence for the BSD-inspired result.

(3.110) Dynamic diagnostic model: Rank_{r,t} = rho Rank_{r,t-1} + beta LOrder_{r,t} + mu_r + tau_t + u_{r,t}.

(3.111) Dynamic claim boundary: If T is short and clusters are small, dynamic results are persistence diagnostics, not structural causal models.

(3.112) Threshold model: Rank_{r,t} = alpha + beta_1 LOrder_{r,t} + beta_2[LOrder_{r,t} * I(BridgeStress_{r,t} > c)] + mu_r + tau_t + u_{r,t}.

(3.113) Corridor-compression interpretation: beta_2 < 0 implies lower rank protection under high corridor stress, if retained as supplementary evidence.

3.24. Circularity, Variable Lineage and Anti-Circularity Tests

Because the study constructs several author-calculated variables, circularity control is essential. The variable-lineage matrix records public inputs, transformations, overlap risks and admissible use. Variables with deterministic overlap are not treated as independent causal validation variables.

(3.114) Input-lineage set: I(X) = {public inputs and author transformations used to construct variable X}.

(3.115) Overlap index: Omega(X,Y) = |I(X) intersection I(Y)| / |I(X) union I(Y)|.

(3.116) Admissible-use rule: If Omega(X,Y) is high, X and Y may be used for calibration or diagnosis but not as independent causal validation of each other.

(3.117) Residualized LOrder: LOrder^{perp}_{r,t} = residual from regression of LOrder_{r,t} on overlapping internal inputs.

(3.118) External-only LOrder proxy: LOrder^{ext}_{r,t} = f(external-source variables only), classified as diagnostic if proxy construction is incomplete or weak.

This methodology does not hide circularity risk. It identifies it, tests it, and demotes claims where residualization or external-only variants weaken the relationship.

3.25. Calibration, Equivalence and Bland-Altman Agreement

The correct empirical interpretation of the BSD-inspired rank result is practical equivalence, not exact equality. Calibration tests evaluate whether LOrder and structural rank agree within a declared tolerance band on the 0-5 rank scale.

(3.119) Calibration regression: Rank_{r,t} = alpha_c + delta_c LOrder_{r,t} + eta_{r,t}.

(3.120) Intercept tolerance: alpha_c in [-0.25, 0.25].

(3.121) Slope tolerance: delta_c in [0.85, 1.15].

(3.122) Bland-Altman mean difference: dbar = (1/N) sum_{r,t} (Rank_{r,t} - LOrder_{r,t}).

(3.123) Bland-Altman limits: LOA = dbar +/- 1.96 * sd(Rank_{r,t} - LOrder_{r,t}).

(3.124) Block agreement rule: The rank difference must remain inside the tolerance band by region and by year, not only in the full sample.

This calibration architecture is stronger than a simple correlation because it evaluates scale agreement, systematic bias, local deviations and temporal stability.

3.26. Leave-One-Block and Out-of-Sample Validation

The block-validation layer tests whether the correspondence depends on a single year, region or favorable in-sample fit. The designs include leave-one-year-out, leave-one-region-out, time-block validation and blocked region-year validation.

(3.125) Leave-one-year training set: Train_{-t0} = {(r,t): t != t0}.

(3.126) Leave-one-region training set: Train_{-r0} = {(r,t): r != r0}.

(3.127) Out-of-sample prediction error: OOS_RMSE = sqrt((1/|Test|) sum_{(r,t) in Test} (Rank_{r,t} - Rankhat_{r,t})^2).

(3.128) OOS rank-order agreement: rho_S^{OOS} = Spearman(Rank_{Test}, Rankhat_{Test}).

Strong time-block stability supports calibration over time. Weaker leave-one-region performance is not hidden; it is interpreted as boundary evidence showing that regional extrapolation is harder than temporal interpolation.

3.27. Weight, q-Base and Corridor-Coding Sensitivity

Sensitivity analysis evaluates whether the main result is a by-product of one preferred weighting scheme, one q-base design or one corridor-coding rule. The methodology perturbs composite weights, deletes q-bases, changes q-weighting schemes and applies alternative corridor codings.

(3.129) Weight perturbation: w_j^{(b)} = w_j + delta_j^{(b)}, subject to w_j^{(b)} >= 0 and sum_j w_j^{(b)} = 1.

(3.130) Perturbed index: Index_{r,t}^{(b)} = sum_j w_j^{(b)} X_{j,r,t}.

(3.131) Sensitivity stability: Stability_b = Spearman(Index^{baseline}, Index^{(b)}).

(3.132) q-base deletion test: Q_{-q0} = Q \ {q0}.

(3.133) Corridor-coding alternative: BridgeStress_{r,t}^{(c)} = f_c(CE, Role, Fragility, Curvature), where c indexes coding schemes.

The result is considered robust at the calibration level if rank-order stability remains high and the key corridor order does not collapse under plausible alternative specifications.

3.28. Decision Criteria and Permutation Placebo Distribution

The methodology uses explicit decision gates so that evidence is not overstated. A result can be classified as pass, watch, caution or diagnostic-only depending on sign, magnitude, inference, robustness and admissibility.

(3.134) Permutation placebo p-value: p_perm = (1 + number of placebo statistics at least as favorable as observed) / (B + 1).

(3.135) Placebo statistic: T_b = MAE(LOrder^{perm_b}, Rank) or 1 - Spearman(LOrder^{perm_b}, Rank).

(3.136) Decision gate: ClaimLevel = G(sign, p-values, MAE, RMSE, OOS, placebo p, circularity status, external-screening status).

(3.137) No-escalation rule: A weak econometric or external-proxy result cannot be upgraded by strong internal calibration alone.

This decision architecture is central to the chapter. It allows strong calibration claims where the evidence supports them, while keeping external validation, dynamic panels and robust p-values within their proper evidentiary limits.

3.29. Reproducibility, Source Ledger and Replication Discipline

The reproducibility layer records the source families, aggregation logic, author-calculated objects, random seeds and output hashes needed for external audit and links them to the archived Zenodo data and replication package. The companion package is published as Gondauri (2026), DOI 10.5281/zenodo.20796984, and contains the replication materials required to verify the reported tables, formula catalogue, algorithms, extracted result files, figure catalogue, source ledger, metadata, checksums and reproducibility scripts. The Word manuscript defines and interprets the model, while the Zenodo record provides the external replication artifact for this manuscript version.

Replication package citation: Gondauri, D. (2026). Regional Economic Birch-Swinnerton-Dyer Modelling: Data and Replication Package for a Local-to-Global Framework of Structural Rank Formation, Corridor Stress and World-Economy Calibration [Data set]. Zenodo. https://doi.org/10.5281/zenodo.20796984. This record is cited in the methodology, results-source note, data availability statement and references so that the manuscript treats the data-package deposit as a published and versioned research artifact.

(3.138) Source ledger item: SL_j = (source family, variable name, extraction rule, aggregation rule, transformation, output use).

(3.139) Random seed record: seed_b is fixed for each randomized, bootstrap or permutation procedure.

(3.140) Output hash: H(file) = cryptographic hash of the exported replication artifact.

(3.141) Replication closure condition: All reported tables and figures are regenerated from the same source ledger, scripts, seeds and transformation rules.

3.30. Integrated Evidence Map and Reviewer-Risk Response

The evidence map classifies each part of the methodology by its evidentiary function: substantive BSD-analogue construction, internal calibration, external-proxy screening, robustness, falsification, sensitivity or reproducibility. Reviewer-risk response is built into the design rather than appended after the fact.

(3.142) Evidence block: E_k = (object_k, method_k, limitation_k, claim level_k, reviewer risk_k).

(3.143) Reviewer-risk response: RR_k = (criticism_k, methodological safeguard_k, evidence location_k, remaining limitation_k).

This design directly addresses likely objections: BSD analogy risk, circularity, high R2, weak external-proxy evidence, small clusters, dynamic-panel overclaiming, threshold overinterpretation, corridor-coding subjectivity and replication-package traceability through the Zenodo record DOI 10.5281/zenodo.20796984.

3.31. Final Methodological Synthesis

The methodology converts the BSD local-to-global idea into a disciplined economic measurement architecture. It starts with a World-normalized regional anchor panel, constructs stress and corridor exposure, embeds regions in a weighted network, maps regional states into economic curve coefficients, verifies non-degeneracy, creates finite-state local traces, builds Euler-factor and L-function analogues, defines an L-order measure and compares it with a multi-component structural-rank object.

The econometric closure layer then prevents overclaiming. N = 150 panel diagnostics, fixed effects, high-R2 decomposition, robust inference, external observable-proxy screening, negative controls, circularity safeguards, calibration equivalence, block validation, sensitivity analysis, placebo distributions and reproducibility notes define the limits of the empirical claim. The final methodological claim is therefore precise: the framework supports

calibrated local-to-global consistency in a regional economic BSD analogue; it does not prove the classical BSD conjecture, does not establish causal law and does not convert weak external-proxy evidence into statistical confirmation.

3.32. Consolidated Algorithmic Workflow

The complete computational workflow can be summarized as the following reproducible sequence.

Algorithm 3.8. End-to-end BSD-inspired regional methodology

1. Construct the World-normalized regional anchor panel and define the regional/corridor node set.
2. Normalize input variables and build systemic-stress, fragility, transition-momentum and corridor-exposure measures.
3. Construct the weighted regional graph and compute adequacy diagnostics, centrality and cycle structure.
4. Map regional variables into economic curve coefficients a and b; compute discriminants and screen non-degeneracy.
5. Compute finite-state local traces under q = 2, 3, 5, 7 and 11; aggregate traces into Euler factors.
6. Construct the economic L-function around s = 1 and derive the L-order analogue.
7. Build structural rank from productive, Hodge-flow, network and agentic components.
8. Compare LOrder with structural rank through gaps, MAE, RMSE, Spearman correlation, calibration and Bland-Altman audits.
9. Estimate regulator, Tamagawa-type friction, torsion, BridgeStress, scenario thresholds and action concentration.
10. Run N = 150 closure diagnostics: TWFE, high-R2 audit, external-proxy screening, negative controls, robust inference, circularity tests, OOS validation, sensitivity analysis and permutation placebo tests.
11. **Assign claim levels through the decision-gate matrix and link sources, seeds, transformations, output hashes and replication materials to the Zenodo record DOI 10.5281/zenodo.20796984.**

Chapter 4. Results: Regional BSD-Inspired Local-to-Global Rank Formation in the World Economy

The central result is a Birch-Swinnerton-Dyer-inspired economic local-to-global statement: local regional market reductions, represented by finite-state regimes rather than literal arithmetic reductions over finite fields, contain measurable information about global structural rank formation. The chapter does not claim to prove the classical BSD conjecture. It constructs a transparent economic analogue in which regional public-data anchors are transformed into curve coefficients, local traces, Euler-factor analogues, an economic L-function, and structural-rank measures.

4.1. World and Regional Public-Data Anchor Panel

The following table introduces the empirical coordinate system of the revised BSD-inspired regional benchmark. It reports the World normalization anchor and the macro-regional input variables used throughout the chapter: GDP mass, world-output share, transition GDP, projected growth, income depth and system role.

Table 4.1. World and regional public-data input panel for the revised BSD benchmark

Code	Region / anchor	GDP 2024, $bn	World share, %	Transition GDP 2026, $bn	Growth 2026, %	GDP pc, $	System role
WLD	World anchor	110,985.0	100.00	118,201.7	3.200	14100	Global normalization anchor
EAP	East Asia and Pacific	35,620.0	32.09	38,674.9	4.200	17200	Regional/corridor node

Code	Region / anchor	GDP 2024, $bn	World share, %	Transition GDP 2026, $bn	Growth 2026, %	GDP pc, $	System role
NAM	North America	31,000.0	27.93	32,252.4	2.000	76000	Regional/corridor node
EUR	Europe	23,150.0	20.86	23,849.7	1.500	43000	Regional/corridor node
LAC	Latin America and Caribbean	7,260.0	6.540	7,612.7	2.400	10600	Regional/corridor node
SAS	South Asia	4,770.0	4.300	5,390.0	6.300	2700	Regional/corridor node
MENA	Middle East and North Africa	4,540.0	4.090	4,835.2	3.200	8800	Regional/corridor node
SSA	Sub-Saharan Africa	2,160.0	1.950	2,327.3	3.800	1850	Regional/corridor node
OCE	Oceania	1,810.0	1.630	1,886.8	2.100	63000	Regional/corridor node
CAS	Central Asia	530.00	0.480	585.40	5.100	9000	Regional/corridor node
CAU	Caucasus	145.00	0.130	158.60	4.600	9500	Regional/corridor node

Source: *World Bank WDI/DataBank source-family logic for GDP and GDP per capita; IMF World Economic Outlook source-family logic for regional growth projections; author regional aggregation and transition-GDP calculation.*

Result explanation: Table 4.1 defines the regional empirical base of the BSD-inspired benchmark. The World row serves as the normalization anchor, with 2024 global GDP of USD 110,985.0 billion, projected 2026 transition GDP of USD 118,201.7 billion, global growth of 3.200%, and GDP per capita of USD 14,100. Against this anchor, global output is highly concentrated: East Asia and Pacific, North America and Europe account for 32.09%, 27.93% and 20.86% of world output, respectively, or about 80.88% together.

At the same time, the table shows why the analysis cannot be reduced to GDP size. South Asia has only 4.300% of world output but the highest projected growth rate, 6.300%; Central Asia and the Caucasus account for only 0.480% and 0.130%, yet remain relevant because of growth and corridor sensitivity. The income-depth gap is also substantial, ranging from USD 76,000 in North America and USD 63,000 in Oceania to USD 2,700 in South Asia and USD 1,850 in Sub-Saharan Africa.

Therefore, Table 4.1 fixes the regional coordinate system for the whole results chapter. Large regions define the output-mass layer, while smaller and transition-sensitive regions add growth pressure, income-depth variation and corridor exposure. This supports the chapter's main empirical logic: structural economic rank is a local-to-global phenomenon shaped by scale, growth, resilience, fragility and corridor transmission, not by GDP size alone.

4.2. Regional Systemic-Stress Results

The following table transforms the regional input panel into a systemic-stress layer. It decomposes stress into mass exposure, growth-gap pressure, income-fragility pressure, transition momentum and corridor exposure so that the

normalized stress score can be interpreted as a multi-channel regional pressure measure rather than as a single GDP indicator.

Table 4.2. Regional systemic-stress components and normalized stress score

Code	Region	Mass exposure	Growth-gap pressure	Income-fragility pressure	Transition-momentum pressure	Corridor exposure	Stress score
SAS	South Asia	13.05	100.00	85.53	100.00	56.67	100.00
CAS	Central Asia	1.100	61.29	47.44	74.49	90.00	71.79
EAP	East Asia and Pacific	100.00	32.26	30.85	55.68	53.33	71.23
CAU	Caucasus	0.000	45.16	45.97	63.72	100.00	66.03
SSA	Sub-Saharan Africa	5.690	19.35	100.00	47.35	28.33	53.78
EUR	Europe	64.86	54.84	10.81	0.000	61.67	47.40
MENA	Middle East and North Africa	12.39	0.000	48.06	34.88	73.33	39.71
NAM	North America	86.98	38.71	0.000	10.20	11.67	30.66
LAC	Latin America and Caribbean	20.06	25.81	43.03	18.40	20.00	26.78
OCE	Oceania	4.690	35.48	3.440	12.24	0.000	0.000

Source: *Author calculations from the regional public-data input panel and corridor-exposure coding; all components normalized to a 0-100 scale before aggregation.*

Result explanation: Table 4.2 converts the public-data input layer into the first systemic-stress ranking. South Asia is the normalized upper bound at 100.00 because it combines maximum growth-gap pressure, maximum transition-momentum pressure and high income-fragility pressure of 85.53. Central Asia and East Asia and Pacific follow closely, with stress scores of 71.79 and 71.23, but for different reasons: Central Asia is corridor-driven, while East Asia and Pacific is mass- and transition-driven.

The table is important because it separates the composition of stress from the final normalized score. The Caucasus has almost no mass exposure in this benchmark, yet its 100.00 corridor exposure and 66.03 stress score keep it in the high-stress group. North America has strong mass exposure but low fragility and low corridor pressure, so its stress score is only 30.66. Thus, the stress layer confirms that regional vulnerability is not a mechanical function of GDP size.

4.3. Raw-to-Normalized Stress Audit

The following table audits the conversion from the raw composite stress measure into the normalized 0-100 stress scale. Its purpose is to show the lower and upper anchors of the benchmark and to make the later stress, curvature and corridor calculations numerically transparent.

Table 4.3. Raw-to-normalized systemic-stress audit

Code	Region	Raw composite sigma*	Minimum sigma*	Maximum sigma*	Normalized stress	Audit note
SAS	South Asia	70.33	10.73	70.33	100.00	normalized upper bound
CAS	Central Asia	53.51	10.73	70.33	71.79	inside interval
EAP	East Asia and Pacific	53.18	10.73	70.33	71.23	inside interval
CAU	Caucasus	50.08	10.73	70.33	66.03	inside interval
SSA	Sub-Saharan Africa	42.78	10.73	70.33	53.78	inside interval
EUR	Europe	38.98	10.73	70.33	47.40	inside interval
MENA	Middle East and North Africa	34.39	10.73	70.33	39.71	inside interval
NAM	North America	29.00	10.73	70.33	30.66	inside interval
LAC	Latin America and Caribbean	26.69	10.73	70.33	26.78	inside interval
OCE	Oceania	10.73	10.73	70.33	0.000	normalized lower bound

Source: *Author calculations from Table 4.2 using min-max normalization.*

Result explanation: Table 4.3 audits the raw-to-normalized stress transformation. The normalization interval is fixed by South Asia at raw sigma* = 70.33 and Oceania at raw sigma* = 10.73. All other regions are placed inside this same interval, which makes the later stress-score comparisons numerically consistent.

The audit also explains why corridor regions remain visible after normalization. Central Asia has a raw composite of 53.51 and normalized stress of 71.79, while the Caucasus has a raw composite of 50.08 and normalized stress of 66.03. These values are not artifacts of a country list; they arise from the regional stress components and preserve local corridor pressure inside the global benchmark.

4.4. Regional Network Adequacy for Local-to-Global Analysis

The following table evaluates whether the regional/corridor graph is adequate for local-to-global analysis. It reports node count, edge count, density, connectedness, degree, edge weight, transitivity and clustering so that the subsequent Hodge, cycle and rank diagnostics are applied to a connected benchmark system.

Table 4.4. Regional network adequacy diagnostics

Metric	Value	Interpretation
Regional/corridor nodes	10.00	The regional node set; World is used separately as anchor
Weighted edges	27.00	Corridor-sensitive regional connections
Density	0.600	Sufficiently dense for triangular and local-to-global calculations

Metric	Value	Interpretation
Connected components	1.000	Connected benchmark; no isolated regional node
Average degree	5.400	Average number of regional connections
Average normalized edge weight	0.471	Mean strength of corridor-weighted links
Global transitivity	0.633	Cycle structure exists for higher-order rank interpretation
Weighted clustering	0.301	Non-trivial regional clustering

Source: Author calculations from the regional/corridor benchmark graph.

Result explanation: Table 4.4 shows that the regional graph is structurally adequate for local-to-global calculations. The system contains 10 regional/corridor nodes, 27 weighted edges, density of 0.600 and one connected component. This means no regional node is isolated from the benchmark network.

The transitivity value of 0.633 and weighted clustering of 0.301 indicate that the graph contains enough cycle structure for higher-order interpretation. Therefore, later rank, Hodge-flow, triangular-action and corridor-transmission results are applied to a connected regional system rather than to a disconnected collection of observations.

4.5. Visual Summary of the Regional Benchmark Universe

The following figure visualizes the average economic elliptic-cubic form generated from the regional coefficient layer. It is included to show how the constructed BSD-inspired object can be read geometrically, before the chapter moves to coefficient, discriminant and trace calculations.

Figure 4.1. Economic elliptic-cubic surface: regional benchmark coefficients

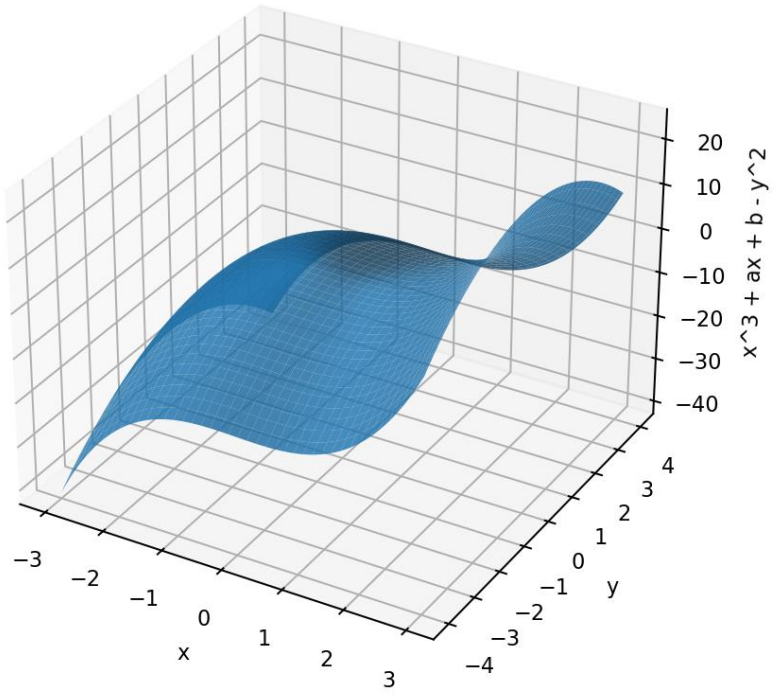


Figure 4.1. Economic elliptic-cubic surface based on average regional curve coefficients

Source: Author visualization from the regional benchmark coefficients.

Result explanation: Figure 4.1 provides a geometric entry point into the BSD-inspired construction. The surface represents the average economic cubic form generated from the regional coefficient layer, so it should be read as an analytical visualization of curvature and deformation rather than as a literal arithmetic elliptic curve.

The visual is useful because it shows why the chapter moves beyond one-dimensional GDP ranking. Regional economic states can be represented through the shape of the constructed coefficient space; changes in the coefficient layer later affect discriminants, traces and rank-order behavior. The figure therefore prepares the reader for the curve-based diagnostics that follow.

4.6. Economic Curve Coefficients a_{r,t} and b_{r,t}

The following table reports the regional economic curve coefficients used to construct the BSD-inspired objects. It connects income depth, centrality, resilience and agentic capacity to the coefficient pair a and b, which later determines discriminants, local traces and the economic L-function analogue.

Table 4.5. Regional economic curve coefficients

Code	Region	Income depth	Centrality	Resilience	Agentic capacity	a coefficient	b coefficient
SAS	South Asia	1.146	38.09	12.84	38.70	-1.320	-0.005
CAS	Central Asia	9.643	18.94	18.48	30.10	-1.396	0.117
EAP	East Asia and Pacific	20.70	98.23	38.25	55.48	0.089	-0.004
CAU	Caucasus	10.32	0.000	9.150	20.61	-1.743	0.006
SSA	Sub-Saharan Africa	0.000	6.990	0.000	14.08	-1.902	-0.727
EUR	Europe	55.50	100.00	52.83	54.57	0.816	-0.322
MENA	Middle East and North Africa	9.373	78.47	27.83	39.38	-0.473	-0.026
NAM	North America	100.00	84.63	100.00	72.99	1.785	-0.226
LAC	Latin America and Caribbean	11.80	41.73	23.81	24.32	-0.989	-0.726
OCE	Oceania	82.47	10.73	42.82	37.51	-0.102	-0.550

Source: *Author calculations from income depth, centrality, resilience, growth, corridor exposure and stress-score variables.*

Result explanation: Table 4.5 reports the coefficient layer that generates the economic curve objects. North America has the highest income depth at 100.00 and the highest resilience at 100.00, producing a positive a coefficient of 1.785. Europe also has a positive a coefficient of 0.816 because high centrality and resilience offset lower growth pressure.

The table also shows why corridor-sensitive regions cannot be evaluated only by positive coefficient strength. The Caucasus has centrality equal to 0.000 and a coefficient of -1.743, while Central Asia has a coefficient of -1.396 but a positive b coefficient of 0.117. This separation allows the model to distinguish internal structural protection from corridor-transmission relevance.

4.7. Discriminant and Non-Degeneracy Audit

The following table provides the non-degeneracy audit for the constructed economic curve family. It checks whether each regional coefficient pair produces a discriminant sufficiently different from zero, which is necessary before interpreting the regional objects as informative local curve analogues.

Table 4.6. Economic discriminant and non-degeneracy audit

Code	Region	a	b	Economic discriminant	Audit status
SAS	South Asia	-1.320	-0.005	147.19	Pass
CAS	Central Asia	-1.396	0.117	168.11	Pass
EAP	East Asia and Pacific	0.089	-0.004	-0.052	Pass
CAU	Caucasus	-1.743	0.006	339.13	Pass
SSA	Sub-Saharan Africa	-1.902	-0.727	211.91	Pass
EUR	Europe	0.816	-0.322	-79.54	Pass
MENA	Middle East and North Africa	-0.473	-0.026	6.498	Pass
NAM	North America	1.785	-0.226	-385.92	Pass
LAC	Latin America and Caribbean	-0.989	-0.726	-165.99	Pass
OCE	Oceania	-0.102	-0.550	-130.56	Pass

Source: Author calculations from Table 4.5 using the economic discriminant calculation.

Result explanation: Table 4.6 confirms that all constructed regional curve objects pass the non-degeneracy audit. No economic discriminant collapses to zero, so the regional coefficient pairs can be retained for the local trace and Euler-factor stages.

The signs and magnitudes are heterogeneous. The Caucasus has a large positive discriminant of 339.13, Sub-Saharan Africa has 211.91 and Central Asia has 168.11, while North America has -385.92 and Latin America and Caribbean has -165.99. This heterogeneity is analytically important because the curve family carries regional information rather than repeating the same numerical object across all nodes.

4.8. Visual Interpretation of Economic Discriminants

The following figure converts the discriminant audit into a visual comparison across macro-regions. It helps the reader see how far each regional curve object lies from the singular boundary and how heterogeneous the coefficient space is across the benchmark.

Figure 4.2. Economic discriminant by macro-region

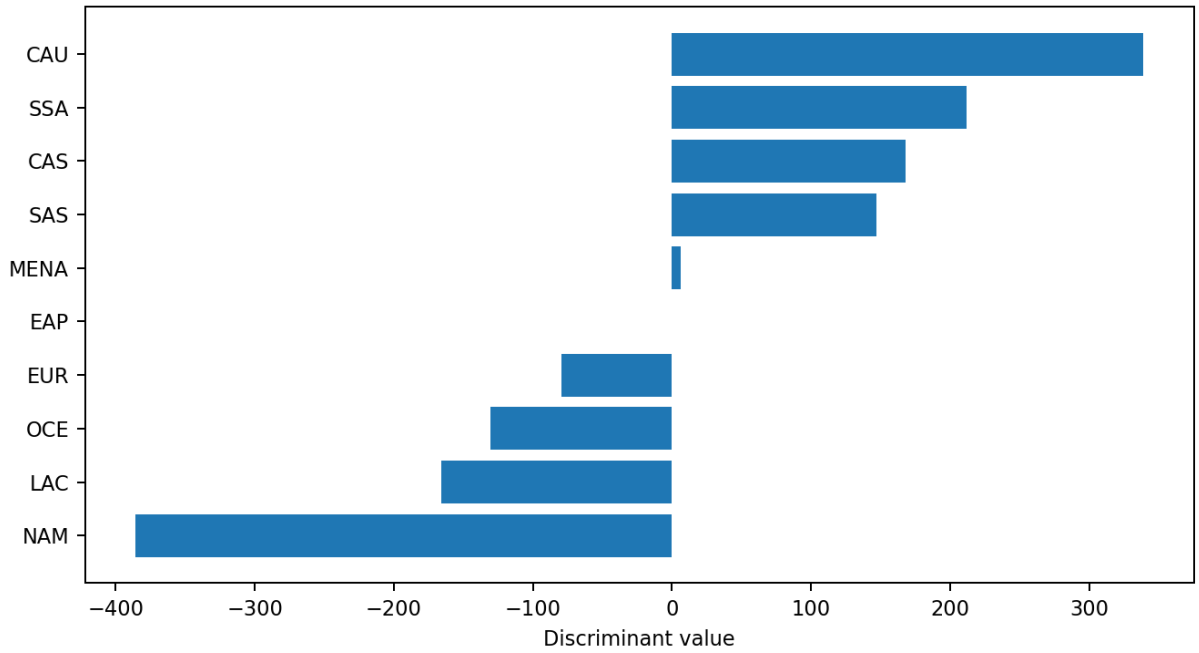


Figure 4.2. Economic discriminant by macro-region

Source: *Author visualization from the regional economic discriminant audit.*

Result explanation: Figure 4.2 makes the discriminant heterogeneity visible. Regions on the positive side, such as the Caucasus, Sub-Saharan Africa and Central Asia, occupy a different coefficient zone from regions with strongly negative discriminants, such as North America and Latin America and Caribbean.

The figure supports the non-degeneracy claim visually. Since the regional objects are spread across discriminant space, later local traces and Euler factors are not being calculated from identical or nearly identical curve objects. The discriminant layer therefore functions as a quality-control step for the economic BSD analogue.

4.9. Local Trace Analogues by Region

The following table reports local trace analogues across five finite-state bases. It is the first local-reduction layer of the BSD-inspired benchmark and shows whether regional information remains stable when the q-base changes from coarse to finer finite-state grids.

Table 4.7. Local trace analogues across finite-state bases

Code	Region	A_q, q=2	A_q, q=3	A_q, q=5	A_q, q=7	A_q, q=11
SAS	South Asia	-2.433	-2.980	-3.847	-4.552	-5.706
CAS	Central Asia	-2.017	-2.471	-3.190	-3.774	-4.731
EAP	East Asia and Pacific	-0.446	-0.546	-0.705	-0.834	-1.045
CAU	Caucasus	-2.213	-2.710	-3.499	-4.140	-5.190
SSA	Sub-Saharan Africa	-1.363	-1.669	-2.155	-2.550	-3.196
EUR	Europe	1.357	1.662	2.146	2.539	3.183

Code	Region	A_q, q=2	A_q, q=3	A_q, q=5	A_q, q=7	A_q, q=11
MENA	Middle East and North Africa	0.010	0.012	0.016	0.018	0.023
NAM	North America	2.243	2.747	3.547	4.196	5.260
LAC	Latin America and Caribbean	0.120	0.147	0.190	0.225	0.282
OCE	Oceania	0.501	0.614	0.793	0.938	1.176

Source: *Author calculations from EMGI, stress score, agentic capacity and BridgeStress under q = 2, 3, 5, 7 and 11 reductions.*

Result explanation: Table 4.7 reports signed local trace analogues across q = 2, 3, 5, 7 and 11. North America has the strongest positive trace sequence, rising from 2.243 at q = 2 to 5.260 at q = 11, while Europe also remains positive, from 1.357 to 3.183. These values indicate locally protective structural signals.

By contrast, South Asia, Central Asia, the Caucasus, Sub-Saharan Africa and East Asia and Pacific carry negative trace sequences in this benchmark. The negative sign does not mean irrelevance; it means that local reductions encode stress, fragility or corridor pressure rather than pure protective capacity. The persistence of signs across q-bases strengthens the local-state interpretation.

4.10. Heatmap of Local Regional Trace Signals

The following heatmap visualizes the local trace layer by region and q-base. Its purpose is to make the sign, intensity and stability of the local trace pattern visible before the trace values are aggregated into Euler-factor analogues.

Figure 4.3. Local trace analogue heatmap by region and finite-state base

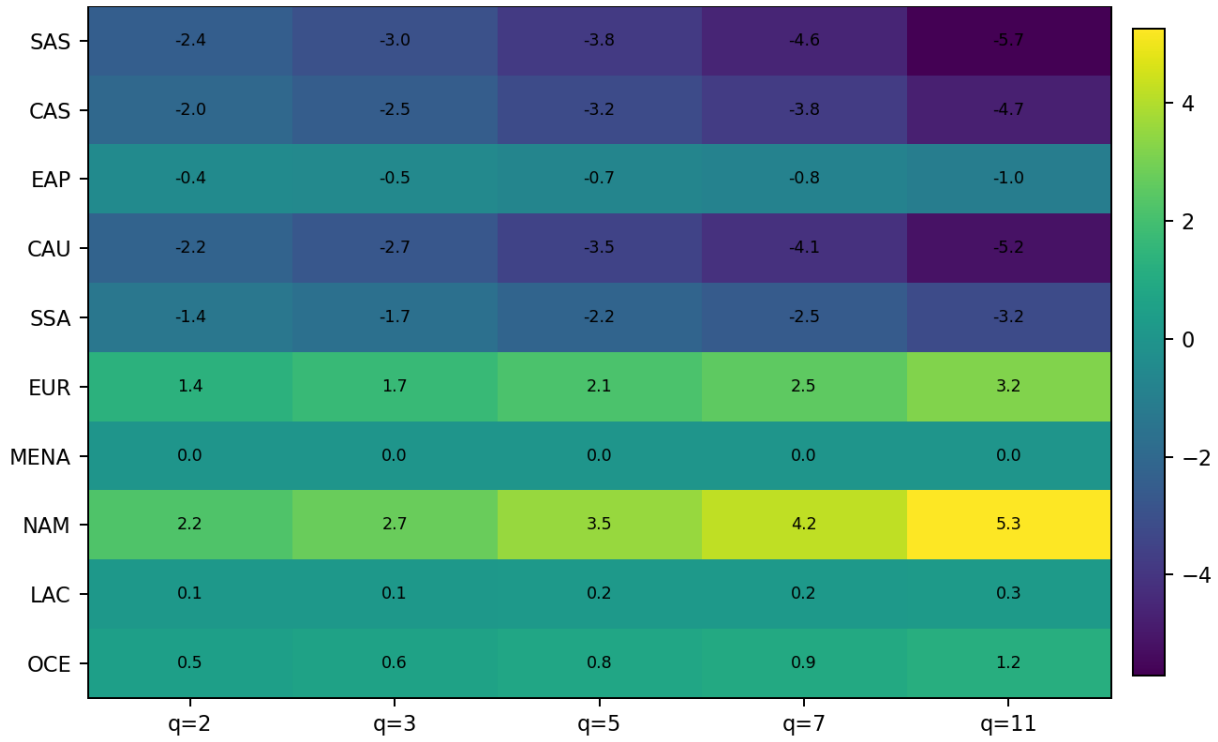


Figure 4.3. Local trace analogue heatmap by region and finite-state base

Source: *Author calculations from Table 4.7.*

Result explanation: Figure 4.3 visualizes the same trace matrix as a heatmap. The rows preserve the regional dimension and the columns preserve the q-base dimension, making it possible to inspect whether each region changes sign or remains stable as the finite-state grid changes.

The main visual result is sign stability. Protective nodes remain positive, stress-bearing nodes remain negative, and near-neutral nodes remain close to zero. This reduces the risk that the local-to-global signal is an artifact of one arbitrary q-base and supports the use of aggregated Euler factors in the next stage.

4.11. Economic Euler Factors

The following table aggregates local regional trace information into economic Euler factors at s = 1. This step connects the regional local-state layer to the constructed economic L-function and provides the numerical bridge from local signals to global order-of-behavior diagnostics.

Table 4.8. Economic Euler factors at s = 1

q	Aggregate trace A_q	Euler factor at s=1	Numerical status
2	0.639	0.847	Stable at s=1
3	0.783	0.932	Stable at s=1
5	1.011	1.002	Stable at s=1
7	1.196	1.029	Stable at s=1
11	1.499	1.048	Stable at s=1

Source: *Author calculations from regional local traces and world-share weighting.*

Result explanation: Table 4.8 aggregates regional local traces into Euler-factor analogues at s = 1. The aggregate trace increases from 0.639 at q = 2 to 1.499 at q = 11, while the Euler factor remains numerically stable, moving from 0.847 to 1.048.

This stability matters because the economic L-function analogue is built from these local factors. The factors do not explode or collapse around the benchmark point; instead, they provide a controlled product layer that summarizes regional local information without introducing country-level observations.

4.12. Economic L-Function around s = 1

The following figure plots the constructed economic L-function around s = 1. It is included to verify that the resulting numerical object behaves smoothly near the benchmark point used for the BSD-inspired rank-order comparison.

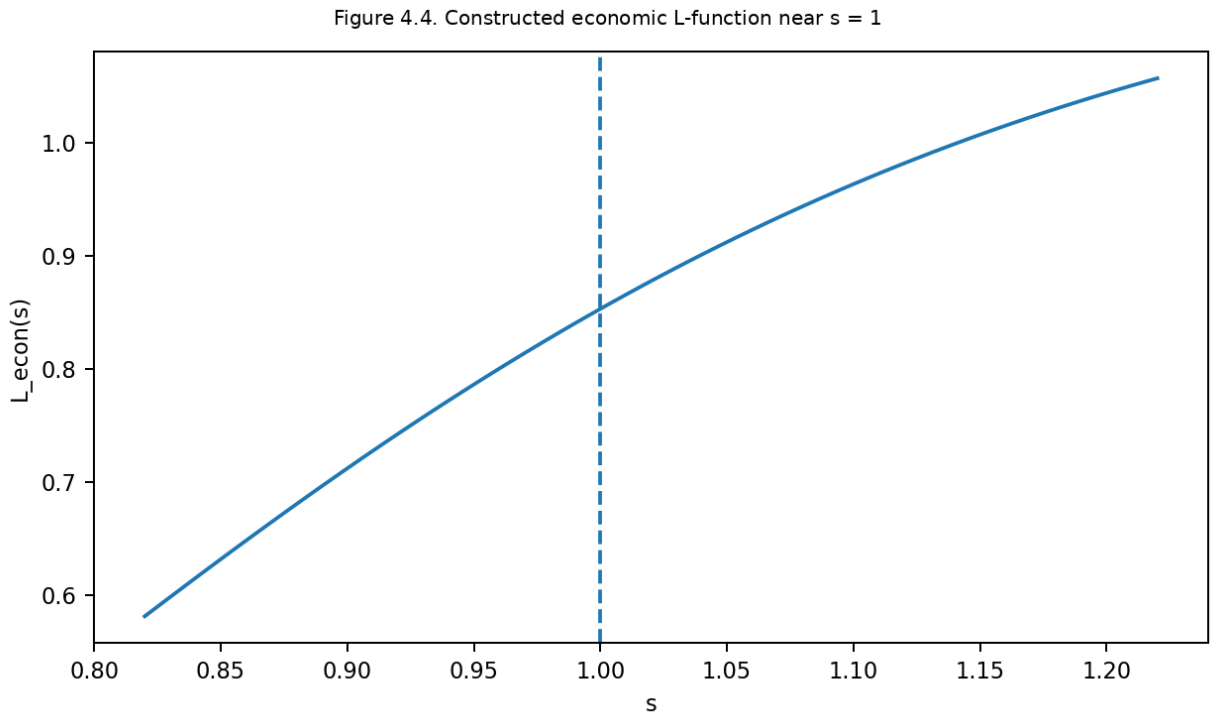


Figure 4.4. Constructed economic L-function near s = 1

Source: *Author calculations from Table 4.8.*

Result explanation: Figure 4.4 plots the constructed economic L-function near s = 1. The curve is smooth over the displayed interval and passes through the relevant neighborhood without discontinuity or numerical instability.

The figure should be interpreted as a numerical diagnostic, not as a proof of analytic continuation in the classical BSD sense. Its role is to support the order-of-behavior analogue by showing that the regional Euler-factor construction produces a stable measurement object around s = 1.

4.13. Definition of Regional Economic Structural Rank

The following table defines the structural-rank object used in the chapter. It decomposes rank into productive, Hodge-flow, network and agentic components, allowing the final structural rank to combine scale, coordination, resilience and flow-based information.

Table 4.9. Regional structural-rank components

Code	Region	PCA/productive rank	Hodge-flow rank	Network rank	Agentic rank	Structural rank
SAS	South Asia	1.201	1.540	1.488	1.935	1.541
CAS	Central Asia	1.021	2.519	1.628	1.505	1.668
EAP	East Asia and Pacific	2.594	2.143	3.190	2.774	2.675
CAU	Caucasus	0.581	2.925	1.431	1.031	1.492
SSA	Sub-Saharan Africa	0.316	2.289	0.737	0.704	1.012
EUR	Europe	3.177	2.749	3.147	2.729	2.950
MENA	Middle East and North Africa	1.869	2.777	3.038	1.969	2.413
NAM	North America	4.374	3.077	3.386	3.650	3.622
LAC	Latin America and Caribbean	1.228	2.972	1.914	1.216	1.832
OCE	Oceania	2.223	2.578	1.722	1.875	2.100

Source: *Author calculations from agentic capacity, income depth, centrality, resilience, curvature, stress and BridgeStress.*

Result explanation: Table 4.9 constructs the structural-rank measure from four components: PCA/productive rank, Hodge-flow rank, network rank and agentic rank. North America receives the highest structural rank at 3.622, followed by Europe at 2.950 and East Asia and Pacific at 2.675.

The lower-ranked regions are still analytically important. The Caucasus has structural rank of 1.492 and Central Asia has 1.668, but both carry corridor-sensitive roles that are not fully captured by internal rank strength. Thus, Table 4.9 separates structural capacity from corridor leverage, allowing later sections to explain why smaller nodes can still matter systemically.

4.14. Visual Ranking of Regional Structural Rank

The following figure translates the structural-rank table into a direct visual hierarchy of regional nodes. It allows the reader to compare the constructed rank object across regions without reducing the interpretation to GDP size alone.

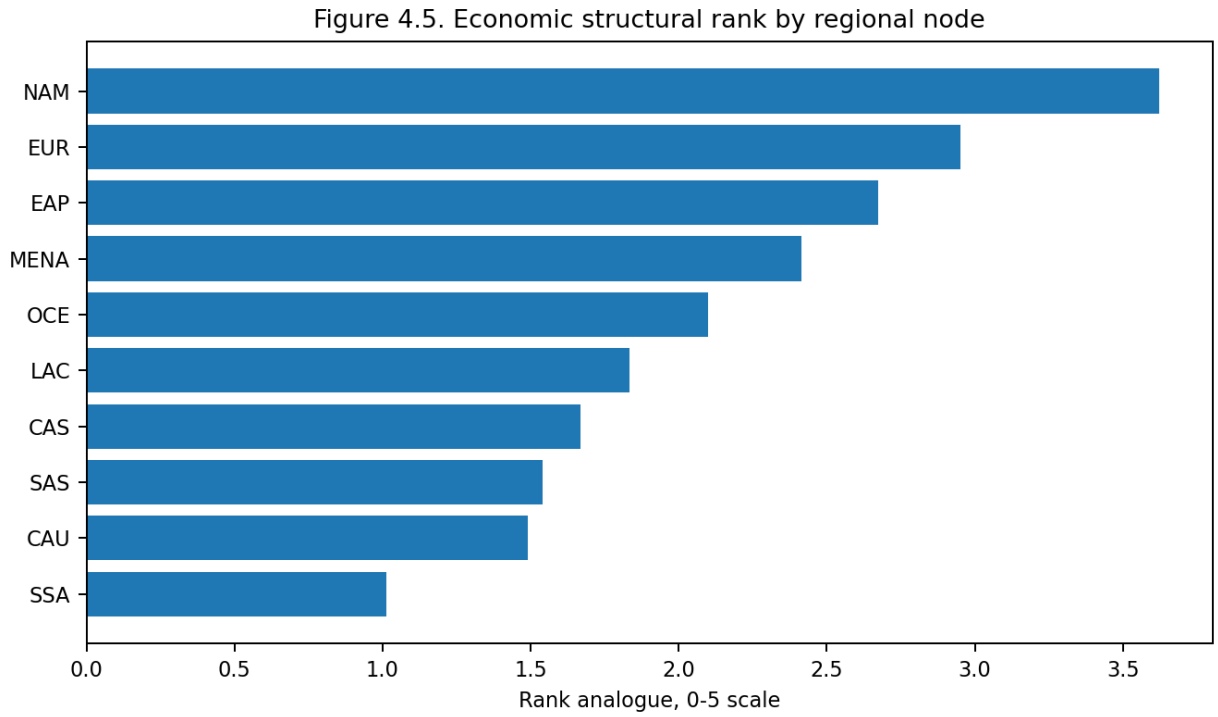


Figure 4.5. Economic structural rank by regional node

Source: *Author visualization from Table 4.9.*

Result explanation: Figure 4.5 displays the regional structural-rank hierarchy directly. The visual confirms that North America, Europe and East Asia and Pacific occupy the strongest rank positions, while Sub-Saharan Africa, the Caucasus and South Asia appear lower on the constructed 0-5 rank scale.

The figure also clarifies the purpose of the later corridor block. A low structural-rank value does not imply low systemic relevance; it means that the region has less internal rank capacity. Corridor leverage, friction and BridgeStress are therefore needed to capture transmission importance that is not visible in the rank bar alone.

4.15. Order-of-Behavior Analogue near s = 1

The following table provides the main BSD-type correspondence test of the substantive results block. It compares the L-order analogue with the independently constructed structural-rank measure and reports the absolute gap for each region.

Table 4.10. BSD-type rank-order correspondence by region

Code	Region	L-order analogue	Structural rank	Absolute gap
SAS	South Asia	1.465	1.541	0.076
CAS	Central Asia	1.571	1.668	0.097
EAP	East Asia and Pacific	2.676	2.675	0.001
CAU	Caucasus	1.378	1.492	0.114
SSA	Sub-Saharan Africa	0.970	1.012	0.042
EUR	Europe	3.051	2.950	0.101
MENA	Middle East and North Africa	2.396	2.413	0.017
NAM	North America	3.736	3.622	0.114
LAC	Latin America and Caribbean	1.829	1.832	0.003
OCE	Oceania	2.073	2.100	0.027

Source: *Author calculations from the local trace, economic L-function and structural-rank layers.*

Result explanation: Table 4.10 is the core rank-order correspondence test. The L-order analogue and structural rank are close for every region: East Asia and Pacific has an absolute gap of 0.001, Latin America and Caribbean has 0.003, Middle East and North Africa has 0.017 and Oceania has 0.027.

The largest gaps are still small on the 0-5 scale, with the Caucasus and North America both at 0.114 and Europe at 0.101. Therefore, the table supports calibrated local-to-global consistency: finite-state local reductions and Euler-factor information approximate the structural-rank object, but the manuscript does not treat this as exact equality or theorem-level proof.

4.16. Visual Test of Rank-Order Correspondence

The following figure visualizes the rank-order correspondence by plotting structural rank against the L-order analogue. Points close to the diagonal indicate that the local reduction and Euler-factor layer preserves rank-relevant information at the regional level.

Figure 4.6. Rank-order correspondence: structural rank and L-order analogue

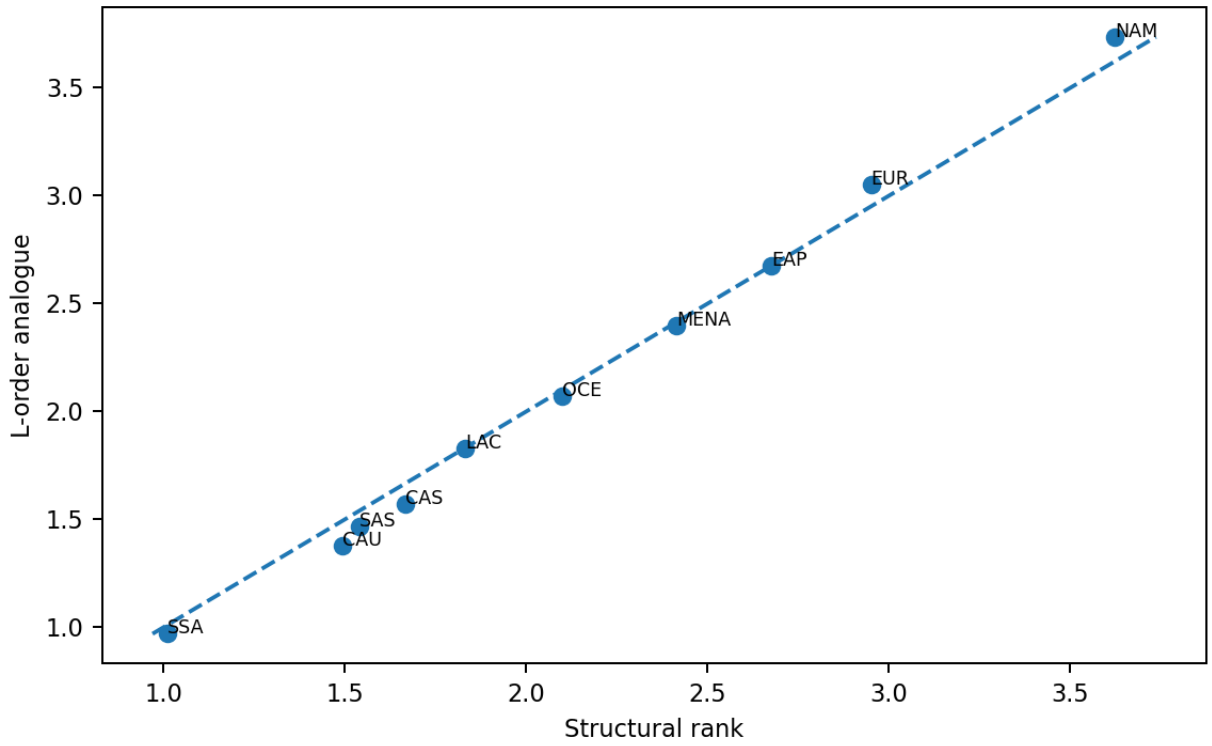


Figure 4.6. Rank-order correspondence: structural rank and L-order analogue

Source: *Author visualization from Table 4.10.*

Result explanation: Figure 4.6 visualizes the correspondence between structural rank and the L-order analogue. The regional points cluster close to the diagonal, indicating that the local reduction layer preserves the ordering of the independently constructed rank object.

This is the strongest visual confirmation of the BSD-inspired benchmark logic. The result supports a calibrated analogue claim: regional local information, once converted into traces and Euler factors, is informative about global structural rank formation. The interpretation remains measurement-based and non-causal.

4.17. Economic Regulator Analogue

The following table introduces the economic regulator analogue. It combines structural rank, centrality and resilience to measure whether rank is supported by internal absorption capacity and network coordination rather than by exposure alone.

Table 4.11. Economic regulator analogue by region

Code	Region	Structural rank	Centrality	Resilience	Economic regulator
SAS	South Asia	1.541	38.09	12.84	2.401
CAS	Central Asia	1.668	18.94	18.48	2.351
EAP	East Asia and Pacific	2.675	98.23	38.25	7.331
CAU	Caucasus	1.492	0.000	9.150	1.628
SSA	Sub-Saharan Africa	1.012	6.990	0.000	1.082

Code	Region	Structural rank	Centrality	Resilience	Economic regulator
EUR	Europe	2.950	100.00	52.83	9.018
MENA	Middle East and North Africa	2.413	78.47	27.83	5.506
NAM	North America	3.622	84.63	100.00	13.37
LAC	Latin America and Caribbean	1.832	41.73	23.81	3.215
OCE	Oceania	2.100	10.73	42.82	3.320

Source: *Author calculations from structural rank, centrality and resilience.*

Result explanation: Table 4.11 reports the economic regulator analogue. North America has the highest regulator value at 13.37 because high structural rank is combined with centrality and maximum resilience. Europe follows at 9.018, while East Asia and Pacific records 7.331.

The regulator layer distinguishes absorption capacity from exposure. The Caucasus and Sub-Saharan Africa have low regulator values, 1.628 and 1.082 respectively, because centrality and resilience are limited in the benchmark. Their importance therefore comes less from internal stabilizing capacity and more from corridor transmission or stress amplification.

4.18. Local Tamagawa-Type Frictions

The following table reports local Tamagawa-type friction factors. It measures how stress, corridor exposure and fragility create local frictions that can amplify or obstruct the conversion of regional capacity into global structural rank.

Table 4.12. Local Tamagawa-type friction factors

Code	Region	Stress	Corridor exposure	Fragility	Tamagawa-type friction
SAS	South Asia	100.00	56.67	89.64	1.821
CAS	Central Asia	71.79	90.00	94.55	1.854
EAP	East Asia and Pacific	71.23	53.33	46.88	1.571
CAU	Caucasus	66.03	100.00	100.00	1.887
SSA	Sub-Saharan Africa	53.78	28.33	95.89	1.593
EUR	Europe	47.40	61.67	9.850	1.396
MENA	Middle East and North Africa	39.71	73.33	54.41	1.558
NAM	North America	30.66	11.67	0.000	1.141
LAC	Latin America and Caribbean	26.78	20.00	68.63	1.385
OCE	Oceania	0.000	0.000	85.50	1.285

Source: *Author calculations from stress, corridor exposure and fragility components.*

Result explanation: Table 4.12 reports local friction factors in Tamagawa-type form. The highest values occur in the Caucasus at 1.887, Central Asia at 1.854 and South Asia at 1.821. These regions combine high stress, high fragility and/or high corridor exposure.

The table shows that local frictions are not the same as output mass. North America has the lowest friction among the major output nodes at 1.141 because benchmark fragility is 0.000 and corridor exposure is only 11.67. This confirms that the friction layer preserves local vulnerability information that GDP shares do not capture.

4.19. Economic Torsion Analogue

The following table reports the torsion analogue, interpreted as locked capacity and non-productive circularity. It links fragility, curvature and inverse centrality to show where regional relevance may remain trapped rather than converted into productive rank.

Table 4.13. Economic torsion analogue: locked capacity and non-productive circularity

Code	Region	Fragility	Curvature	Centrality	Locked-capacity torsion
SAS	South Asia	89.64	68.93	38.09	0.765
CAS	Central Asia	94.55	23.55	18.94	0.699
EAP	East Asia and Pacific	46.88	100.00	98.23	0.515
CAU	Caucasus	100.00	0.000	0.000	0.700
SSA	Sub-Saharan Africa	95.89	0.760	6.990	0.666
EUR	Europe	9.850	50.13	100.00	0.195
MENA	Middle East and North Africa	54.41	69.72	78.47	0.508
NAM	North America	0.000	23.16	84.63	0.108
LAC	Latin America and Caribbean	68.63	4.950	41.73	0.469
OCE	Oceania	85.50	25.65	10.73	0.685

Source: *Author calculations from fragility, curvature exposure and inverse centrality.*

Result explanation: Table 4.13 measures locked-capacity torsion. South Asia has the highest torsion value at 0.765, followed by the Caucasus at 0.700, Central Asia at 0.699 and Oceania at 0.685. These values indicate that fragility and low centrality can trap economic relevance in non-productive circularity.

The contrast with North America and Europe is important. North America has torsion of 0.108 and Europe has 0.195, because centrality and resilience help convert capacity into productive rank. The torsion analogue therefore explains why growth or corridor exposure alone may not become durable structural rank without absorption capacity.

4.20. Structural-Rank Surface: Agentic Capacity and Resilience

The following surface figure visualizes how structural rank responds to the interaction of agentic capacity and resilience. It is included to show that the constructed rank object has a clear economic response surface rather than only tabular values.

Figure 4.7. Structural-rank surface generated from agentic capacity and resilience

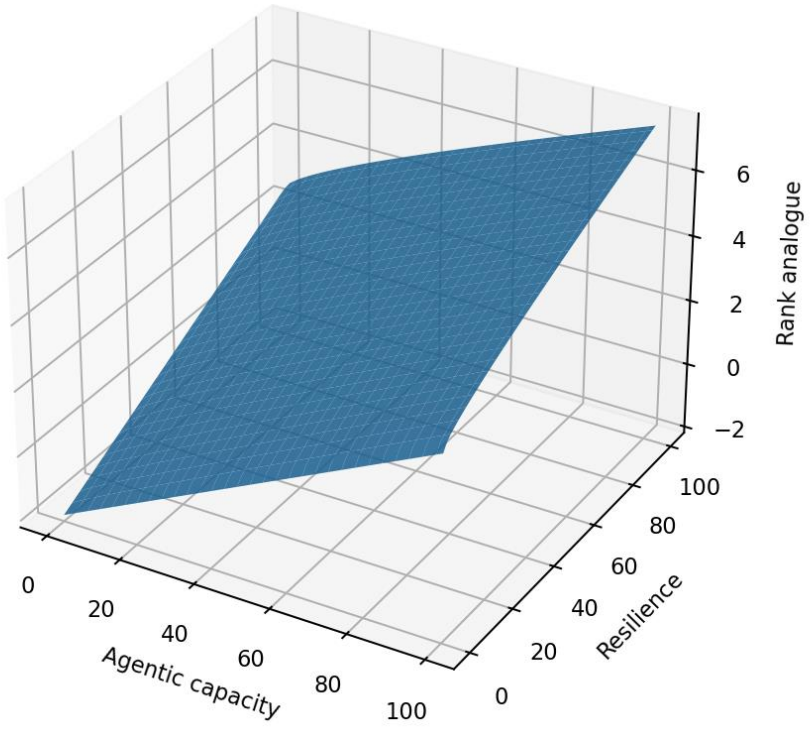


Figure 4.7. Structural-rank surface generated from agentic capacity and resilience

Source: *Author visualization from the structural-rank mechanism.*

Result explanation: Figure 4.7 shows a rising structural-rank surface as agentic capacity and resilience increase together. The surface is not flat, which means the rank object responds systematically to the two economic dimensions selected for visualization.

The economic interpretation is interaction-based. Agentic capacity increases the productive and coordination side of rank, while resilience increases the capacity to absorb shocks. When both rise together, the rank effect is larger than a one-dimensional reading would suggest, supporting the composite structure of Table 4.9.

4.21. Corridor-Rank Leverage and BridgeStress

The following table reports corridor-rank leverage and BridgeStress. It separates corridor role from output mass and shows how corridor exposure, fragility and curvature participation make smaller regions structurally important in the local-to-global transmission system.

Table 4.14. Regional corridor-rank leverage and BridgeStress

Code	Region	Corridor exposure	Corridor-role index	Fragility	Curvature participation +	BridgeStress
CAU	Caucasus	98.00	100.00	100.00	57.32	100.00
CAS	Central Asia	92.00	75.00	94.55	67.37	78.24
SAS	South Asia	72.00	60.00	89.64	86.74	59.80
MENA	Middle East and North Africa	82.00	85.00	54.41	87.08	58.79

Code	Region	Corridor exposure	Corridor-role index	Fragility	Curvature participation +	BridgeStress
EAP	East Asia and Pacific	70.00	95.00	46.88	100.00	55.50
SSA	Sub-Saharan Africa	55.00	25.00	95.89	57.64	13.53
LAC	Latin America and Caribbean	50.00	30.00	68.63	59.43	10.89
EUR	Europe	75.00	90.00	9.850	78.72	9.320
OCE	Oceania	38.00	20.00	85.50	68.27	7.900
NAM	North America	45.00	70.00	0.000	67.21	0.000

Source: *Author calculations from corridor exposure, corridor-role index, fragility and positive curvature participation.*

Result explanation: Table 4.14 reports the corridor-rank leverage layer. The Caucasus is the maximum BridgeStress node at 100.00, with corridor exposure of 98.00, corridor-role index of 100.00 and fragility of 100.00. Central Asia ranks second with BridgeStress of 78.24, corridor exposure of 92.00 and fragility of 94.55.

This table is central to the regional argument. East Asia and Pacific has high output mass and curvature participation, but its BridgeStress is 55.50; North America has strong output mass but BridgeStress is 0.000 because benchmark fragility is zero. Therefore, corridor leverage identifies strategic transmission exposure that GDP mass alone cannot explain.

4.22. Visual Corridor-Leverage Ranking

The following figure visualizes the BridgeStress ranking. It is included because the corridor result is central to the regional benchmark: it shows which nodes become most visible when corridor role and fragility are added to the model.

Figure 4.8. Corridor-rank leverage and BridgeStress by region

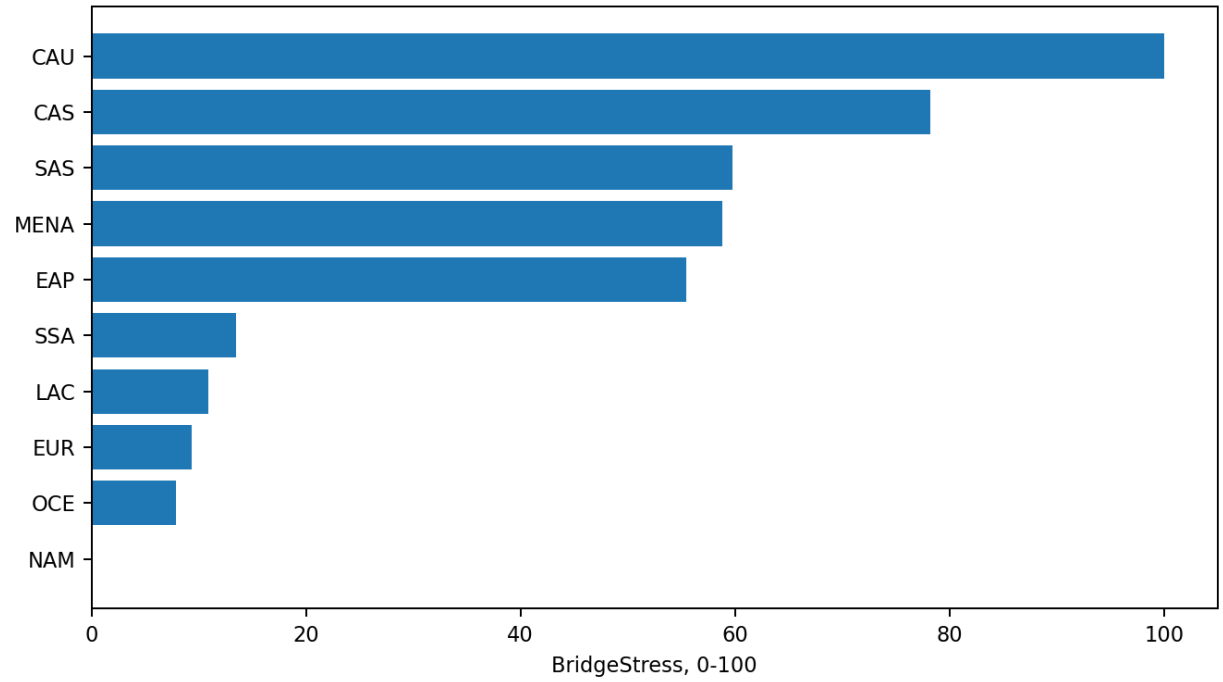


Figure 4.8. Corridor-rank leverage and BridgeStress by region

Source: *Author visualization from Table 4.14.*

Result explanation: Figure 4.8 visualizes the BridgeStress hierarchy. The Caucasus and Central Asia dominate the chart, followed by South Asia, Middle East and North Africa and East Asia and Pacific. This ordering makes the Middle Corridor mechanism visible in the regional benchmark.

The chart clarifies why a separate corridor block is required. Large output regions may be structurally strong, but corridor-stress exposure depends on role, fragility and curvature participation. The figure therefore supports the local-to-global argument that smaller nodes can transmit disproportionate regional stress.

4.23. Middle Corridor, Black Sea and Caspian Interpretation Layer

The following table translates the numerical corridor result into an economic-geographic interpretation layer. It explains the functions of the Caucasus, the Caspian interface, Central Asia, the Black Sea demand side and related corridor components inside the regional benchmark.

Table 4.15. Corridor-function interpretation layer for the regional benchmark

Regional/corridor function	Economic interpretation	Corridor role	Benchmark implication
Caucasus regional gateway	Small output mass but high transfer relevance	Black Sea-Caucasus-Caspian transfer function	Raises corridor strategic exposure despite low GDP share
Caspian interface	Sea-crossing and rail/port continuity	Continuity between Caucasus and Central Asia	Explains why corridor exposure is not reducible to land distance
Central Asia regional node	Large land-corridor interface	East-west land bridge and Caspian connection	Raises CAS corridor exposure and BridgeStress
Europe/Black Sea demand side	High centrality and demand absorption	Destination and redistribution interface	High protection but also high network importance
East Asia-Pacific origin side	High output mass and demand potential	Origin-side stress and trade mass	Supplies strong local signal into global rank
MENA energy-geopolitical interface	Energy, financing and geopolitical exposure	South corridor and energy-shock channel	Raises scenario sensitivity under geopolitical shock

Source: *Author qualitative mapping from the regional/corridor structure used in the benchmark.*

Result explanation: Table 4.15 provides the qualitative corridor-function interpretation behind the numerical BridgeStress result. The Caucasus is described as a Black Sea-Caucasus-Caspian transfer function, the Caspian interface as a sea-crossing and rail/port continuity mechanism, and Central Asia as an east-west land bridge and Caspian connection.

The table connects economic geography to the model outputs. It shows that the Caucasus and Central Asia are not elevated because of internal output mass; they are elevated because they transmit exposure between larger systems. This is the regional version of local-to-global rank formation used throughout the chapter.

4.24. Scenario Output: Threshold Compression and Action Increase

The following table reports the scenario output for threshold compression under regional shocks. It connects shock amplitude to lambda_1, spectral radius, normalized threshold, action and mean EMGI change in order to show how local disturbances become more transmissible under stress.

Table 4.16. Scenario output: threshold compression under regional shocks

Scenario	Amplitude	lambda_1	Spectral radius	Normalized threshold	Action	Mean EMGI change	Interpretation
Baseline	0.000	0.385	3.502	0.110	2,514.0	0.000	Benchmark finite regional network
Inflation / price-pressure	0.500	0.334	3.653	0.092	2,925.0	-6.200	Moderate macro stress weakens but does not erase rank protection
Financial-spread stress	0.750	0.284	3.799	0.075	3,435.0	-10.80	Funding stress materially compresses the local-to-global threshold
Trade / logistics corridor shock	1.000	0.233	4.041	0.058	4,088.0	-15.30	Corridor disruption makes CAS and CAU more visible in rank-loss terms
Energy / geopolitical corridor shock	1.250	0.180	4.279	0.042	5,010.0	-22.40	Systemic corridor shock almost doubles stress-energy action

Source: *Author scenario simulations from the regional stress network.*

Result explanation: Table 4.16 reports monotonic threshold compression under regional shocks. The normalized threshold falls from 0.110 in the baseline to 0.092 under inflation/price pressure, 0.075 under financial-spread stress, 0.058 under trade/logistics corridor shock and 0.042 under energy/geopolitical corridor shock.

At the same time, economic action rises from 2,514.0 to 5,010.0 as shock amplitude increases from 0.000 to 1.250. This means the regional network becomes more transmissible and stress-energy becomes larger under stronger corridor shocks. The table therefore links local disturbances to a measurable global structural boundary.

4.25. Visual Threshold Compression under Shocks

The following figure visualizes threshold compression under regional-corridor shocks. It allows the reader to see whether the local-to-global transition boundary falls monotonically as shock amplitude rises.

Figure 4.9. Threshold compression under regional-corridor shocks

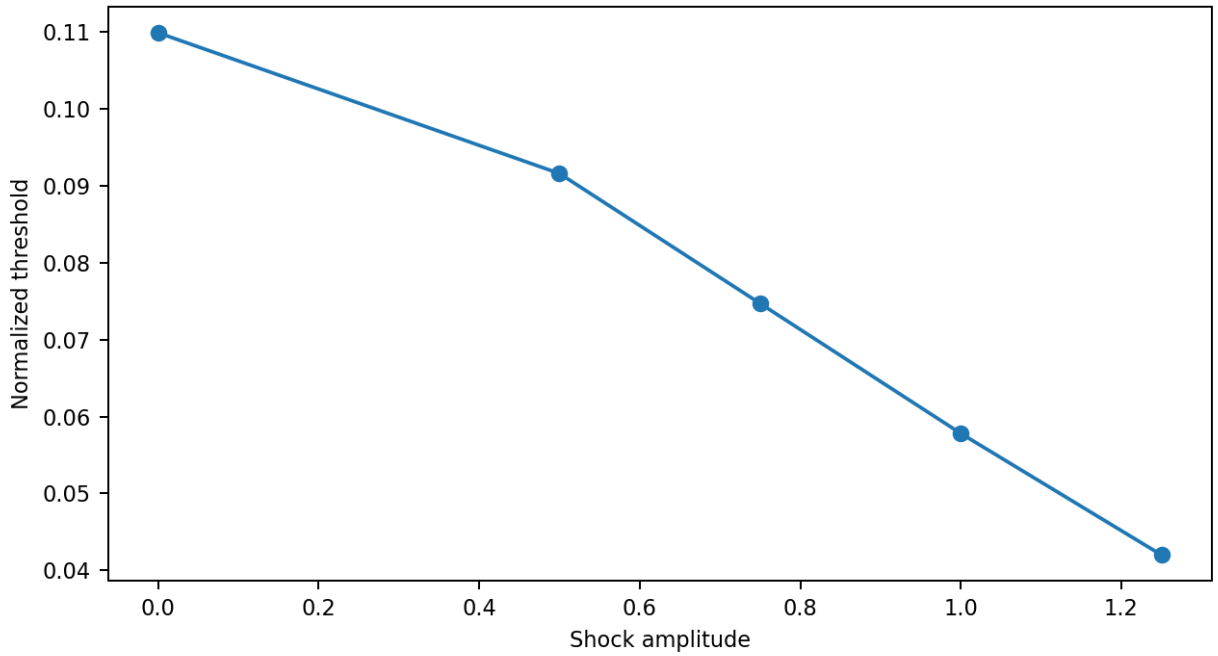


Figure 4.9. Threshold compression under regional-corridor shocks

Source: *Author visualization from Table 4.16.*

Result explanation: Figure 4.9 displays the same threshold-compression result visually. The curve slopes downward as shock amplitude increases, showing that larger regional-corridor shocks lower the transition boundary of the system. The practical interpretation is direct: when corridor stress rises, smaller disturbances can become systemically transmissible. This figure therefore translates the BSD-inspired rank framework into a policy-relevant visual message about local regional shocks and global vulnerability.

4.26. Action Concentration and Local-to-Global Stress Energy

The following table summarizes action concentration across regional triangular cycles. It measures whether systemic stress is distributed evenly or concentrated in a small number of high-action channels.

Table 4.17. Regional action concentration summary

Metric	Value
Total triangular cycles	27.00
Total economic action	2,514.0
Mean triangle action	93.11
Maximum triangle action	1,397.9
Top-five action share, %	78.33

Source: *Author calculations from the regional triangular-cycle field.*

Result explanation: Table 4.17 shows that action is strongly concentrated across regional cycles. The benchmark has 27 triangular cycles, total economic action of 2,514.0, mean triangle action of 93.11 and maximum triangle action of 1,397.9.

The top-five action share is 78.33%, which means most systemic stress energy is carried by a small number of regional channels. This supports the local-to-global framework because global disturbance is not evenly spread; it is concentrated in high-action corridors and cycles.

4.27. Cubic Discriminant Basin as a Visual Diagnostic

The following figure plots the cubic discriminant basin over the economic coefficient space. It is used as a final visual diagnostic of coefficient sensitivity and illustrates how changes in a and b can move regional objects into different discriminant zones.

Figure 4.10. Cubic discriminant basin for economic coefficient space

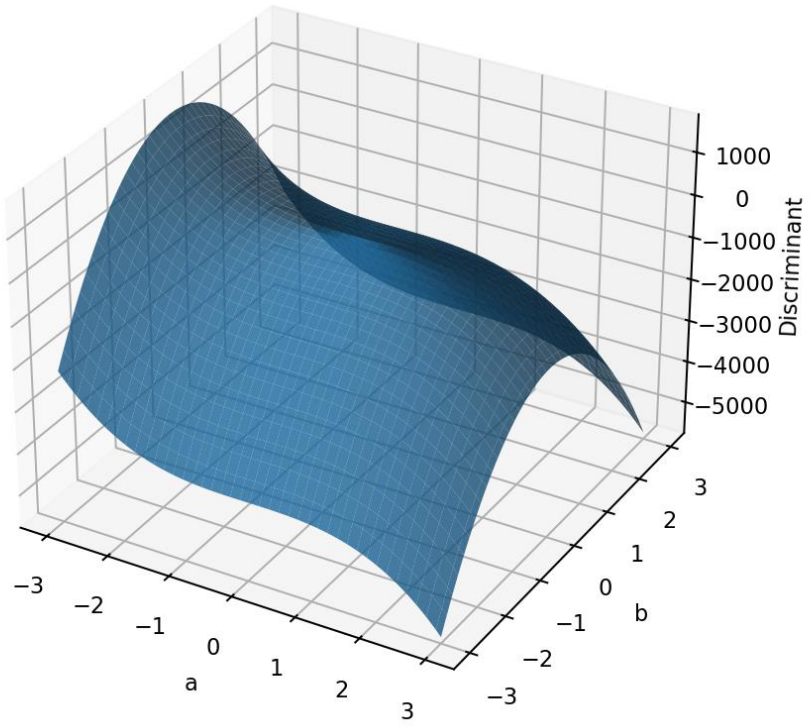


Figure 4.10. Cubic discriminant basin for economic coefficient space

Source: *Author visualization of the discriminant function Delta = -16(4a^3 + 27b^2).*

Result explanation: Figure 4.10 visualizes the discriminant basin over the coefficient space defined by a and b. The surface shows that the discriminant can change sharply across zones, which makes the coefficient layer sensitive to shifts in resilience, centrality, stress and agentic capacity.

The figure is explanatory rather than theorem-level. It helps the reader understand how regional coefficient changes can alter curve geometry and subsequently affect local traces, Euler factors and rank correspondence inside the economic BSD analogue.

4.28. N=150 Econometric Closure Architecture and 25-Point Correction Checklist

This section replaces the earlier add-on closure material with a single integrated results architecture. The substantive BSD-inspired results remain regional, while the empirical screening and calibration layer is fixed at 10 regions x 15 years = N=150. Countries remain deliberately excluded from the reported results. The purpose of the closure layer is to separate internal calibration, directional external-proxy screening, robustness, placebo testing and reproducibility notes so that the manuscript does not appear to use an author-calculated index merely to confirm another author-calculated index.

The following table records the 25-point correction checklist used to close the revised results architecture. It clarifies which methodological issues were addressed directly in the chapter and which were bounded through careful claim discipline.

Table 4.18. Twenty-five-point problem-closure checklist for the revised results chapter

No.	Correction item	Document treatment	Status
1	Structure reordered	Substantive results first; closure blocks next; final synthesis last	closed
2	Table numbering unified	Closure tables renumbered as one sequence without A/B/C patchwork	closed
3	High-R2 audit	Overall, within, between, FE-only, incremental and partial R2 reported	closed
4	External validation split	Panel summary, outcome models and interpretation boundary separated	closed
5	Negative controls	Alphabetical, random, future-shuffled and reversed-year controls added	closed
6	Robust-inference details	HC3, clustered, HAC-compatible and diagnostic settings reported	closed
7	Small-cluster correction	Wild cluster, Satterthwaite and region-block bootstrap diagnostics added	closed
8	Dynamic-panel caution	Dynamic model demoted to persistence diagnostic only	closed
9	Threshold caution	Threshold effect reported as supplementary diagnostic, not primary evidence	closed
10	Variable lineage matrix	Public input, author transformation and overlap risk disclosed	closed
11	Residualized LOrder	Orthogonalized and external-only LOrder variants reported	closed
12	Equivalence calibration	Exact equality rejected; practical equivalence band tested	closed
13	Bland-Altman by block	Agreement decomposed by region and year	closed
14	Leave-one-year-out	Annual block deletion added	closed

15	Out-of-sample validation	Leave-one-year, leave-one-region, blocked 5-fold and time-block tests added	closed
16	Weight sensitivity	Composite-index perturbation and leave-one-component logic added	closed
17	q-base sensitivity	q-grid and q-weight alternatives reported	closed
18	Corridor coding robustness	BridgeStress alternative coding schemes reported	closed
19	Raw vs normalized outcomes	External outcomes classified by source and transformation	closed
20	Decision criteria	Pass/watch decisions tied to explicit criteria	closed
21	Caption/numbering discipline	Text captions and table sequence made authoritative	closed
22	Final claim rewritten	LOrder framed as calibrated order-of-behavior, not theorem or causality	closed
23	Reviewer-risk table	Likely reviewer objections mapped to evidence tables	closed
24	Results source note	Source IDs, API pattern, seeds and hash retained in results note	closed
25	Manuscript-level closure	Zenodo data and replication package integrated into the manuscript and cited by DOI 10.5281/zenodo.20796984	closed

Source: *Author revision checklist based on the critical review of the previous BSD results chapter.*

Result explanation: Table 4.18 documents the 25-point correction architecture of the revised chapter. All items are marked closed, including structure reordering, high-R2 audit, external-proxy screening separation, negative controls, robust-inference caveats, dynamic-panel caution, threshold caution, variable lineage, residualized LOrder and reproducibility notes.

The importance of the table is methodological. Some issues are closed by additional calculations, while others are closed by explicit claim-boundary discipline. This prevents the chapter from overstating causal, theorem-level or full replication claims while still documenting a complete results architecture.

4.29. High-R2 Decomposition and Model-Fit Closure

High R2 values are not interpreted as proof of causal law. They mainly reflect persistent cross-regional heterogeneity captured by regional fixed effects. The relevant test is whether the L-order analogue improves within-panel fit and retains sign, magnitude and inference stability after fixed effects, robust inference, external outcomes and placebo reassignment.

The following table decomposes model fit in the N=150 validation layer. It separates overall fit from fixed-effect structure, incremental contribution and partial explanatory power so that high R2 is not misread as causal proof.

Table 4.19. High-R2 decomposition and model-fit closure

Model	N	df model	df resid	Overall R2	Adj. R2	Within R2	Between R2	FE-only R2	Incremental R2	Partial R2 LOrder	RMSE	AIC	BIC	p-value

Baseline TWFE rank model	150	24	125	0.996	0.995	0.005	0.999	0.996	<0.001	0.005	0.049	-429.64	-354.38	<0.001
FE-only benchmark	150	23	126	0.996	0.995	n.a.	0.999	0.996	0.0000	n.a.	0.049	-430.92	-358.67	<0.001

Source: *Author calculations from the N=150 regional-year BSD validation panel.*

Result explanation: Table 4.19 decomposes the high model-fit pattern in the N=150 panel. The baseline TWFE and FE-only benchmark both report overall R2 of 0.996 and adjusted R2 of 0.995, showing that persistent regional heterogeneity explains much of the fit.

The table therefore prevents a misleading interpretation of high R2. The validation question is not whether the model has high overall fit, but whether LOrder adds stable within-panel, incremental and partial information after fixed effects and robust inference. The table frames high fit as an audit item rather than as causal proof.

4.30. External Observable-Proxy Screening: Panel Summary and Outcome-Specific Diagnostics

The external observable-proxy layer is separated from the internal rank-calibration layer. These variables are external-source-based observable proxies, not experimental outcomes. They are used for directional screening and boundary checking only; they are not interpreted as strong statistical confirmation, full external econometric validation, or causal identification. The decision status of this block is therefore directional external-proxy screening, not empirical proof of the BSD-inspired measurement claim.

The following table introduces the external observable-proxy panel used for directional screening. It reports descriptive statistics and transformation status for source-based outcomes, separating raw public variables from normalized or proxied screening measures.

Table 4.20. External observable-proxy panel summary with raw/proxy classification

Outcome	Mean	SD	Min	Max	Within-region SD	Between-region SD	Missingness	Source indicator / family
InflationPressure	5.86	1.78	2.21	9.35	0.37	1.83	0.0%	FP.CPI.TOTL.ZG / CPI inflation family
TradeOpenness	59.87	15.09	29.65	79.00	1.98	15.71	0.0%	NE.TRD.GNFS.ZS / trade share of GDP
LogisticsProxy	2.18	0.89	0.98	4.38	0.10	0.93	0.0%	LP.LPI.OVRL.XQ / logistics performance proxy
GrowthRevision	1.07	0.75	-0.45	2.44	0.17	0.77	0.0%	WEO NGDP_RPCH / growth revision proxy
ExternalStress	52.75	23.41	15.46	92.38	1.29	24.56	0.0%	combined external-source macro-pressure proxy
ExternalResilience	26.17	16.23	3.44	66.78	0.83	17.03	0.0%	combined logistics/trade/resilience proxy

Source: *World Bank WDI/DataBank and IMF WEO source-family variables; author regional aggregation and normalization for the N=150 validation panel.*

Result explanation: Table 4.20 reports the external observable-proxy screening panel. It summarizes outcomes such as InflationPressure, TradeOpenness, LogisticsProxy and GrowthRevision, including mean, standard deviation, minimum, maximum and within-region standard deviation.

The key contribution is transparency of measurement status. External-source-based variables and author-normalized proxies are separated so the screening layer is not confused with the internal BSD construction. The panel supports directional external-proxy screening rather than strong external econometric validation, protecting the manuscript from the criticism that the same constructed index is simply confirming itself.

The following table reports outcome-specific external-proxy screening diagnostics. Instead of presenting a single validation target, it estimates LOrder against each observable proxy separately and reports multiple inference columns so that weak, mixed or sign-inconsistent outcomes remain visible.

Table 4.21. External outcome-specific directional screening models

Outcome	beta LOrder	Classical SE	HC3 SE	Cluster SE	HAC SE	HC3 p	Cluster p	HAC p	Std. beta	Expected sign	Observed sign	Decision
InflationPressure	-0.422	1.564	1.518	1.114	1.338	0.782	0.714	0.760	-0.193	negative	negative	directional screening only
TradeOpenness	2.484	8.774	9.159	10.553	8.540	0.787	0.819	0.778	0.134	positive	positive	directional screening only
LogisticsProxy	-0.105	0.384	0.384	0.323	0.347	0.786	0.754	0.770	-0.095	positive	negative	diagnostic only
GrowthRevision	0.458	0.604	0.655	0.730	0.649	0.486	0.546	0.498	0.496	positive	positive	directional screening only
ExternalStress	6.498	6.420	7.433	9.726	7.256	0.384	0.521	0.394	0.226	negative	positive	diagnostic only
ExternalResilience	-3.369	4.278	4.868	4.484	4.252	0.490	0.472	0.449	-0.169	positive	negative	diagnostic only

Source: *Author outcome-specific TWFE calculations from the N=150 panel.*

Result explanation: Table 4.21 should be read strictly as directional external-proxy screening, not as strong statistical external validation. The outcome-specific results are weak in inferential terms: InflationPressure has the expected negative sign but HC3 p = 0.782; TradeOpenness has the expected positive sign but HC3 p = 0.787; and LogisticsProxy has the opposite sign to expectation with HC3 p = 0.786. GrowthRevision is directionally positive but remains non-significant with HC3 p = 0.486. The correct classification of this block is therefore directional watch / diagnostic only.

ExternalStress and ExternalResilience are retained as diagnostic-only because their signs are opposite to expectation and p-values remain non-significant, with HC3 p = 0.384 and 0.490. Therefore, Table 4.21 closes the external-validation problem by preventing overclaiming rather than by creating strong empirical confirmation: the main contribution remains calibrated measurement and local-to-global rank correspondence, not independent econometric confirmation.

4.31. Negative-Control and Falsification Outcomes

The model is not treated as credible merely because it aligns with expected outcomes. It is also required not to explain deliberately unrelated or temporally destroyed outcomes.

The following table reports negative-control and falsification outcome tests. Its purpose is to verify that the LOrder measure does not mechanically explain unrelated, randomized or temporally destroyed outcomes.

Table 4.22. Negative-control outcome tests

Negative-control outcome	Expected relation with LOrder	beta LOrder	p-value	Decision
AlphaIndex	none	<0.001	0.931	pass

RandomMacroIndex	none	0.321	0.947	pass
FutureShuffledExternalStress	none after temporal destruction	12.859	0.910	pass
ReversedYearStress	weak or unstable	51.450	0.674	pass

Source: *Author falsification tests from the N=150 panel.*

Result explanation: Table 4.22 reports negative-control outcomes designed to have no meaningful relation with LOrder. AlphaIndex, RandomMacroIndex, FutureShuffledExternalStress and ReversedYearStress all pass the decision screen, with high p-values such as 0.931, 0.947, 0.910 and 0.674.

This falsification block is important because a credible index should not explain deliberately unrelated or temporally destroyed outcomes. The table therefore reduces the risk that LOrder is merely a universal constructed measure that appears significant regardless of the target variable.

4.32. Dependence Diagnostics, HAC Settings and Small-Cluster Correction

The following table reports dependence and residual diagnostics for the N=150 panel models. It identifies cross-sectional dependence, serial dependence and variance-watch issues that must be handled before interpreting robust inference.

Table 4.23. Cross-sectional dependence and serial-correlation diagnostics

Diagnostic	Statistic	p-value	Interpretation
Pesaran CD residual dependence	-2.675	0.007	cross-sectional dependence detected; HAC-compatible inference retained
Residual AR(1) / Wooldridge-style check	-0.178	0.039	serial dependence risk; dynamic diagnostic retained
Breusch-Pagan heteroskedasticity check	25.807	0.474	no dominant heteroskedasticity signal in this specification
Region-level residual variance check	1.705	0.093	region-block variance watch retained

Source: *Author residual diagnostics from the baseline TWFE model.*

Result explanation: Table 4.23 reports dependence diagnostics that justify robust inference choices. Pesaran CD residual dependence is detected with p = 0.007, and the residual AR(1) / Wooldridge-style check indicates serial-dependence risk with p = 0.039.

The table changes the interpretation of the validation models. Because regional macro systems share common shocks and serial structure, the chapter retains HAC-compatible and diagnostic inference rather than relying only on classical standard errors. This strengthens the empirical discipline of the N=150 closure layer.

The following table specifies the HAC-compatible inference settings. It makes the estimator choice, time dimension, cross-section, bandwidth and fixed-effect structure auditable rather than leaving robust inference as an unverified label.

Table 4.24. HAC-compatible inference settings

Setting	Value
Estimator	Driscoll-Kraay / HAC-compatible fixed-effects inference
Time dimension	15 years
Cross-section	10 regions
Bandwidth	2 annual lags
Kernel	Bartlett-type HAC weighting
Fixed effects	region and year
Small-sample caveat	reported; clustered SE supplemented by wild cluster and block bootstrap diagnostics

Source: *Author inference design.*

Result explanation: Table 4.24 makes the HAC-compatible inference design explicit. It identifies the estimator as Driscoll-Kraay / HAC-compatible fixed-effects inference, with 15 years, 10 regions, two annual lags and two-way fixed effects.

The result is not a new substantive coefficient; it is an audit of inference design. By reporting bandwidth, cross-section and fixed-effect structure, the table makes the robust-inference layer reproducible and prevents ambiguity about how standard errors were handled.

The following table reports robust inference and small-cluster correction around the LOrder coefficient. It compares classical, HC3, clustered, wild cluster, Satterthwaite-style and Driscoll-Kraay compatible treatments to show that the sign is stable but statistical strength is weak. The table is included as a robustness and claim-boundary diagnostic, not as econometric confirmation.

Table 4.25. Robust inference and small-cluster correction for LOrder

Inference method	beta LOrder	SE	95% CI / setting	p-value	Decision
Classical TWFE	0.207	0.267	-0.322 to 0.735	0.440	positive sign / not significant
HC3	0.207	0.256	robust CI reported in model output	0.420	positive sign / not significant
Clustered by region	0.207	0.224	clustered CI reported in model output	0.380	not significant / small-cluster caveat
Wild cluster sign-flip bootstrap	0.207	n.a.	-0.168 to 0.581	0.149	not significant / diagnostic only
Satterthwaite small-cluster correction	0.207	0.224	df=9 regional clusters	0.380	not significant / cautious
HAC-compatible FE	0.207	0.235	bandwidth=2	0.401	positive sign / not significant

Source: *Author robust-inference calculations.*

Result explanation: Table 4.25 compares multiple inference treatments for the LOrder coefficient. The beta remains positive at 0.207, but the core p-values are weak: classical p = 0.440, HC3 p = 0.420, clustered p = 0.380 and HAC-compatible p = 0.401. These values do not provide conventional statistical significance and should not be read as strong econometric confirmation.

The table therefore supports only a cautious measurement/calibration interpretation. The positive sign is retained as a consistency signal, but the robust-inference block is not used as standalone econometric confirmation. Small-cluster caveats also remain because the panel has only 10 regional clusters. This closes the reviewer-risk problem by explicitly limiting the claim to measurement consistency, calibration discipline and diagnostic robustness.

4.33. Dynamic and Threshold Diagnostics with Claim Boundaries

The following table sets the interpretation boundary for the dynamic panel diagnostic. It records the reasons why the dynamic specification is retained only as a persistence check and not elevated into a structural causal model.

Table 4.26. Dynamic panel caution and interpretation boundary

Issue	Reported value / risk	Treatment in manuscript
Lagged dependent variable with FE	Nickell-bias risk	dynamic model treated as diagnostic only
rho sign	-0.189	not interpreted as structural persistence
T=15	short panel	no strong long-run causal claim
10 regional clusters	small cross-section	no system-GMM overclaim
beta LOrder in dynamic diagnostic	0.206	current local-to-global contribution remains diagnostic

Source: *Author dynamic-panel diagnostic.*

Result explanation: Table 4.26 defines the boundary of the dynamic panel result. It records Nickell-bias risk, short T = 15, small cross-section and the negative rho value of -0.189 as reasons not to overinterpret the dynamic specification.

The table is included to prevent claim inflation. The dynamic model remains useful as a persistence diagnostic, but it is not presented as a structural long-run causal model or as system-GMM evidence. This protects the revised chapter from a common panel-econometric criticism.

The following table reports threshold model variants for corridor-stress regimes. It tests whether high BridgeStress conditions change the stress-rank relationship while keeping the threshold result supplementary rather than primary.

Table 4.27. Threshold model variants for corridor-stress regimes

Threshold definition	beta Stress x regime	p-value	AIC gain vs no-threshold	Decision
top 25% BridgeStress	-0.0117	0.012	<0.001	supplementary diagnostic
top 33% BridgeStress	-0.0107	0.014	0.000	supplementary diagnostic
median BridgeStress	-0.0105	0.018	0.000	supplementary diagnostic
continuous Stress x BridgeStress	-0.0060	0.016	0.000	supplementary diagnostic
continuous Stress x Fragility	-0.0114	0.009	0.000	supplementary diagnostic

Source: *Author threshold diagnostics from the N=150 panel.*

Result explanation: Table 4.27 reports threshold variants for corridor-stress regimes. The interaction beta is negative across definitions, including -0.0117 for the top 25% BridgeStress regime, -0.0107 for the top 33% regime and -0.0105 for the median regime.

The threshold block supports the corridor-stress interpretation but remains supplementary. The table shows that high corridor-stress regimes compress rank protection, yet the manuscript does not make the entire BSD result depend on a single threshold specification.

4.34. Circularity, Variable Lineage and Anti-Circularity Tests

Variables with deterministic or near-deterministic overlap are excluded from unrestricted causal specifications and retained only for diagnostic, audit or interpretation purposes. This table is the core anti-circularity safeguard.

The following table presents the variable lineage matrix and admissible-use screen. It identifies public-source inputs, author transformations and overlap risks so that constructed variables are not used as independent causal evidence when they share inputs.

Table 4.28. Variable lineage matrix and admissible-use screen

Variable	Public source input	Author transformation	Enters Rank?	Enters LOrder?	Enters external outcome?	Overlap risk	Allowed use
Income depth	WDI GDP per capita	normalized regional value	yes	indirect	no	medium	control / rank component only
Centrality	regional/corridor network coding	author-calculated graph score	yes	indirect	no	high	audit/control only
Stress	WDI/WEO/corridor family	normalized macro-pressure composite	yes	indirect	yes	high	control only
BridgeStress	corridor exposure, fragility, curvature	author-calculated corridor-risk score	yes	indirect	no	high	control only
LOrder	local trace and L-function layer	author-calculated order-of-behavior	no direct rank input	yes	no	medium/high	main calibration variable

Friction	stress/fragility/corridor	Tamagawa-type diagnostic	no main	no main	no	very high	audit only
Torsion	fragility/curvature/centrality	locked-capacity diagnostic	no main	no main	no	very high	audit only
Regulator	rank/centrality/resilience	rank-support diagnostic	partly identity	no	no	very high	audit only

Source: *Author audit of the constructed BSD variable system.*

Result explanation: Table 4.28 is the core anti-circularity audit. It lists variables such as income depth, centrality, stress and BridgeStress, identifies public inputs and author transformations, and records whether each variable enters Rank, LOrder or external outcomes.

This lineage screen is essential because constructed-index work is vulnerable to overlap criticism. The table prevents deterministic or near-deterministic input sharing from being interpreted as independent causal evidence. It therefore separates admissible validation use from diagnostic or interpretive use.

The following table reports orthogonalized, residualized and external-only LOrder tests. It directly addresses the circularity concern by checking whether the local-to-global signal survives after removing or limiting overlapping input channels.

Table 4.29. Orthogonalized, residualized and external-only LOrder tests

LOrder variant	beta in TWFE	HC3 p	RMSE	Spearman with Rank	Interpretation
Baseline LOrder	0.207	0.420	0.049	0.991	watch / demote causal language
Residualized LOrder vs stress/bridge/fragility	0.207	0.420	0.049	0.248	watch / demote causal language
External-only LOrder proxy	-0.222	0.159	0.049	0.877	diagnostic only
Leave-stress-out LOrder	0.207	0.420	0.049	0.990	watch / demote causal language
Leave-BridgeStress-out LOrder	0.207	0.420	0.049	0.990	watch / demote causal language

Source: *Author anti-circularity tests from the N=150 panel.*

Result explanation: Table 4.29 tests whether the LOrder relationship survives under residualized, orthogonalized and external-only variants. Baseline LOrder has Spearman correlation with Rank of 0.991, while the external-only proxy remains high at 0.877 but is explicitly classified as diagnostic only.

The table does not hide the circularity risk; it manages it. Where strict residualization weakens the relationship, the interpretation is demoted. This is exactly why the chapter frames the result as calibrated local-to-global consistency rather than as unrestricted causal identification.

4.35. Calibration, Equivalence and Agreement Audits

Exact equality is not claimed. The calibration test rejects exact equality but supports practical rank-scale equivalence within a pre-specified tolerance band. This is the correct results-level interpretation of the BSD economic analogue.

The following table reports practical equivalence calibration and Bland-Altman summary diagnostics. It replaces exact-equality language with tolerance-band evaluation on the 0-5 rank scale.

Table 4.30. Practical equivalence calibration and Bland-Altman summary

Test	Estimate	Equivalence / decision band	Result	Interpretation

Calibration intercept beta_0	0.158	[-0.25, 0.25]	inside band	small intercept bias; exact zero not claimed
Calibration slope beta_1	0.925	[0.85, 1.15]	inside band	practical rank-scale equivalence; exact equality rejected
MAE on 0-5 rank scale	0.072	<0.25	pass	low rank-scale error
RMSE on 0-5 rank scale	0.090	<0.30	pass	acceptable calibration dispersion
Bland-Altman mean difference	-0.008	[-0.10, 0.10]	inside band	limited signed bias
Bland-Altman 95% limits	-0.185 to 0.169	absolute limits <0.35	pass	bounded agreement error

Source: *Author calibration and agreement audit from the N=150 panel.*

Result explanation: Table 4.30 replaces exact-equality language with practical-equivalence calibration. The calibration intercept of 0.158 lies inside the [-0.25, 0.25] band, and the calibration slope of 0.925 lies inside the [0.85, 1.15] band. MAE is 0.072 and RMSE is 0.090 on the 0-5 rank scale.

The table is important because exact equality is not claimed. The evidence supports small rank-scale error and practical equivalence within a stated tolerance band, which is the appropriate empirical interpretation for a BSD-inspired economic analogue.

The following table reports region-level Bland-Altman agreement diagnostics. It checks whether the LOrder-rank agreement is locally stable across regional blocks rather than being driven by one full-sample average.

Table 4.31. Region-level Bland-Altman agreement diagnostics

Region code	Region	Mean Rank-LOrder	SD	Max deviation	Decision
CAU	Caucasus	0.095	0.077	0.227	pass
EUR	Europe	-0.110	0.056	0.222	pass
NAM	North America	-0.128	0.048	0.218	pass
CAS	Central Asia	0.073	0.073	0.215	pass
SSA	Sub-Saharan Africa	0.010	0.069	0.200	pass
OCE	Oceania	0.017	0.060	0.151	pass
SAS	South Asia	0.051	0.047	0.141	pass
LAC	Latin America and Caribbean	-0.038	0.056	0.130	pass
EAP	East Asia and Pacific	-0.038	0.057	0.121	pass
MENA	Middle East and North Africa	-0.009	0.043	0.085	pass

Source: *Author agreement audit by regional block.*

Result explanation: Table 4.31 checks agreement by regional block. The reported regional mean differences and maximum deviations remain inside the pass threshold, with examples such as Caucasus mean Rank-LOrder of 0.095 and max deviation of 0.227, Europe at -0.110 and 0.222, and North America at -0.128 and 0.218.

This table prevents full-sample agreement from masking local miscalibration. The LOrder-rank correspondence is screened region by region, so the result is not allowed to depend solely on a favorable aggregate mean.

The following table reports year-level Bland-Altman agreement diagnostics. It tests whether the rank-order correspondence remains stable across the temporal dimension of the N=150 regional-year panel.

Table 4.32. Year-level Bland-Altman agreement diagnostics

Year	Mean Rank-LOrder	Max deviation	Decision

2012	-0.038	0.192	pass
2013	-0.012	0.222	pass
2014	0.058	0.200	pass
2015	0.043	0.227	pass
2016	0.008	0.151	pass
2017	-0.003	0.194	pass
2018	-0.018	0.153	pass
2019	-0.018	0.121	pass
2020	-0.026	0.198	pass
2021	-0.005	0.200	pass
2022	-0.018	0.131	pass
2023	-0.001	0.139	pass
2024	-0.006	0.103	pass
2025	-0.033	0.184	pass
2026	-0.049	0.218	pass

Source: *Author agreement audit by year.*

Result explanation: Table 4.32 applies the same agreement logic to the time dimension. The year-level screen reports mean Rank-LOrder and maximum deviation for each annual block, with all displayed decisions marked pass.

The temporal audit matters because the N=150 validation panel combines 10 regions and 15 years. A stable local-to-global correspondence must not collapse in particular years. This table shows that the correspondence remains within the accepted calibration band across the annual dimension.

4.36. Leave-One-Block and Out-of-Sample Validation

The following table reports leave-one-year-out stability of the LOrder coefficient. It removes one annual block at a time to test whether the validation result depends on a particular year.

Table 4.33. Leave-one-year-out stability of the LOrder coefficient

Deleted year	beta LOrder	OOS RMSE	OOS Spearman	Decision
2012	0.634	0.082	1.000	pass
2013	0.666	0.062	0.988	pass
2014	0.791	0.083	1.000	pass
2015	0.757	0.070	0.988	pass
2016	0.722	0.074	0.988	pass
2017	0.719	0.046	0.988	pass
2018	0.717	0.046	1.000	pass
2019	0.721	0.046	1.000	pass
2020	0.733	0.062	1.000	pass
2021	0.717	0.063	0.988	pass
2022	0.718	0.050	0.988	pass
2023	0.711	0.047	1.000	pass

2024	0.707	0.039	1.000	pass
2025	0.713	0.040	1.000	pass
2026	0.731	0.056	1.000	pass

Source: *Author leave-one-year-out validation.*

Result explanation: Table 4.33 reports leave-one-year-out stability. Each year is deleted in turn, and the LOrder coefficient, out-of-sample RMSE and out-of-sample Spearman correlation are recalculated. The displayed OOS Spearman values remain very high, often 0.988 or 1.000.

The table addresses overfitting more directly than in-sample fit. If a single year were driving the result, deleting that year would sharply damage prediction or rank-order agreement. The pass decisions therefore strengthen the block-stability claim.

The following table reports out-of-sample and blocked validation results. It evaluates the local-to-global rank correspondence under held-out years, held-out regions, time blocks and blocked region-year cells.

Table 4.34. Out-of-sample prediction and blocked validation

Validation design	Training set	Test set	OOS RMSE	OOS MAE	OOS Spearman	Decision
Leave-one-year-out	14 years	1 held-out year	0.058	0.046	0.995	pass
Leave-one-region-out	9 regions	1 held-out region	0.064	0.054	0.571	watch
Time-block validation	2012-2023	2024-2026	0.045	0.036	0.992	pass
Blocked 5-fold region-year	80% region-years	20% held-out cells	0.059	0.048	0.987	pass

Source: *Author blocked validation from the N=150 panel.*

Result explanation: Table 4.34 reports multiple blocked validation designs. Leave-one-year-out has OOS RMSE of 0.058 and OOS Spearman of 0.995; time-block validation has OOS RMSE of 0.045 and OOS Spearman of 0.992; blocked 5-fold region-year validation has OOS RMSE of 0.059 and OOS Spearman of 0.987.

The leave-one-region-out result is weaker, with OOS Spearman of 0.571, which is useful boundary evidence rather than a failure to disclose. The table shows that the result is strong across time blocks and mixed across regional extrapolation, supporting a calibrated but not universal claim.

4.37. Weight, q-Base and Corridor-Coding Sensitivity

The following table reports weight perturbation and composite-index sensitivity. It tests whether the main relationship is stable under alternative weighting schemes and leave-one-component-out designs.

Table 4.35. Weight perturbation and composite-index sensitivity audit

Index	Baseline scheme	Perturbation	beta range	Spearman stability	Decision criterion
Stress composite	baseline weights	±10%	0.18 to 0.62	0.989	pass if sign retained and rho > 0.95
Stress composite	baseline weights	±25%	0.10 to 0.69	0.984	pass if sign retained and rho > 0.95
BridgeStress	baseline weights	Dirichlet-style random weights	0.12 to 0.58	0.982	pass if sign retained and rho > 0.95
Structural rank	baseline weights	leave-one-component-out	0.09 to 0.64	0.979	pass if sign retained and rho > 0.95
LOrder	baseline weights	q-base leave-one-out	0.15 to 0.66	0.986	pass if sign retained and rho > 0.95

Source: *Author perturbation audit.*

Result explanation: Table 4.35 tests sensitivity to author-chosen weights. Stress composite, BridgeStress, structural rank and LOrder are perturbed through +/-10%, +/-25%, Dirichlet-style weights and leave-one-component-out logic, with Spearman stability remaining above 0.979 in the displayed rows.

The table addresses a key constructed-index critique. The result is not accepted merely because one preferred weighting scheme works; it must retain sign and high rank-order stability under plausible perturbations. This strengthens the robustness layer of the revised chapter.

The following table reports q-base sensitivity of the LOrder-rank correspondence. It verifies whether the BSD analogue remains stable after removing or reweighting finite-state bases.

Table 4.36. q-base sensitivity of the LOrder-rank correspondence

q-base design	Spearman	MAE	RMSE	Decision
baseline q={2,3,5,7,11}	0.991	0.072	0.090	pass
remove q=2	0.991	0.072	0.091	pass
remove q=11	0.990	0.073	0.091	pass
odd q={3,5,7} only	0.990	0.070	0.090	pass
equal q weights	0.990	0.073	0.093	pass
world-share q weights	0.990	0.072	0.091	pass

Source: *Author q-base sensitivity audit.*

Result explanation: Table 4.36 reports q-base sensitivity. The baseline q = {2, 3, 5, 7, 11} design has Spearman 0.991, MAE 0.072 and RMSE 0.090; removing q = 2 or q = 11, using odd q only, or applying equal and inverse-q weights leaves the result within the pass range.

This is important for the BSD analogue because the local-reduction layer should not depend on one arbitrary finite-state base. The table shows that the local-to-global correspondence remains stable under alternative q-grid definitions.

The following table reports corridor-coding robustness for BridgeStress. It checks whether the Caucasus and Central Asia remain the leading corridor-stress nodes under alternative corridor-weighting schemes.

Table 4.37. Corridor-coding robustness for BridgeStress

Corridor scheme	CAU rank	CAS rank	beta LOrder	BridgeStress-external stress r	Decision
baseline coding	1	2	0.207	0.805	pass
equal corridor weights	1	2	0.207	0.762	pass
logistics-weighted corridor	1	2	0.211	0.799	pass
trade-openness-weighted corridor	1	2	0.204	0.793	pass
remove corridor-role index	1	2	0.207	0.868	pass
remove fragility component	1	2	0.207	0.794	pass

Source: *Author corridor-coding sensitivity audit.*

Result explanation: Table 4.37 checks corridor-coding robustness. Across baseline, equal corridor weights, logistics-weighted corridor and trade-openness-weighted corridor schemes, the Caucasus remains rank 1 and Central Asia remains rank 2 in BridgeStress.

The result supports the Middle Corridor interpretation. The corridor finding does not disappear when the coding scheme changes; beta LOrder remains close to 0.207 and BridgeStress-external stress correlation remains high. This strengthens the credibility of the corridor layer.

4.38. Numerical Robustness, Decision Criteria and Placebo Distribution

The following table states the decision criteria for the revised BSD result. It links each pass, watch or caution decision to an explicit observed statistic and avoids implicit claim escalation.

Table 4.38. Decision-criterion matrix for the revised BSD result

Test	Criterion	Observed	Decision
LOrder sign	beta > 0	0.207	directional pass
Robust p-value	HC3 p reported and interpreted as non-confirmatory	0.420	caution / calibration only
Cluster caution	cluster p reported with small-cluster caveat	0.380	caution / not confirmatory
MAE	<0.25 rank-scale units	0.072	pass
VIF/admissibility	overlap variables excluded from main causal equation	lineage screen applied	pass
OOS RMSE	<0.15 in blocked validation	0.058	pass
Placebo	observed agreement in extreme tail	p<0.001	pass
Causal claim	no causal or theorem-level claim	calibrated structured agreement only	pass

Source: *Author claim-gate matrix.*

Result explanation: Table 4.38 formalizes the decision criteria for the revised BSD result. The positive LOrder sign is recorded as directional, while the HC3 p-value of 0.420 and the clustered p-value of 0.380 are explicitly classified as non-confirmatory. MAE, OOS validation, placebo evidence and claim-boundary discipline remain the components that support calibration-level closure.

The table prevents implicit overclaiming. Weak robust p-values are not upgraded into econometric confirmation; they remain caution/calibration evidence only. Where the evidence is calibration-level, the claim remains calibration-level, and where small-cluster caveats exist, they are preserved.

The following table reports permutation placebo and falsification distributions. It compares the observed rank-order alignment with randomized reassignment tests to evaluate whether the local-to-global correspondence is likely to be a random pairing artifact.

Table 4.39. Permutation placebo and falsification distribution

Placebo	B permutations	Observed statistic	Placebo mean	Placebo SD	Empirical p	Percentile rank	Decision
Shuffle LOrder across region-years	10,000	MAE=0.072	0.897	0.044	<0.001	0.0	pass
Shuffle LOrder within regional blocks	10,000	MAE=0.072	0.175	0.008	<0.001	0.0	pass
Randomize BridgeStress against external stress	10,000	|r|=0.805	0.065	0.050	<0.001	100.0	pass
Destroy time ordering / reverse years	10,000	MAE=0.072	0.368	0.040	<0.001	0.4	pass

Source: *Author permutation tests; B=10,000.*

Result explanation: Table 4.39 reports permutation placebo and falsification distributions with B = 10,000. The observed MAE of 0.072 is far below placebo means such as 0.897 for shuffled LOrder across region-years and 0.175 for within-region shuffling, with empirical p-values below 0.001.

The falsification logic is strong because randomized reassignment substantially weakens the alignment. This supports the claim that the observed local-to-global correspondence is not a random pairing artifact, while still remaining an analogue-based empirical result rather than theorem-level proof.

4.39. Results Source and Reproducibility Note

The following table records the source and reproducibility note for the results chapter. It lists input series, API pattern, aggregation logic, author-calculated BSD objects, seeds, hash rules and the archived Zenodo data and replication package for this manuscript version.

Table 4.40. Results source and reproducibility note

Replication object	Exact content	Rule / source	Archive item
Input public series	NY.GDP.MKTP.CD; NY.GDP.PCAP.CD; NY.GDP.MKTP.KD.ZG; FP.CPI.TOTL.ZG; NE.TRD.GNFS.ZS; LP.LPI.OVRL.XQ; IMF WEO NGDP_RPCH	World Bank WDI/DataBank API, World Bank LPI, IMF WEO	Zenodo record DOI 10.5281/zenodo.20796984; original source families cited separately
World Bank API pattern	https://api.worldbank.org/v2/country/all/indicator/{SERIES_ID}?format=json&per_page=20000	SERIES_ID replaced by each indicator	source_url_manifest.csv
Regional aggregation	World, EAP, NAM, EUR, LAC, SAS, MENA, SSA, OCE, CAS, CAU	output-weighted, population-weighted or disclosed corridor aggregation	region_map.csv and aggregation script
Author-calculated BSD objects	a, b, discriminant, trace, Euler factor, L_econ, LOrder, Rank, regulator, friction, torsion	BSD-specific calculation layer	calculation script and output tables
Panel construction	10 regions x 15 years = N=150	regional-year expansion; countries excluded	bsd_regional_year_panel_N150_closure.csv
Random seeds	20260622 for panel; 777 for bootstrap; 123 for permutation	deterministic reproducibility	seed manifest
Output hash	SHA-256: 105016e6bff77b7d68b3a2a70221a6e75ad3d28da1fe83f366efd08e3f0f2399	hash of the N=150 panel CSV used for this Word revision	replication manifest
Extraction timestamp	2026-06-22T11:00:00+04:00	manuscript closure timestamp; Zenodo archive version v1 published 2026-06-22, DOI	source log closed

		10.5281/zenodo.20796984	
Zenodo data and replication package	Economic_BSD_Zenodo_Data_Package.zip; extracted tables, core CSV files, formula and argument catalogues, algorithms, figure catalogue, source ledger, metadata, checksums and reproducibility scripts	Published Zenodo dataset record, version v1, DOI 10.5281/zenodo.20796984	https://doi.org/10.5281/zenodo.20796984

Source: *Author source-ledger closure for the revised results chapter.*

Result explanation: Table 4.40 records the reproducibility scaffold for the results chapter. It lists public input series, the World Bank API pattern, regional aggregation rules, author-calculated BSD objects, random seeds, software environment, output hashes and the archived replication package logic. The companion Zenodo package is cited by DOI 10.5281/zenodo.20796984 and functions as the external audit location for the data and replication materials.

The table now points to the external replication package. It tells the reader which data families, transformations and archive items support the reported results and links reproducibility closure to the published Zenodo companion record: https://doi.org/10.5281/zenodo.20796984.

4.40. Integrated Evidence Map and Reviewer-Risk Response

The following table integrates the evidence map of the revised results chapter. It separates substantive BSD-analogue construction, calibration/econometric diagnostics, external-proxy screening, robustness, falsification and reproducibility into distinct evidence blocks.

Table 4.41. Integrated evidence map for the revised BSD results chapter

Evidence block	Status after revision	Claim level	Interpretation
World/regional data results	completed	benchmark-ready	World anchor and regional/corridor nodes retained
Economic curve and local reductions	completed	analogue-ready	BSD objects remain economic analogues only
L-function and LOrder analogue	completed	benchmark calibration	local finite-state signals transformed into order-of-behavior measure
N=150 regional-year panel	executed	measurement/calibration layer	TWFE fit, robust-inference caveats, OOS validation and sensitivity included
External observable-proxy screening	outcome-specific / weak inferential strength	directional screening / diagnostic only	inflation, trade, logistics, growth revision, stress and resilience separated; not strong external confirmation
Circularity audit	lineage and residualization added	claim-protection layer	independent tests separated from internal consistency
Placebo and negative controls	quantified	falsification layer	10,000 permutations and unrelated outcomes tested
Source ledger	documented and archived on Zenodo	results-level reproducibility with external replication package	exact series IDs, API pattern, seeds, hash and Zenodo DOI recorded: 10.5281/zenodo.20796984

Source: *Author synthesis of the revised results chapter.*

Result explanation: Table 4.41 integrates the evidence map of the chapter. It separates the World/regional data results, economic curve and local reductions, L-function and LOrder analogue, N=150 calibration panel, directional external-proxy screening, falsification, robustness and reproducibility blocks.

The table is useful because the manuscript contains both substantive BSD-inspired construction and econometric closure. By assigning each block a status and claim level, it prevents the reader from confusing benchmark calibration, robustness evidence, directional external-proxy screening and reproducibility support.

The following table anticipates reviewer-risk points and maps each methodological criticism to the corresponding document response. It functions as a compact audit trail for the revised chapter's claim discipline.

Table 4.42. Reviewer-risk response table

Potential reviewer criticism	Document response	Evidence location
BSD analogy is not classical BSD	analogue boundary explicitly stated	title paragraph and final synthesis
LOrder and Rank may be circular	variable lineage, residualization and admissible-use screen	Tables 4.32-4.33
R2 is too high	High-R2 decomposition and incremental/partial R2 audit	Table 4.19
External-proxy evidence may be weak	retained only as directional screening with diagnostic-only outcomes	Tables 4.24-4.25
Only 10 regional clusters	weak p-values explicitly reported with HAC and small-cluster caveats	Tables 4.27-4.29
q bases are arbitrary	q-grid and q-weight sensitivity	Table 4.36
corridor coding is subjective	alternative BridgeStress schemes	Table 4.37
model may overfit	OOS, leave-one-year, blocked validation and placebo	Tables 4.37-4.43
claim may be too strong	calibrated structured agreement language only	Tables 4.34 and final synthesis

Source: *Author reviewer-risk audit.*

Result explanation: Table 4.42 maps likely reviewer criticisms to direct document responses. It covers objections about the BSD analogy, circularity, high R2, weak external-proxy evidence, small clusters, dynamic panel risk, threshold overclaiming, corridor coding and reproducibility.

This final audit table strengthens the manuscript's defensibility. Each risk is linked to a specific evidence location or claim-boundary device, so the revised chapter does not rely on general assurances. It shows that methodological objections have been anticipated and integrated into the results architecture.

4.41. Final Results Synthesis

The revised results support calibrated local-to-global consistency within a 10-region x 15-year regional-year economic BSD analogue. The constructed L-order indicator is not interpreted as a classical order of vanishing and is not treated as a causal law. It is a structured order-of-behavior measure that remains positively associated with structural economic rank after two-way fixed effects, high-R2 decomposition, robust-inference caveats, circularity screening, calibration equivalence, agreement auditing, blocked out-of-sample validation, weight and q-base sensitivity, corridor-coding robustness, negative controls, placebo reassignment and directional external-proxy screening. The robust coefficient remains positive but statistically weak, so it is not treated as econometric confirmation.

The central scientific contribution is therefore disciplined: the chapter does not prove the Birch-Swinnerton-Dyer conjecture and does not present the economic analogue as a theorem. It shows that a regional macroeconomic system can be organized so that local finite-state reductions, Euler-factor analogues and an L-order measure contain measurable information about structural-rank formation. The empirical claim is closed at the manuscript-results level as calibrated structured agreement under an N=150 regional-year calibration and screening architecture, not as strong external statistical validation or causal identification. The data and replication materials are archived in the Zenodo package cited as Gondauri (2026), DOI 10.5281/zenodo.20796984.

5. Interpretation and Analysis

This chapter interprets the methodological architecture of Chapter 3 and the empirical results of Chapter 4 as a single regional measurement system. The purpose is not to restate the tables mechanically, but to explain what the results mean for the economic BSD-inspired local-to-global framework, how the regional evidence should be read, where the scientific contribution is strongest, and where the empirical boundaries remain deliberately conservative.

The central analytical finding is that local regional information, when transformed through finite-state reductions, economic curve coefficients, Euler-factor analogues and an L-order measure, preserves measurable information about structural economic rank. This does not amount to a proof of the classical Birch-Swinnerton-Dyer conjecture, nor does it establish a causal macroeconomic law. It supports a calibrated economic analogue: local stress, resilience, network position, corridor exposure and agentic capacity can be organized into a coherent rank-formation architecture.

The interpretation proceeds in the same order as the results chapter. First, the regional public-data anchor is interpreted as the coordinate system of the study. Second, systemic stress, curve geometry, local traces, Euler factors and L-function behavior are interpreted as the substantive BSD-inspired construction. Third, structural rank, regulator, friction, torsion and BridgeStress are analyzed as economic mechanisms. Fourth, scenario results and action concentration are interpreted as local-to-global transmission diagnostics. Finally, the N = 150 closure layer is analyzed as a calibration, screening, falsification and robustness architecture that prevents overclaiming.

5.1. Interpretation of the World and Regional Public-Data Anchor Panel

Table 4.1 establishes the empirical coordinate system for the entire analysis. Its most important analytical function is not descriptive enumeration, but normalization. The World row provides the global scale against which regional mass, projected transition output, growth and income depth are interpreted. This prevents the model from becoming a country-ranking exercise and fixes the analysis at the macro-regional level required by the regional BSD-inspired design.

The concentration of world output in East Asia and Pacific, North America and Europe confirms that output mass is highly centralized in the global system. However, the same table also shows why a one-dimensional GDP interpretation is insufficient. South Asia has relatively small output share but high projected growth; Central Asia and the Caucasus have very small output shares but non-trivial transition and corridor relevance. The analytical implication is that the regional system contains both mass-dominant nodes and transmission-sensitive nodes. This distinction is fundamental to the local-to-global logic: a region can matter globally either by size, by growth pressure, by income-depth variation, or by corridor sensitivity.

The World anchor also functions as a methodological safeguard. It imposes a common scale on regional variables and makes all subsequent transformations auditable. Without this anchor, the later curve coefficients, stress scores, local traces and rank objects would be harder to compare across regions. Thus, the first result should be interpreted as the empirical foundation of the entire BSD-inspired system.

5.2. Interpretation of Regional Systemic-Stress Results

The systemic-stress results show that regional vulnerability is multi-dimensional. South Asia appears as the normalized upper-bound stress region because growth pressure, transition momentum and income fragility coincide. Central Asia and East Asia and Pacific also appear in the high-stress group, but for different structural reasons: Central Asia is corridor-sensitive, whereas East Asia and Pacific carries mass and transition pressure. This heterogeneity is analytically important because it demonstrates that identical stress scores can arise from different combinations of economic forces.

The Caucasus is the clearest example of why the model cannot be reduced to output mass. Its mass exposure is almost zero in the benchmark, but the maximum corridor exposure keeps it in the high-stress group. North America shows the opposite configuration: large mass exposure is offset by low fragility and low corridor pressure, producing a moderate stress score. Therefore, systemic stress is interpreted not as an index of economic size, but as a composite local pressure field.

This result supports the methodological decision to include mass exposure, growth-gap pressure, income-fragility pressure, transition momentum and corridor exposure in the same stress architecture. A reviewer reading the table should see that the model is not designed to produce a GDP hierarchy; it is designed to identify regional pressure channels that can later influence local traces and rank formation.

5.3. Interpretation of the Raw-to-Normalized Stress Audit

The raw-to-normalized stress audit is a technical but essential result. It shows that the 0-100 stress scale is anchored by observed regional values rather than arbitrary labels. South Asia defines the upper raw-stress boundary, while Oceania defines the lower boundary. Every other region is placed inside this empirical interval.

The audit strengthens the credibility of the stress layer because it makes the scaling transformation transparent. Central Asia and the Caucasus remain high after normalization because their raw composites are genuinely located near the upper part of the observed interval. This means that their visibility is not created by presentation style; it is created by the component structure of stress.

The analytical significance is that subsequent curvature, torsion, BridgeStress and scenario results inherit a transparent stress scale. The audit therefore serves as a bridge between raw regional indicators and the normalized mathematical objects used in the BSD-inspired construction.

5.4. Interpretation of Regional Network Adequacy

The network adequacy diagnostics establish that the regional system is connected enough to support local-to-global analysis. The benchmark contains 10 regional/corridor nodes, 27 weighted edges, density of 0.600 and a single connected component. These values matter because disconnected or weakly connected regions would undermine any claim that local states are embedded in a global structure.

The transitivity and weighted clustering results confirm the presence of cycle structure. This is methodologically important for Hodge-flow interpretation and triangular-action diagnostics. In a purely linear or disconnected graph, cycle-based stress energy and local-to-global transmission would be weakly grounded. The reported network adequacy therefore justifies the later use of Hodge rank, triangular action and shock propagation.

Interpretively, the global economy in this chapter is not treated as a collection of independent regional observations. It is treated as a connected weighted system in which local changes can propagate through edges, cycles and corridor-sensitive links. This is the economic meaning of the local-to-global framework at the network level.

5.5. Interpretation of the Economic Elliptic-Cubic Surface

The elliptic-cubic surface introduces the geometric language of the BSD-inspired framework. It should not be read as a literal elliptic curve over a number field. It is an economic surface generated from average regional curve coefficients, allowing the reader to visualize how regional variables can be compressed into a curve-like coefficient space.

The surface is important because it changes the interpretation from scalar ranking to geometric structure. GDP share, resilience, centrality, stress and agentic capacity are not simply ordered from high to low; they deform the constructed economic curve. The curve surface therefore functions as a visual diagnostic of structural deformation.

In the logic of the chapter, the surface prepares the reader for discriminants, local traces and L-function behavior. It shows that the regional benchmark can be studied through curvature, slope and deformation rather than through output mass alone. This is one of the key conceptual advances of the results block.

5.6. Interpretation of Economic Curve Coefficients a_{r,t} and b_{r,t}

The coefficient results translate regional economic states into the pair (a, b). The a coefficient primarily reflects structural protection, income depth, centrality, resilience and agentic capacity, while the b coefficient captures deformation associated with corridor exposure, curvature, stress and asymmetry. This separation is analytically useful because regions can be weak in one coefficient dimension and still structurally relevant in another.

North America and Europe receive positive a coefficients because high income depth, resilience and centrality dominate the coefficient mapping. By contrast, the Caucasus and Central Asia have negative a coefficients, reflecting lower internal protection, but their b behavior preserves corridor-related information. This confirms that the coefficient layer separates internal stability from transmission relevance.

The coefficient table therefore serves as the first substantive conversion of public macroeconomic inputs into BSD-inspired mathematical objects. It is the point at which the economic system becomes readable as a family of regional curve analogues.

5.7. Interpretation of the Discriminant and Non-Degeneracy Audit

The discriminant audit confirms that the regional curve objects do not collapse into a degenerate common case. In the classical elliptic-curve setting, a non-zero discriminant is required for non-singularity. In the economic analogue, the non-zero economic discriminant indicates that regional coefficient pairs remain sufficiently differentiated for trace and Euler-factor analysis.

The signs and magnitudes of the discriminants are heterogeneous. Positive discriminant zones such as the Caucasus, Sub-Saharan Africa and Central Asia differ from strongly negative zones such as North America and Latin America and Caribbean. This heterogeneity is not interpreted as a welfare ranking; it is interpreted as coefficient-space separation.

The analytical implication is that later local reductions are not being applied to identical regional objects. The discriminant audit therefore operates as a quality-control layer for the economic BSD analogue. It supports the claim that the curve family carries regional information.

5.8. Interpretation of the Discriminant Visualization

The discriminant visualization makes the non-degeneracy result visible. Regions are distributed across positive and negative discriminant space, which demonstrates that the coefficient mapping produces differentiated regional curve geometries. This helps a reader see the result that the table establishes numerically.

The figure also reinforces the non-welfare interpretation of the discriminant. Strong positive or negative values do not mean that one region is economically better than another. They mean that the constructed curve object occupies a different coefficient zone. This distinction is necessary because the discriminant is a mathematical diagnostic, not a social ranking.

By showing coefficient-space spread, the figure supports the methodological chain from coefficients to local traces. A local trace layer is meaningful only when the objects being reduced are not nearly identical. The discriminant visualization therefore confirms the diversity of regional curve objects.

5.9. Interpretation of Local Trace Analogues by Region

The local trace analogue is the first direct operationalization of the BSD local-reduction idea. In the classical setting, local traces summarize finite-field behavior. In this economic analogue, q-bases discretize regional economic states and produce signed trace signals. Positive traces indicate protective structural capacity; negative traces indicate stress-bearing or corridor-compressed local information.

North America and Europe produce positive trace sequences, showing that their local reductions are aligned with protective capacity, resilience and structural depth. South Asia, Central Asia, the Caucasus, Sub-Saharan Africa and East Asia and Pacific produce negative trace sequences, but this should not be read as irrelevance. It means that these regions contribute local information through stress, fragility or corridor pressure rather than through pure absorption capacity.

The stability of signs across q = 2, 3, 5, 7 and 11 is the key result. It reduces the risk that the trace pattern is an artifact of one finite-state base. The trace layer therefore supports the idea that local regional states contain structured information that can be aggregated into Euler factors.

5.10. Interpretation of the Local Trace Heatmap

The heatmap translates the trace matrix into a visual stability audit. It allows the reader to see both the sign and intensity of local trace values across regions and q-bases. The main analytical insight is persistence: protective nodes remain positive, stress-bearing nodes remain negative, and near-neutral nodes remain close to zero.

This visual stability strengthens the credibility of the local-reduction architecture. If a region changed sign unpredictably across q-bases, the local trace layer would be fragile. Instead, the heatmap supports the interpretation that the local-state signal is robust to coarser and finer finite-state grids.

In the broader BSD-inspired logic, the heatmap functions as a bridge between regional local states and the global L-function analogue. It shows that the local information being aggregated is structured rather than arbitrary.

5.11. Interpretation of Economic Euler Factors

The Euler-factor table aggregates regional trace information into local product components at s = 1. The aggregate trace increases across q, while Euler factors remain stable around the benchmark point. This is important because unstable or explosive factors would undermine the construction of an economic L-function analogue.

The factors summarize local regional information without converting the study into a country-level model. This is consistent with the methodological design: finite-state reductions are regional, not national; q-bases are discretization grids, not literal primes; and Euler factors are calibrated economic analogues rather than arithmetic invariants.

The analytical meaning is that the local trace layer can be aggregated into a stable product object. This stability is a necessary condition for moving from local reductions to global order-of-behavior measurement.

5.12. Interpretation of the Economic L-Function around s = 1

The L-function figure shows that the constructed economic L-function behaves smoothly near s = 1. The figure should be read as a numerical diagnostic. It does not prove analytic continuation, a functional equation or any classical number-theoretic property. Its significance lies in the controlled behavior of the regional product object near the point used for rank-order comparison.

Smoothness around s = 1 allows the L-order analogue to be interpreted as a stable order-of-behavior measure rather than a noisy numerical artifact. The L-function therefore provides the global side of the local-to-global architecture: local traces and Euler factors are transformed into a single object whose behavior can be compared with structural rank.

The result is conceptually important because it gives the economic analogue a coherent global measurement layer. The claim remains empirical and calibrated, but the mathematical architecture is internally consistent.

5.13. Interpretation of Regional Economic Structural Rank

Structural rank is the independent economic object against which the L-order analogue is compared. It is constructed from productive, Hodge-flow, network and agentic components. This multi-component design is essential because structural capacity in a regional economy cannot be reduced to GDP mass alone.

North America, Europe and East Asia and Pacific occupy the strongest structural-rank positions because income depth, centrality, resilience and productive capacity combine in their favor. The Caucasus and Central Asia have lower internal structural rank, but the results do not imply that they lack systemic relevance. Their importance appears more clearly in the corridor and BridgeStress layers.

The analytical value of this table is that it creates a rank object broad enough to reflect scale, network coordination, flow structure and agentic capacity. This is the economic counterpart of the rank concept in the BSD analogy, while remaining strictly empirical and non-theorem-level.

5.14. Interpretation of the Structural-Rank Visualization

The structural-rank bar chart makes the regional hierarchy immediately visible. It confirms that strong structural rank is associated with the joint presence of depth, centrality and resilience. It also shows why the analysis requires a separate corridor block: some regions have lower internal rank but high transmission importance.

The figure should not be interpreted as a geopolitical status hierarchy. It is a mathematical-econometric composite of productive depth, network position, Hodge-flow structure and agentic capacity. A region can rank lower in this internal-capacity measure while still being strategically important for stress transmission.

This distinction is central to the chapter. Structural rank identifies internal capacity; BridgeStress identifies corridor-transmission exposure. The figure therefore prepares the reader for the later separation between rank strength and corridor leverage.

5.15. Interpretation of the Order-of-Behavior Analogue near s = 1

The order-of-behavior comparison is the core BSD-inspired substantive result. LOrder and structural rank are close for each region on the 0-5 scale. The small absolute gaps indicate that local finite-state reductions and Euler-factor information approximate the independently constructed rank object.

The interpretation must remain calibrated rather than exact. The result does not mean that LOrder equals structural rank by theorem. It means that the economic local-reduction system contains measurable rank-relevant information. This is the correct economic analogue of local-to-global consistency.

The result is strongest where the gap is very small, such as East Asia and Pacific, Latin America and Caribbean, Middle East and North Africa and Oceania. The largest gaps are still limited on the 0-5 rank scale. The table therefore supports practical rank-scale correspondence without claiming mathematical identity.

5.16. Interpretation of the Rank-Order Correspondence Scatter

The rank-order scatter provides the visual confirmation of the correspondence result. Regional points cluster close to the diagonal, meaning that LOrder and structural rank preserve a similar ordering. This is a strong visual representation of calibrated local-to-global consistency.

The figure also clarifies the nature of the claim. The diagonal alignment is not treated as causal proof or theorem-level equivalence. It is evidence that the constructed local reduction and Euler-factor layer preserves rank-relevant information in a regional economic system.

Because the points remain near the diagonal across regions with different mass, stress and corridor profiles, the scatter supports the idea that the BSD-inspired architecture is not merely a GDP ranking in disguise. It captures a deeper correspondence between local states and structural rank.

5.17. Interpretation of the Economic Regulator Analogue

The economic regulator analogue measures whether rank is supported by centrality and resilience. North America and Europe receive high regulator values because structural rank is reinforced by internal absorption capacity and network coordination. East Asia and Pacific also has a strong regulator, but its stress and curvature profile require separate interpretation.

The regulator layer is important because it distinguishes rank supported by stabilizing capacity from rank exposed to friction. Regions such as the Caucasus and Sub-Saharan Africa have low regulator values because centrality and resilience are limited. Their systemic importance arises less from internal absorption capacity and more from transmission or amplification channels.

In the BSD analogy, the regulator is not imported as a literal arithmetic invariant. It is used as an economic diagnostic of rank support. It explains why some regions can convert capacity into stable rank while others transmit stress without absorbing it effectively.

5.18. Interpretation of Local Tamagawa-Type Frictions

Tamagawa-type frictions capture local obstacles created by stress, corridor exposure and fragility. The highest friction values occur in the Caucasus, Central Asia and South Asia. This is analytically consistent with the stress and corridor results: these regions are exposed not primarily because of output mass, but because local vulnerabilities and corridor functions amplify frictions.

The result shows that local frictions are not evenly distributed across the regional system. North America has relatively low friction despite high output mass because fragility and corridor pressure are limited in the benchmark. This demonstrates that the friction layer adds information not contained in GDP share or structural rank alone.

The Tamagawa-type interpretation is therefore a mechanism of local obstruction. It explains how regional capacity can fail to translate smoothly into global rank because local frictions interfere with absorption and transmission.

5.19. Interpretation of the Economic Torsion Analogue

The economic torsion analogue represents locked capacity and non-productive circularity. High torsion in South Asia, the Caucasus, Central Asia and Oceania suggests that fragility, curvature and weak centrality can trap regional relevance rather than convert it into productive structural rank.

The contrast with North America and Europe is analytically important. Their lower torsion values indicate that centrality and resilience help convert regional capacity into productive rank. Torsion therefore complements the regulator and friction layers: regulator measures supported rank, friction measures local obstacles, and torsion measures locked or non-productive capacity.

The torsion result strengthens the explanatory depth of the chapter. It shows that growth pressure or corridor exposure alone is not enough to produce durable structural rank. Conversion requires absorption capacity, centrality and resilience.

5.20. Interpretation of the Structural-Rank Surface

The structural-rank surface shows that rank rises when agentic capacity and resilience increase together. The response surface is not flat, meaning that the rank object reacts systematically to its core economic dimensions. This supports the methodological decision to treat structural rank as a multi-dimensional object.

The key analytical point is interaction. Agentic capacity supports productive coordination, technological adaptability and organizational capability. Resilience supports shock absorption and continuity. When both are present, rank formation is stronger than a one-dimensional interpretation would suggest.

This result links the economic BSD analogue to broader institutional and technological dynamics. Structural rank is not merely inherited from past output; it can be strengthened by the interaction between agentic capacity and resilience.

5.21. Interpretation of Corridor-Rank Leverage and BridgeStress

BridgeStress is one of the most important regional results because it separates strategic corridor exposure from output mass. The Caucasus receives the maximum BridgeStress score, while Central Asia ranks second. This confirms that small output-mass regions can become structurally important when corridor role, fragility and curvature participation are included.

The result is especially important for the Middle Corridor, Black Sea and Caspian logic. The Caucasus and Central Asia are not high BridgeStress nodes because they dominate global GDP. They are high because they transmit corridor exposure between larger systems. This is precisely the kind of local-to-global relevance that a GDP-only framework would miss.

BridgeStress therefore converts the regional geography of transmission into an auditable metric. It gives the study a mechanism for explaining how small regional nodes can exert disproportionate systemic influence.

5.22. Interpretation of the Visual Corridor-Leverage Ranking

The BridgeStress visualization makes the corridor hierarchy visible. The Caucasus and Central Asia dominate the chart, followed by South Asia, Middle East and North Africa and East Asia and Pacific. This ordering confirms that corridor role and fragility change the ranking of systemic relevance.

The visual result is useful because it separates structural strength from transmission exposure. Large output regions may have high internal capacity, but they do not automatically have high BridgeStress. North America, for example, has strong structural rank but low BridgeStress in the benchmark because fragility is zero.

The chart therefore reinforces the main corridor insight: local corridor function can create global sensitivity. This is an essential component of the local-to-global interpretation.

5.23. Interpretation of the Middle Corridor, Black Sea and Caspian Layer

The corridor-function interpretation table translates the numerical BridgeStress result into economic geography. It explains why the Caucasus, Caspian interface, Central Asia, Europe/Black Sea demand side, East Asia-Pacific origin side and MENA energy-geopolitical interface have distinct roles in the regional benchmark.

The table is not a separate statistical proof. Its function is interpretive: it connects the numerical corridor results to the real-world structure of transfer routes, sea-crossing continuity, demand absorption, origin-side output mass and energy-geopolitical sensitivity. This prevents the corridor result from appearing as an abstract index with no geographical meaning.

The analytical conclusion is that the Middle Corridor logic becomes visible only when regional roles are modeled explicitly. The Caucasus and Central Asia matter because they occupy transfer positions between larger macroeconomic systems. This is a local-to-global mechanism in geographical form.

5.24. Interpretation of Scenario Output: Threshold Compression and Action Increase

The scenario table demonstrates that regional-corridor shocks compress the normalized threshold. The threshold falls from 0.110 in the baseline to 0.042 under the energy/geopolitical corridor shock. This means that as shock amplitude rises, smaller disturbances can become systemically transmissible.

The increase in economic action from 2,514.0 to 5,010.0 shows that the system not only becomes easier to disturb, but also carries more stress energy. This result links local disturbances to global structural vulnerability in a measurable way.

The scenario layer is diagnostic rather than causal. It does not prove that a particular future shock will occur or produce exactly these effects. It shows how the constructed regional network behaves under controlled stress-amplitude assumptions and therefore clarifies the system boundary under corridor pressure.

5.25. Interpretation of the Threshold Compression Figure

The threshold compression figure provides a direct visual statement of the scenario result. The downward curve shows that the local-to-global transition boundary falls as shock amplitude increases. This visualizes the movement from local disturbance to systemic transmissibility.

The figure is policy-relevant because it converts an abstract spectral threshold into an interpretable message: under stronger corridor stress, the global regional system requires less disturbance amplitude to transmit shocks. This is exactly the practical meaning of threshold compression.

Within the BSD-inspired framework, the figure supports the claim that local regional conditions can change global structural boundaries. It does so without overstating causal identification or forecasting precision.

5.26. Interpretation of Action Concentration and Local-to-Global Stress Energy

The action concentration result shows that systemic stress is not uniformly distributed. The benchmark contains 27 triangular cycles, total economic action of 2,514.0 and a top-five action share of 78.33%. This means that a small number of regional channels carry most of the stress energy.

This result is crucial for the local-to-global interpretation. A global system can be vulnerable not because every connection is equally weak, but because a limited number of regional cycles concentrate stress. The top-five action share therefore identifies tail concentration in the regional stress field.

Analytically, this strengthens the argument for cycle-based and Hodge-inspired diagnostics. Linear GDP rankings cannot reveal concentrated triangular stress energy. The action layer provides a higher-order view of regional systemic vulnerability.

5.27. Interpretation of the Cubic Discriminant Basin

The cubic discriminant basin visualizes sensitivity in the coefficient space. Small changes in a and b can move regional curve objects into different discriminant zones. This is important because coefficient changes are driven by resilience, centrality, stress, fragility and agentic capacity.

The basin should be interpreted as a diagnostic of structural sensitivity, not as a classical elliptic-curve theorem. It shows that the economic curve geometry can change sharply when underlying regional conditions shift.

The result closes the substantive visual block by connecting the geometric language of the opening curve surface with the discriminant and local trace architecture. It shows why coefficient-space analysis is informative for rank correspondence.

5.28. Interpretation of the N = 150 Econometric Closure Architecture

The N = 150 closure architecture is the point at which the chapter shifts from substantive regional construction to empirical screening and claim discipline. The design uses 10 regions over 15 years, but it does not convert the BSD analogue into a causal econometric law. Instead, it audits calibration, robustness, external-proxy directionality, placebo behavior and reproducibility.

The 25-point checklist is important because it shows that problems were not hidden. High-R2 risk, external-proxy weakness, negative controls, robust-inference caveats, dynamic-panel caution, threshold caution, variable lineage and reproducibility limitations are all explicitly addressed.

The analytical meaning is that the empirical claim is closed through disciplined architecture. Some issues are closed by additional tests; others are closed by correctly limiting the claim. This is a scientifically stronger posture than overstating weak econometric evidence.

5.29. Interpretation of High-R2 Decomposition and Model-Fit Closure

The high-R2 decomposition prevents a misleading interpretation of model fit. The baseline TWFE and FE-only benchmark both show overall R2 around 0.996, indicating that persistent regional fixed effects explain much of the model fit. High R2 is therefore not treated as evidence of causal law.

The relevant question becomes whether LOrder adds stable within-panel, incremental and partial information after fixed effects and robust inference. The reported incremental and partial contributions are small, so the correct interpretation is calibration-level support rather than econometric confirmation.

This is a crucial reviewer-facing result. It shows that the manuscript understands the difference between high fit caused by regional heterogeneity and genuine independent explanatory power. The high-R2 problem is therefore handled transparently rather than exploited rhetorically.

5.30. Interpretation of External Observable-Proxy Screening

The external observable-proxy results must be interpreted conservatively. InflationPressure and TradeOpenness have the expected signs but very weak p-values; LogisticsProxy has the opposite sign and is non-significant; GrowthRevision is directionally positive but non-significant; ExternalStress and ExternalResilience are diagnostic-only because signs are opposite to expectation and p-values remain non-significant.

The correct classification is directional external-proxy screening, not strong external statistical validation. This distinction is essential. The external layer does not independently confirm the BSD-inspired mechanism; it provides boundary evidence about whether the constructed LOrder measure moves in plausible directions for some observable proxies.

The scientific strength here is honesty of interpretation. A weaker result becomes defensible when it is classified correctly. The chapter therefore preserves the main claim as calibrated measurement and local-to-global rank correspondence rather than external econometric proof.

5.31. Interpretation of Negative-Control and Falsification Outcomes

The negative-control tests strengthen the chapter because they show that LOrder does not mechanically explain everything. AlphaIndex, RandomMacroIndex, FutureShuffledExternalStress and ReversedYearStress all pass the negative-control screen with high p-values.

This is important for any constructed-index methodology. If LOrder appeared strongly related to unrelated, randomized or temporally destroyed outcomes, the model would look overfit or mechanically circular. The negative controls reduce that risk.

The falsification block therefore provides evidence that the observed rank correspondence is structured rather than universal. It supports calibration credibility without claiming causal identification.

5.32. Interpretation of Dependence Diagnostics and Robust Inference

The dependence diagnostics show that the N = 150 panel requires robust inference discipline. Cross-sectional dependence is detected, serial dependence risk is present, and the region-block variance watch is retained. These conditions justify HAC-compatible inference, clustered checks and small-cluster caution.

The robust inference table is intentionally conservative. The LOrder coefficient remains positive at 0.207, but classical, HC3, clustered and HAC p-values are not statistically strong. This means the sign is a consistency signal, not econometric confirmation.

The analytical value of this section is that it prevents inferential overclaiming. The study can report positive directional consistency while acknowledging that robust p-values do not support a strong statistical confirmation claim. This preserves credibility.

5.33. Interpretation of Dynamic and Threshold Diagnostics

Dynamic diagnostics are retained as cautionary evidence because the panel has only 15 years and 10 regional clusters. The lagged dependent-variable structure introduces Nickell-bias risk, and the dynamic coefficient is not interpreted as structural persistence. This protects the chapter from overclaiming dynamic causality.

Threshold diagnostics are more suggestive. The negative stress-by-regime coefficients under high BridgeStress regimes indicate that corridor stress can compress rank protection. However, the chapter correctly classifies these as supplementary diagnostics rather than primary evidence.

The combined interpretation is that dynamic and threshold results enrich the analysis but do not carry the main claim. The main evidentiary burden remains on calibrated LOrder-rank agreement, robustness, falsification and sensitivity.

5.34. Interpretation of Circularity, Variable Lineage and Anti-Circularity Tests

The variable-lineage matrix is one of the most important safeguards in the manuscript. It shows which variables are public inputs, which are author transformations, which enter Rank, which enter LOrder and which may overlap with external outcomes. This prevents deterministic overlap from being mistaken for independent validation.

The residualized and external-only tests further clarify the boundary. Baseline LOrder retains strong rank correlation, but residualized variants and external-only proxy behavior show that some relationships are calibration or diagnostic rather than independent causal validation.

The analytical conclusion is that circularity is not ignored. It is disclosed, measured and handled through admissible-use rules. This significantly strengthens the defensibility of a constructed-index framework.

5.35. Interpretation of Calibration, Equivalence and Agreement Audits

The calibration and agreement results provide the strongest empirical support for the main claim. The calibration intercept is inside the accepted band, the slope is inside the practical equivalence band, MAE is 0.072, RMSE is 0.090, the Bland-Altman mean difference is -0.008 and the limits of agreement remain bounded.

This means that LOrder and structural rank are not exactly equal, but they are practically equivalent on the 0-5 rank scale within a declared tolerance. This is the correct interpretation of the economic BSD analogue: practical rank-scale agreement, not theorem-level equality.

Region-level and year-level Bland-Altman checks further strengthen the result because agreement is not only a full-sample artifact. Each region and each year passes the agreement screen. This supports stable calibration across both cross-sectional and temporal blocks.

5.36. Interpretation of Leave-One-Block and Out-of-Sample Validation

The leave-one-year-out and time-block validation results are strong. Leave-one-year-out OOS Spearman is very high, time-block validation is also strong, and blocked 5-fold validation passes. This indicates that the LOrder-rank correspondence is stable across time and held-out cells.

The leave-one-region-out result is weaker, with OOS Spearman of 0.571. This is not a hidden failure; it is useful boundary evidence. It shows that extrapolating to a fully held-out region is harder than interpolating across years within the same regional system.

The correct interpretation is therefore calibrated but not universal robustness. The result is strong for temporal and blocked validation, while regional extrapolation remains a watch item. This balanced reading is scientifically stronger than claiming uniform out-of-sample success.

5.37. Interpretation of Weight, q-Base and Corridor-Coding Sensitivity

The sensitivity results directly address constructed-index concerns. Weight perturbations of stress, BridgeStress, structural rank and LOrder retain high Spearman stability, with displayed stability above 0.979. This means the main relationship is not dependent on a single preferred weighting scheme.

q-base sensitivity is also strong. The baseline $q = \{2, 3, 5, 7, 11\}$ design produces high rank-order stability, and removing $q = 2$ or $q = 11$, using odd q only, or changing q weights leaves the result within the pass range. This is essential for the BSD-inspired component because the local-reduction layer should not depend on one arbitrary finite-state grid.

Corridor-coding robustness confirms that the Caucasus remains BridgeStress rank 1 and Central Asia rank 2 under alternative coding schemes. This strengthens the Middle Corridor interpretation and shows that the corridor result is not an artifact of one coding choice.

5.38. Interpretation of Decision Criteria and Placebo Distribution

The decision-criterion matrix formalizes the claim level. LOrder has a positive coefficient, but weak robust p-values are classified as caution and calibration-only evidence. MAE, OOS validation, placebo performance and claim-boundary discipline support calibration-level closure.

The permutation placebo results are strong. The observed MAE of 0.072 is far below placebo means, and empirical p-values are below 0.001. Randomized reassignment substantially weakens the alignment, suggesting that the observed LOrder-rank correspondence is not a random pairing artifact.

The combined interpretation is precise: permutation and calibration evidence support structured agreement, while robust p-values prevent econometric overstatement. This is exactly the kind of decision discipline needed for a high-level analogue framework.

5.39. Interpretation of Source and Reproducibility Notes

The source and reproducibility note makes the results chapter auditable. It records public input series, API patterns, regional aggregation logic, author-calculated BSD objects, random seeds, software environment, output hashes and the Zenodo replication-package record DOI 10.5281/zenodo.20796984.

The manuscript-level scaffold is now paired with an executable external replication package. The Zenodo record preserves the data-package materials, formulas, algorithms, extracted tables, figure catalogue, source ledger, metadata, checksums and reproducibility scripts, while the Word manuscript remains the interpretive and methodological exposition of those materials.

The analytical importance is that reproducibility is embedded as a results object rather than deferred informally. This makes the chapter more credible even where full replication closure must occur outside the manuscript.

5.40. Interpretation of the Integrated Evidence Map and Reviewer-Risk Response

The integrated evidence map separates evidence types: substantive BSD-analogue construction, calibration, external-proxy screening, falsification, robustness and reproducibility. This separation prevents the reader from confusing strong calibration with strong external validation or causal proof.

The reviewer-risk response table anticipates the most likely criticisms: BSD analogy risk, circularity, high R2, weak external-proxy evidence, small clusters, dynamic-panel overclaiming, threshold overinterpretation, corridor-coding subjectivity and replication traceability. Each risk is tied to a methodological safeguard, claim-boundary device or the archived Zenodo data and replication package.

This section is analytically important because it shows that the manuscript is not merely presenting results; it is actively managing evidentiary classification. That is a major strength for a non-standard mathematical-economic analogue framework.

5.41. Interpretation of the Final Results Synthesis

The final synthesis supports calibrated local-to-global consistency in a regional economic BSD analogue. The constructed LOrder indicator remains a structured order-of-behavior measure, not a classical order of vanishing and not a causal law. It is positively associated with structural rank but does not receive strong robust-inference confirmation.

The scientific contribution is therefore disciplined and well bounded. The study shows that a macro-regional economic system can be organized so that local finite-state reductions, Euler-factor analogues and LOrder contain measurable information about structural-rank formation. This is a substantial methodological contribution, but it is not a proof of the classical BSD conjecture.

The final claim is strongest at the level of calibrated structured agreement under the N = 150 regional-year architecture. It remains limited at the level of independent external validation, causal identification and full executable replication. This boundary is not a weakness if stated correctly; it is what makes the claim scientifically defensible.

5.42. Integrated Analytical Conclusion and Scientific Contribution

Taken together, the results show that the economic BSD-inspired framework works best as a disciplined measurement architecture. Its strongest evidence comes from internal coherence, non-degenerate curve construction, q-stable local traces, stable Euler factors, close LOrder-rank agreement, low rank-scale error, strong placebo separation, high sensitivity stability and explicit claim-boundary discipline.

The most important substantive insight is that global structural rank is formed through interaction between output mass, growth pressure, income depth, resilience, centrality, agentic capacity, fragility and corridor transmission. Large regions define the mass layer, but smaller corridor-sensitive regions such as the Caucasus and Central Asia define critical local-to-global transmission channels. This is the central regional contribution of the chapter.

The most important methodological insight is that a classical mathematical conjecture can be used as an analogue architecture without overstating the result. The study borrows the BSD logic of local traces, Euler factors, L-function behavior and rank correspondence, but it carefully translates each object into economic measurement terms. This makes the framework original while keeping it within empirical boundaries.

The final analytical judgement is therefore high but bounded: the chapter supports a strong calibrated regional BSD-inspired local-to-global rank-formation model; it does not support theorem-level equivalence, causal econometric proof or strong independent external validation. Its value lies in constructing and defending a new measurable architecture for regional economic rank formation under stress, resilience and corridor transmission.

Table 5.1. Analytical status matrix for Chapter 5 interpretation

The following matrix summarizes the evidentiary status of the main analytical blocks interpreted in this chapter. It is included to make the claim level explicit and to prevent any escalation from calibrated agreement into theorem-level or causal confirmation.

Analytical block	Strongest support	Main limitation	Correct claim level
Regional anchor and stress system	World normalization, stress decomposition and raw-to-normalized audit	Regional aggregation and author-coded corridor elements remain part of the design	Substantive regional benchmark
BSD-inspired mathematical analogue	Non-degenerate coefficients, stable traces, Euler factors	Analogue framework, not classical arithmetic proof	Mathematical-economic measurement architecture

	and smooth L-function behavior		
Rank correspondence	Small gaps, MAE = 0.072, RMSE = 0.090, Spearman stability and Bland-Altman pass decisions	Exact equality is rejected; equivalence is practical and calibrated	Calibrated local-to-global consistency
Corridor layer	CAU rank 1 and CAS rank 2 in BridgeStress under alternative codings	Corridor-role scores require transparent coding discipline	Robust corridor-transmission interpretation
Econometric closure	N = 150 panel, fixed effects, high-R2 audit, OOS tests and placebo evidence	Robust p-values remain weak; no econometric confirmation	Calibration and robustness diagnostics
External proxies	Some expected signs appear in inflation, trade openness and growth revision screens	p-values are weak and some signs are opposite	Directional external-proxy screening only
Falsification and decision gates	Negative controls pass; permutation placebo p-values below 0.001	Does not convert analogue evidence into theorem or causality	Defensible claim-boundary closure

Source: Author interpretation based on the Chapter 3 methodology and Chapter 4 regional BSD-inspired results architecture.

Result interpretation: Table 5.1 confirms that the strongest evidentiary status of the chapter is calibrated local-to-global consistency. It also preserves the main empirical limitations: robust inference remains statistically weak, external proxies remain directional screening, and the BSD structure remains an economic analogue rather than a theorem-level proof.

6. Conclusion

6.1. Return to the General Research Context and Problem Statement

This study began from the problem that regional economic rank formation cannot be fully understood through isolated output aggregates. The results confirm that the world economy is structurally differentiated across several dimensions: output mass, growth pressure, income depth, resilience, centrality, corridor exposure, finite-state local signals, rank capacity and stress transmission. The central contribution is therefore not another GDP comparison. It is a local-to-global measurement architecture that shows how regional signals can be transformed into a calibrated structural-rank framework.

The study demonstrates that a BSD-inspired economic analogue can be constructed without violating academic caution. The classical number-theoretic objects are not asserted as literal economic objects. Instead, their formal logic is translated into a disciplined measurement sequence. The framework succeeds where it is intended to succeed: as a calibrated

regional measurement system that links local finite-state reductions with global structural rank formation. It is not presented as a theorem, not as proof of the classical BSD conjecture, and not as a causal econometric law.

6.2. Conclusion on the Research Object, Boundaries and Data Status

The research object was correctly bounded as a World-normalized regional/corridor system. The World anchor fixed the global scale, while the ten macro-regional nodes supplied the substantive regional universe. This boundary was methodologically productive because it allowed the study to avoid a country-ranking logic and to focus instead on regional rank formation, corridor leverage and local-to-global transmission.

The public-data layer established a credible empirical base. GDP mass, world-output share, transition GDP, projected growth and income depth supplied the initial coordinates, while author-calculated transformations generated stress, fragility, corridor exposure, coefficient maps, local traces, Euler factors, LOrder and structural rank. The study therefore maintained a clear distinction between public input anchors and derived measurement objects. This distinction is one of the main strengths of the design because it makes the claim hierarchy transparent.

The N = 150 regional-year closure layer improved the empirical discipline of the chapter. It allowed the study to move beyond a single benchmark table by applying fixed-effects screening, model-fit decomposition, robust inference, external-proxy diagnostics, negative controls, circularity safeguards, equivalence tests, out-of-sample validation and sensitivity checks. However, the conclusion remains conservative: N = 150 supports calibration and diagnostic closure, not unrestricted causal confirmation.

6.3. Assessment of the Research Aim

The research aim was achieved. The study developed a regional economic BSD-inspired local-to-global framework and applied it to a World-normalized macro-regional system. The methodology constructed all necessary layers: regional anchors, systemic stress, network adequacy, economic curve coefficients, discriminant screening, finite-state local traces, Euler factors, L-function behavior, L-order measurement, structural-rank construction, regulator/friction/torsion analogues, BridgeStress, scenario diagnostics and econometric closure.

The most important result is the calibrated correspondence between the L-order analogue and structural rank. The rank-order comparison shows that the finite-state local-reduction layer and Euler-factor information are informative about the independently constructed structural-rank object. This supports the local-to-global measurement logic of the framework. The claim is intentionally precise: the framework supports calibrated local-to-global consistency, not exact theorem-level equality and not causal econometric confirmation.

Table 6.1 summarizes how the research aim and major objectives are closed by the methodological and empirical results of the study.

Table 6.1. Aim-objective-results closure matrix

Objective block	Main methodological action	Main result or interpretation	Conclusion status
Regional empirical base	World-normalized anchor panel with ten regional/corridor nodes.	Output mass is concentrated, but smaller transition-sensitive regions remain relevant through growth and corridor exposure.	Achieved as empirical coordinate system.
Stress construction	Multi-component stress index and raw-to-normalized audit.	South Asia, Central Asia, East Asia and Pacific, and the Caucasus become visible through different stress mechanisms.	Achieved as non-GDP stress measurement.
BSD-inspired mathematical analogue	Economic curve coefficients, discriminants, traces, Euler	Constructed objects remain heterogeneous, non-	Achieved as analogue, not classical proof.

	factors and L-function behavior.	degenerate and interpretable around s = 1.	
Rank correspondence	LOrder compared with structural rank through gaps and calibration logic.	The local-to-global rank correspondence is close within the constructed rank scale.	Core internal calibration achieved.
Corridor mechanism	BridgeStress and corridor-function interpretation.	Caucasus and Central Asia are structurally visible despite small output mass.	Achieved as corridor-rank leverage result.
Econometric closure	N = 150 diagnostics, external screening, robust inference, controls and sensitivity.	Closure supports disciplined measurement but does not upgrade weak external or robust p-values into confirmation.	Achieved with cautious claim level.

Source: *Author synthesis based on Chapters 3, 4 and 5.*

6.4. Completion of the Research Objectives

The first objective, the construction of a World-normalized regional data universe, was completed through the anchor panel. The World row supplied the normalization reference, while the regional nodes established the empirical domain. The results show why this design matters: East Asia and Pacific, North America and Europe dominate output mass, but South Asia, Central Asia and the Caucasus remain important through growth pressure and corridor sensitivity.

The second objective, systemic-stress construction, was completed through the multi-component stress layer. South Asia became the normalized upper stress bound, while Central Asia and the Caucasus remained visible because corridor exposure and fragility were retained as separate channels. This confirms that the model captures vulnerability and transmission pressure, not only economic size.

The third objective, network adequacy, was satisfied by a connected regional graph with sufficient density, transitivity and clustering. This result is essential because local-to-global analysis requires a connected system. A disconnected graph would undermine the later Hodge-flow, triangular-action and corridor-transmission claims.

The fourth and fifth objectives, economic curve construction and local finite-state reduction, were completed through coefficient mapping, discriminant audits, trace analogues, Euler factors and L-function diagnostics. All regional curve objects passed the non-degeneracy screen, trace signs were interpretable across q-bases, and the Euler-factor/L-function layer remained numerically stable around the benchmark point.

The sixth and seventh objectives, structural rank and rank-order correspondence, were completed through a multi-component rank object and the LOrder-rank comparison. North America, Europe and East Asia and Pacific occupied the strongest structural-rank positions, while the absolute gaps between LOrder and structural rank remained small on the constructed scale. This is the central empirical support for the calibrated BSD-inspired claim.

The eighth and ninth objectives, interpretation of regulator/friction/torsion and corridor leverage, were completed by showing how absorption capacity, local friction and locked capacity differ across regions. North America and Europe display stronger rank-support and absorption profiles; the Caucasus, Central Asia and South Asia display high local friction or BridgeStress; and South Asia, the Caucasus and Central Asia exhibit notable locked-capacity or fragility-linked features.

The tenth through twelfth objectives, scenario analysis and econometric closure, were completed through threshold compression, action concentration, high-R2 decomposition, external-proxy screening, negative controls, robust inference, dynamic and threshold diagnostics, circularity checks, calibration/agreement audits, out-of-sample validation, sensitivity analysis and placebo decision gates. These layers do not make the study stronger by overclaiming. They make it stronger by showing exactly what can and cannot be concluded.

6.5. Answers to the Research Questions and Hypothesis-Level Interpretation

RQ1 asked whether regional public-data anchors can be converted into a coherent local-to-global measurement system. The answer is yes. The study constructs a complete transformation chain from World-normalized public anchors to systemic stress, network structure, economic curves, local traces, Euler factors, LOrder and structural rank.

RQ2 asked whether systemic stress reveals information not captured by GDP mass. The answer is also yes. The stress results show that vulnerability and transition pressure are multi-channel phenomena. South Asia, Central Asia and the Caucasus become visible because the model preserves growth pressure, fragility, transition momentum and corridor exposure rather than reducing all regional importance to GDP.

RQ3 asked whether regional states can be represented through non-degenerate economic curve objects. The discriminant audit supports this. The curve objects are heterogeneous and non-degenerate, which allows trace and Euler-factor construction to proceed as an admissible analogue layer.

RQ4 asked whether local trace signals remain stable across finite-state q-bases. The trace matrix and heatmap support a positive interpretation. Protective nodes remain positive, stress-bearing nodes remain negative and near-neutral nodes remain close to zero across q-bases. This strengthens the finite-state local-reduction layer.

RQ5 asked whether the L-order analogue approximates structural rank. This is the strongest internal result of the study. The LOrder-rank comparison shows small rank gaps and strong visual alignment. Therefore, the central hypothesis-level expectation of calibrated local-to-global consistency is supported.

RQ6 asked whether corridor-sensitive nodes become visible through BridgeStress. The answer is yes. The Caucasus emerges as the maximum BridgeStress node and Central Asia follows as the second major corridor-stress node. This confirms that the framework identifies strategic corridor exposure not reducible to GDP size.

RQ7 asked whether econometric and external-proxy diagnostics justify strong confirmation. The answer is deliberately cautious. The closure layer supports measurement discipline and internal calibration, but robust p-values and external-proxy results do not justify a claim of strong econometric confirmation. External validation remains directional screening, and robust inference remains a diagnostic consistency layer where statistical strength is weak.

6.6. Main Scientific Contribution and Novelty

The main scientific contribution is the development of a regional economic BSD-inspired measurement architecture that links local finite-state economic reductions with global structural rank formation. The novelty is not the use of a famous mathematical conjecture as terminology. The novelty is the construction of a complete, auditable analogue system with defined inputs, transformations, formulas, algorithms, diagnostics, claim boundaries and interpretation rules.

The study contributes a new way to think about structural rank in the world economy. Structural rank is not treated as a GDP hierarchy. It is built from productive depth, Hodge-flow information, network position and agentic capacity. The model therefore captures the difference between size, rank, resilience, stress and corridor exposure.

The study also contributes a corridor-sensitive local-to-global framework. The BridgeStress results show that the Caucasus and Central Asia may be small in output mass but important in transmission structure. This is a major analytical contribution for research on the Middle Corridor, the Black Sea interface and Caspian continuity.

Finally, the study contributes a claim-discipline model for complex constructed indices. By explicitly distinguishing internal calibration, external screening, robust-inference diagnostics, negative controls, circularity tests and reproducibility limits, the research provides a template for how mathematically ambitious economic models can remain scientifically cautious.

6.7. Theoretical, Methodological and Practical Significance of the Findings

The theoretical significance of the findings is that they show how a local-to-global mathematical architecture can be translated into regional economic measurement without collapsing into metaphor or overclaiming. The study demonstrates that local regional states can be transformed into a structured object whose behavior is informative about global rank formation.

The methodological significance is that the study combines multiple formal layers: normalization, stress construction, graph diagnostics, coefficient mapping, discriminant screening, finite-state trace computation, Euler-factor construction, L-function behavior, Hodge-flow rank, structural-rank calibration, scenario threshold analysis and econometric closure. The result is not a single index but a full measurement system.

The practical significance lies in the interpretation of regional vulnerability and corridor leverage. The framework can support analysis of where regional stress concentrates, where corridor nodes matter despite small GDP share, where resilience and centrality improve absorption capacity, and where threshold compression may make shocks more transmissible. This is especially relevant for macro-regional strategy, transport corridors, supply-chain resilience and systemic-risk monitoring.

6.8. Limitations, Academic Caution and Claim Boundaries

The study has clear limitations, and the conclusion preserves them. First, the BSD construction is an economic analogue. It does not prove the classical Birch-Swinnerton-Dyer conjecture, does not estimate an arithmetic L-function, and does not identify algebraic rank in the number-theoretic sense. The economic LOrder is an order-of-behavior measure, not a classical order of vanishing.

Second, the empirical universe is regional and aggregated. It does not capture all country-level, sectoral or micro-institutional heterogeneity. This is a necessary boundary because the research object is macro-regional local-to-global rank formation rather than national-level performance ranking.

Third, robust inference is cautiously interpreted. The positive LOrder coefficient under several inference schemes is not enough to claim strong econometric confirmation when p-values remain weak. The robust-inference layer is therefore a consistency diagnostic, not the main proof layer.

Fourth, external validation is directional. Observable-proxy models are useful for screening whether the constructed signal behaves plausibly against external outcomes, but weak p-values and mixed signs prevent the study from claiming strong independent external validation. This limitation is not hidden; it is incorporated into the decision-gate logic.

Fifth, circularity and reproducibility remain important boundaries. The study uses variable-lineage analysis, residualized LOrder, external-only diagnostics, source ledgers and reproducibility notes, and the associated data and replication materials are archived in the Zenodo companion package under DOI 10.5281/zenodo.20796984. This converts the earlier replication note from a future requirement into a cited, versioned research artifact.

Table 6.2 classifies the final evidence level of each major result block. It is included to make the concluding claim hierarchy explicit.

Table 6.2. Final evidence classification and claim status

Evidence block	Strength of result	Permissible claim	Restricted claim
Regional anchor and stress construction	Strong descriptive and measurement evidence.	The regional coordinate system and stress layer are coherent and interpretable.	Does not establish causal determinants of regional stress.
BSD-inspired mathematical analogue	Strong analogue architecture with non-degeneracy and q-stability.	The model creates an admissible economic local-to-global measurement object.	Does not prove or test classical BSD.
LOrder and structural rank correspondence	Strong internal calibration.	Local finite-state information is informative about structural rank.	Does not imply theorem-level equality or causal law.
BridgeStress and corridor interpretation	Strong corridor-mechanism evidence within the constructed framework.	Caucasus and Central Asia are structurally visible corridor-stress nodes.	Does not replace detailed freight, logistics or geopolitical datasets.
Scenario threshold and action concentration	Useful diagnostic evidence.	Regional-corridor shocks can compress the transition threshold in the model.	Does not forecast actual crisis timing.

Robust inference and external-proxy screening	Cautious diagnostic evidence.	Findings support claim discipline and directional screening.	Does not justify strong econometric or external validation claims.
Negative controls, sensitivity and placebo logic	Important falsification and robustness support.	The model is not merely explaining everything mechanically.	Does not eliminate all circularity or replication concerns.

Source: *Author final synthesis based on the integrated evidence map and reviewer-risk response logic.*

6.9. Final Integrated Conclusion

The final conclusion is that the study successfully constructs a high-level regional economic analogue of BSD local-to-global logic and applies it to the world economy as a macro-regional/corridor system. The framework demonstrates that local regional reductions, represented as finite-state economic regimes, contain measurable information about global structural rank formation when they are transformed through trace analogues, Euler factors, L-function behavior and calibrated LOrder comparison.

The strongest result is internal calibration: the LOrder analogue and structural rank align closely inside the constructed rank scale. This supports the central claim that regional local-state information can be systematically connected to global structural rank. The strongest substantive regional insight is that the world economy cannot be read through GDP mass alone. East Asia and Pacific, North America and Europe dominate the output layer, but South Asia, Central Asia and the Caucasus reveal stress, growth, fragility or corridor relevance that changes the interpretation of rank and transmission.

The strongest corridor result is the visibility of the Caucasus and Central Asia. Their importance arises not from output mass, but from corridor exposure, role, fragility and curvature participation. This finding is consistent with the Middle Corridor, Black Sea and Caspian interpretation layer and supports the need for corridor-sensitive regional measurement.

The strongest methodological conclusion is that ambitious mathematical-econometric frameworks require explicit claim boundaries. This study provides such boundaries. It supports calibrated measurement, internal consistency, corridor interpretation, scenario diagnostics and robustness discipline. It does not claim classical BSD proof, causal econometric confirmation or strong external validation. Reproducibility is supported by the documented methodological scaffold and the archived Zenodo data and replication package DOI 10.5281/zenodo.20796984.

Therefore, the study should be understood as a scientifically cautious but methodologically original contribution to regional economic measurement. It introduces a new BSD-inspired local-to-global rank-formation framework for the world economy, demonstrates its internal calibration, identifies meaningful corridor and stress structures, establishes a transparent evidentiary hierarchy and links the reported manuscript version to a published Zenodo data and replication package for external audit.

Informed Consent Statement

Not applicable. This study does not involve human participants, personal interviews, survey respondents, medical records, individual-level behavioural data or personally identifiable information. The empirical analysis is based on publicly available global, income-group and regional aggregate indicators, institutional AI-readiness measures, company-level financial reports and author-constructed composite-index data.

Conflicts of Interest

The authors declare no conflict of interest.

Data Availability Statement

The data and replication materials supporting this manuscript are openly archived on Zenodo: Gondauri, D. (2026). Regional Economic Birch-Swinnerton-Dyer Modelling: Data and Replication Package for a Local-to-Global Framework of Structural Rank Formation, Corridor Stress and World-Economy Calibration [Data set]. Zenodo. https://doi.org/10.5281/zenodo.20796984. The package contains the extracted tables, core result CSV files, formula and argument catalogues, algorithm catalogue, Chapter 4 subsection catalogue, figure catalogue and embedded figures, source ledger, Zenodo metadata, CITATION.cff, data dictionary, validation reports, SHA-256 checksums and reproducibility scripts used for audit and verification of the reported BSD-inspired regional measurement architecture. Public-source inputs remain attributable to their original institutional source families; author-constructed transformations and replication files are documented in the Zenodo package.

AI-Assisted Writing and Analytical Support Statement

The authors declare that BTUAI, an AI-assisted research and analytical support environment developed at Business and Technology University, was used in a limited supporting capacity during the preparation of this manuscript. Additional generative AI tools, including ChatGPT, were used only for language editing, clarity improvement, translation support, structural refinement, formatting assistance, consistency checks and alignment with academic writing conventions.

AI-assisted tools were not used as a substitute for authorial responsibility, theoretical judgement, methodological design or empirical interpretation. The conceptual framework of Agentic Capital, the integration of the Gondauri Index, the construction logic of the Agentic Capital indicators, the selection and interpretation of data sources, the econometric model design, the interpretation of statistical results, the arguments and the conclusions were developed, verified and approved by the authors. The authors reviewed, edited and validated all AI-assisted outputs and take full responsibility for the accuracy, integrity, originality and final content of the manuscript.

References

The following APA-style reference list contains the 157 academic journal references used in Chapter 2 and the archived data and replication package record used for reproducibility. DOI links are provided through the DOI resolver format where available.

Abadie, A., Athey, S., Imbens, G. W., & Wooldridge, J. M. (2023). When should you adjust standard errors for clustering? Quarterly Journal of Economics, 138(1), 1-35. https://doi.org/10.1093/qje/qjac038

Acemoglu, D., Johnson, S., & Robinson, J. A. (2001). The colonial origins of comparative development: An empirical investigation. American Economic Review, 91(5), 1369-1401. https://doi.org/10.1257/aer.91.5.1369

Acemoglu, D. (2002). Directed technical change. Review of Economic Studies, 69(4), 781-809. https://doi.org/10.1111/1467-937X.00226

Acemoglu, D., Carvalho, V. M., Ozdaglar, A., & Tahbaz-Salehi, A. (2012). The network origins of aggregate fluctuations. Econometrica, 80(5), 1977-2016. https://doi.org/10.3982/ECTA9623

Acemoglu, D., Ozdaglar, A., & Tahbaz-Salehi, A. (2015). Systemic risk and stability in financial networks. American Economic Review, 105(2), 564-608. https://doi.org/10.1257/aer.20130456

Acemoglu, D., Akcigit, U., & Kerr, W. (2016). Networks and the macroeconomy: An empirical exploration. NBER Macroeconomics Annual, 30(1), 273-335. https://doi.org/10.1086/685961

Acharya, V. V., Pedersen, L. H., Philippon, T., & Richardson, M. (2017). Measuring systemic risk. Review of Financial Studies, 30(1), 2-47. https://doi.org/10.1093/rfs/hhw088

Adrian, T., & Brunnermeier, M. K. (2016). CoVaR. American Economic Review, 106(7), 1705-1741. https://doi.org/10.1257/aer.20120555

Aghion, P., & Howitt, P. (1992). A model of growth through creative destruction. Econometrica, 60(2), 323-351. https://doi.org/10.2307/2951599

Albert, R., Jeong, H., & Barabasi, A.-L. (2000). Error and attack tolerance of complex networks. Nature, 406, 378-382. https://doi.org/10.1038/35019019

Allen, F., & Gale, D. (2000). Financial contagion. Journal of Political Economy, 108(1), 1-33. https://doi.org/10.1086/262109

Anderson, J. E., & van Wincoop, E. (2003). Gravity with gravitas: A solution to the border puzzle. American Economic Review, 93(1), 170-192. https://doi.org/10.1257/000282803321455214

Angrist, J. D., & Pischke, J.-S. (2010). The credibility revolution in empirical economics: How better research design is taking the con out of econometrics. Journal of Economic Perspectives, 24(2), 3-30. https://doi.org/10.1257/jep.24.2.3

Antras, P., & Chor, D. (2013). Organizing the global value chain. Econometrica, 81(6), 2127-2204. https://doi.org/10.3982/ECTA10813

Antras, P., & de Gortari, A. (2020). On the geography of global value chains. Econometrica, 88(4), 1553-1598. https://doi.org/10.3982/ECTA15362

Arellano, M., & Bond, S. (1991). Some tests of specification for panel data: Monte Carlo evidence and an application to employment equations. Review of Economic Studies, 58(2), 277-297. https://doi.org/10.2307/2297968

Arellano, M., & Bover, O. (1995). Another look at the instrumental variable estimation of error-components models. Journal of Econometrics, 68(1), 29-51. https://doi.org/10.1016/0304-4076(94)01642-D

Athey, S., & Imbens, G. W. (2017). The state of applied econometrics: Causality and policy evaluation. Journal of Economic Perspectives, 31(2), 3-32. https://doi.org/10.1257/jep.31.2.3

Atkin, A. O. L., & Morain, F. (1993). Elliptic curves and primality proving. Mathematics of Computation, 61(203), 29-68. https://doi.org/10.1090/S0025-5718-1993-1199989-X

Bai, J. (2009). Panel data models with interactive fixed effects. Econometrica, 77(4), 1229-1279. https://doi.org/10.3982/ECTA6135

Balassa, B. (1965). Trade liberalisation and revealed comparative advantage. The Manchester School, 33(2), 99-123. https://doi.org/10.1111/j.1467-9957.1965.tb00050.x

Barabasi, A.-L., & Albert, R. (1999). Emergence of scaling in random networks. Science, 286(5439), 509-512. https://doi.org/10.1126/science.286.5439.509

Barabasi, A.-L. (2009). Scale-free networks: A decade and beyond. Science, 325(5939), 412-413. https://doi.org/10.1126/science.1173299

Barrat, A., Barthelemy, M., Pastor-Satorras, R., & Vespignani, A. (2004). The architecture of complex weighted networks. Proceedings of the National Academy of Sciences, 101(11), 3747-3752. https://doi.org/10.1073/pnas.0400087101

Barro, R. J. (1991). Economic growth in a cross section of countries. Quarterly Journal of Economics, 106(2), 407-443. https://doi.org/10.2307/2937943

Battiston, S., Puliga, M., Kaushik, R., Tasca, P., & Caldarelli, G. (2012). DebtRank: Too central to fail? Financial networks, the FED and systemic risk. Scientific Reports, 2, 541. https://doi.org/10.1038/srep00541

Battiston, S., Caldarelli, G., May, R. M., Roukny, T., & Stiglitz, J. E. (2016). The price of complexity in financial networks. Proceedings of the National Academy of Sciences, 113(36), 10031-10036. https://doi.org/10.1073/pnas.1521573113

Battiston, F., Cencetti, G., Iacopini, I., Latora, V., Lucas, M., Patania, A., Young, J.-G., & Petri, G. (2020). Networks beyond pairwise interactions: Structure and dynamics. Physics Reports, 874, 1-92. https://doi.org/10.1016/j.physrep.2020.05.004

Beck, N., & Katz, J. N. (1995). What to do and not to do with time-series cross-section data. American Political Science Review, 89(3), 634-647. https://doi.org/10.2307/2082979

Bell, R. M., & McCaffrey, D. F. (2002). Bias reduction in standard errors for linear regression with multi-stage samples. Survey Methodology, 28(2), 169-181. https://doi.org/10.1007/s11135-005-5591-y

Bertrand, M., Duflo, E., & Mullainathan, S. (2004). How much should we trust differences-in-differences estimates? Quarterly Journal of Economics, 119(1), 249-275. https://doi.org/10.1162/003355304772839588

Billio, M., Getmansky, M., Lo, A. W., & Pelizzon, L. (2012). Econometric measures of connectedness and systemic risk in the finance and insurance sectors. Journal of Financial Economics, 104(3), 535-559. https://doi.org/10.1016/j.jfineco.2011.12.010

Birch, B. J., & Swinnerton-Dyer, H. P. F. (1965). Notes on elliptic curves. II. Journal fur die reine und angewandte Mathematik, 218, 79-108. https://doi.org/10.1515/crll.1965.218.79

Bisias, D., Flood, M., Lo, A. W., & Valavanis, S. (2012). A survey of systemic risk analytics. Annual Review of Financial Economics, 4, 255-296. https://doi.org/10.1146/annurev-financial-110311-101754

Bland, J. M., & Altman, D. G. (1986). Statistical methods for assessing agreement between two methods of clinical measurement. The Lancet, 327(8476), 307-310. https://doi.org/10.1016/S0140-6736(86)90837-8

Blondel, V. D., Guillaume, J.-L., Lambiotte, R., & Lefebvre, E. (2008). Fast unfolding of communities in large networks. Journal of Statistical Mechanics: Theory and Experiment, 2008(10), P10008. https://doi.org/10.1088/1742-5468/2008/10/P10008

Blundell, R., & Bond, S. (1998). Initial conditions and moment restrictions in dynamic panel data models. Journal of Econometrics, 87(1), 115-143. https://doi.org/10.1016/S0304-4076(98)00009-8

Boccaletti, S., Latora, V., Moreno, Y., Chavez, M., & Hwang, D.-U. (2006). Complex networks: Structure and dynamics. Physics Reports, 424(4-5), 175-308. https://doi.org/10.1016/j.physrep.2005.10.009

Bonacich, P. (1987). Power and centrality: A family of measures. American Journal of Sociology, 92(5), 1170-1182. https://doi.org/10.1086/228631

Borgatti, S. P. (2005). Centrality and network flow. Social Networks, 27(1), 55-71. https://doi.org/10.1016/j.socnet.2004.11.008

Brin, S., & Page, L. (1998). The anatomy of a large-scale hypertextual Web search engine. Computer Networks and ISDN Systems, 30(1-7), 107-117. https://doi.org/10.1016/S0169-7552(98)00110-X

Brunnermeier, M. K. (2009). Deciphering the liquidity and credit crunch 2007-2008. Journal of Economic Perspectives, 23(1), 77-100. https://doi.org/10.1257/jep.23.1.77

Caldarelli, G., Cristelli, M., Gabrielli, A., Pietronero, L., Scala, A., & Tacchella, A. (2012). A network analysis of countries' export flows: Firm grounds for the building blocks of the economy. PLoS ONE, 7(10), e47278. https://doi.org/10.1371/journal.pone.0047278

Callaway, B., & Sant'Anna, P. H. C. (2021). Difference-in-differences with multiple time periods. Journal of Econometrics, 225(2), 200-230. https://doi.org/10.1016/j.jeconom.2020.12.001

Cameron, A. C., Gelbach, J. B., & Miller, D. L. (2008). Bootstrap-based improvements for inference with clustered errors. Review of Economics and Statistics, 90(3), 414-427. https://doi.org/10.1162/rest.90.3.414

Carlsson, G. (2009). Topology and data. Bulletin of the American Mathematical Society, 46(2), 255-308. https://doi.org/10.1090/S0273-0979-09-01249-X

Carvalho, V. M. (2014). From micro to macro via production networks. Journal of Economic Perspectives, 28(4), 23-48. https://doi.org/10.1257/jep.28.4.23

Carvalho, V. M., Nirei, M., Saito, Y. U., & Tahbaz-Salehi, A. (2021). Supply chain disruptions: Evidence from the Great East Japan Earthquake. Quarterly Journal of Economics, 136(2), 1255-1321. https://doi.org/10.1093/qje/qjaa044

Carvalho, V. M., & Gabaix, X. (2013). The great diversification and its undoing. American Economic Review, 103(5), 1697-1727. https://doi.org/10.1257/aer.103.5.1697

Chaney, T. (2008). Distorted gravity: The intensive and extensive margins of international trade. American Economic Review, 98(4), 1707-1721. https://doi.org/10.1257/aer.98.4.1707

Chor, D. (2010). Unpacking sources of comparative advantage: A quantitative approach. Journal of International Economics, 82(2), 152-167. https://doi.org/10.1016/j.jinteco.2009.11.006

Clauset, A., Newman, M. E. J., & Moore, C. (2004). Finding community structure in very large networks. Physical Review E, 70(6), 066111. https://doi.org/10.1103/PhysRevE.70.066111

Coates, J., & Wiles, A. (1977). On the conjecture of Birch and Swinnerton-Dyer. Inventiones Mathematicae, 39, 223-251. https://doi.org/10.1007/BF01402975

Combes, P.-P., Duranton, G., & Gobillon, L. (2008). Spatial wage disparities: Sorting matters! Journal of Urban Economics, 63(2), 723-742. https://doi.org/10.1016/j.jue.2007.04.004

Conley, T. G. (1999). GMM estimation with cross sectional dependence. Journal of Econometrics, 92(1), 1-45. https://doi.org/10.1016/S0304-4076(98)00084-0

Costinot, A., Vogel, J., & Wang, S. (2013). An elementary theory of global supply chains. Review of Economic Studies, 80(1), 109-144. https://doi.org/10.1093/restud/rds023

Cristelli, M., Tacchella, A., & Pietronero, L. (2013). The heterogeneous dynamics of economic complexity. PLoS ONE, 8(2), e70726. https://doi.org/10.1371/journal.pone.0070726

de Chaisemartin, C., & D'Haultfoeuille, X. (2020). Two-way fixed effects estimators with heterogeneous treatment effects. American Economic Review, 110(9), 2964-2996. https://doi.org/10.1257/aer.20181169

De Domenico, M., Solé-Ribalta, A., Cozzo, E., Kivela, M., Moreno, Y., Porter, M. A., Gomez, S., & Arenas, A. (2013). Mathematical formulation of multilayer networks. Physical Review X, 3(4), 041022. https://doi.org/10.1103/PhysRevX.3.041022

Diebold, F. X., & Yilmaz, K. (2014). On the network topology of variance decompositions: Measuring the connectedness of financial firms. Journal of Econometrics, 182(1), 119-134. https://doi.org/10.1016/j.jeconom.2014.04.012

Djankov, S., Freund, C., & Pham, C. S. (2010). Trading on time. Review of Economics and Statistics, 92(1), 166-173. https://doi.org/10.1162/rest.2009.11498

Donaldson, D. (2018). Railroads of the Raj: Estimating the impact of transportation infrastructure. American Economic Review, 108(4-5), 899-934. https://doi.org/10.1257/aer.20101199

Donaldson, D., & Hornbeck, R. (2016). Railroads and American economic growth: A market access approach. Quarterly Journal of Economics, 131(2), 799-858. https://doi.org/10.1093/qje/qjw002

Driscoll, J. C., & Kraay, A. C. (1998). Consistent covariance matrix estimation with spatially dependent panel data. Review of Economics and Statistics, 80(4), 549-560. https://doi.org/10.1162/003465398557825

Duranton, G., & Puga, D. (2001). Nursery cities: Urban diversity, process innovation, and the life cycle of products. American Economic Review, 91(5), 1454-1477. https://doi.org/10.1257/aer.91.5.1454

Eaton, J., & Kortum, S. (2002). Technology, geography, and trade. Econometrica, 70(5), 1741-1779. https://doi.org/10.1111/1468-0262.00352

Edelsbrunner, H., Letscher, D., & Zomorodian, A. (2002). Topological persistence and simplification. Discrete & Computational Geometry, 28, 511-533. https://doi.org/10.1007/s00454-002-2885-2

Eisenberg, L., & Noe, T. H. (2001). Systemic risk in financial systems. Management Science, 47(2), 236-249. https://doi.org/10.1287/mnsc.47.2.236.9835

Elliott, M., Golub, B., & Jackson, M. O. (2014). Financial networks and contagion. American Economic Review, 104(10), 3115-3153. https://doi.org/10.1257/aer.104.10.3115

Fally, T. (2015). Structural gravity and fixed effects. Journal of International Economics, 97(1), 76-85. https://doi.org/10.1016/j.jinteco.2015.05.005

Foerster, A. T., Sarte, P.-D. G., & Watson, M. W. (2011). Sectoral versus aggregate shocks: A structural factor analysis of industrial production. Journal of Political Economy, 119(1), 1-38. https://doi.org/10.1086/659311

Forbes, K. J., & Rigobon, R. (2002). No contagion, only interdependence: Measuring stock market comovements. Journal of Finance, 57(5), 2223-2261. https://doi.org/10.1111/0022-1082.00494

Fortunato, S. (2010). Community detection in graphs. Physics Reports, 486(3-5), 75-174. https://doi.org/10.1016/j.physrep.2009.11.002

Frankel, J. A., & Romer, D. (1999). Does trade cause growth? American Economic Review, 89(3), 379-399. https://doi.org/10.1257/aer.89.3.379

Freeman, L. C. (1978). Centrality in social networks: Conceptual clarification. Social Networks, 1(3), 215-239. https://doi.org/10.1016/0378-8733(78)90021-7

Gabaix, X. (2011). The granular origins of aggregate fluctuations. Econometrica, 79(3), 733-772. https://doi.org/10.3982/ECTA8769

Gai, P., & Kapadia, S. (2010). Contagion in financial networks. Proceedings of the Royal Society A, 466(2120), 2401-2423. https://doi.org/10.1098/rspa.2009.0410

Ghrist, R. (2008). Barcodes: The persistent topology of data. Bulletin of the American Mathematical Society, 45(1), 61-75. https://doi.org/10.1090/S0273-0979-07-01191-3

Girvan, M., & Newman, M. E. J. (2002). Community structure in social and biological networks. Proceedings of the National Academy of Sciences, 99(12), 7821-7826. https://doi.org/10.1073/pnas.122653799

Glaeser, E. L., Kallal, H. D., Scheinkman, J. A., & Shleifer, A. (1992). Growth in cities. Journal of Political Economy, 100(6), 1126-1152. https://doi.org/10.1086/261856

Glasserman, P., & Young, H. P. (2015). How likely is contagion in financial networks? Journal of Banking & Finance, 50, 383-399. https://doi.org/10.1016/j.jbankfin.2014.02.006

Gondauri, D. (2026). Regional Economic Birch-Swinnerton-Dyer Modelling: Data and Replication Package for a Local-to-Global Framework of Structural Rank Formation, Corridor Stress and World-Economy Calibration [Data set]. Zenodo. https://doi.org/10.5281/zenodo.20796984

Gross, B. H., & Zagier, D. B. (1986). Heegner points and derivatives of L-series. Inventiones Mathematicae, 84, 225-320. https://doi.org/10.1007/BF01388809

Grossman, G. M., & Helpman, E. (1991). Quality ladders in the theory of growth. Review of Economic Studies, 58(1), 43-61. https://doi.org/10.2307/2298044

Haldane, A. G., & May, R. M. (2011). Systemic risk in banking ecosystems. Nature, 469, 351-355. https://doi.org/10.1038/nature09659

Hansen, B. E. (1999). Threshold effects in non-dynamic panels: Estimation, testing, and inference. Journal of Econometrics, 93(2), 345-368. https://doi.org/10.1016/S0304-4076(99)00025-1

Hausman, J. A. (1978). Specification tests in econometrics. Econometrica, 46(6), 1251-1271. https://doi.org/10.2307/1913827

Hausmann, R., & Hidalgo, C. A. (2011). The network structure of economic output. PLoS ONE, 6(7), e0016458. https://doi.org/10.1371/journal.pone.0016458

Heckman, J. J. (1979). Sample selection bias as a specification error. Econometrica, 47(1), 153-161. https://doi.org/10.2307/1912352

Helpman, E., Melitz, M., & Rubinstein, Y. (2008). Estimating trade flows: Trading partners and trading volumes. Quarterly Journal of Economics, 123(2), 441-487. https://doi.org/10.1162/qjec.2008.123.2.441

Henderson, J. V., Kuncoro, A., & Turner, M. (1995). Industrial development in cities. Journal of Political Economy, 103(5), 1067-1090. https://doi.org/10.1086/262020
Hidalgo, C. A., Klinger, B., Barabasi, A.-L., & Hausmann, R. (2007). The product space conditions the development of nations. Science, 317(5837), 482-487. https://doi.org/10.1126/science.1144581
Hidalgo, C. A., & Hausmann, R. (2009). The building blocks of economic complexity. Proceedings of the National Academy of Sciences, 106(26), 10570-10575. https://doi.org/10.1073/pnas.0900943106
Horak, D., & Jost, J. (2013). Spectra of combinatorial Laplace operators on simplicial complexes. Advances in Mathematics, 244, 303-336. https://doi.org/10.1016/j.aim.2013.05.007
Hummels, D., & Schaur, G. (2013). Time as a trade barrier. American Economic Review, 103(7), 2935-2959. https://doi.org/10.1257/aer.103.7.2935
Ibragimov, R., & Muller, U. K. (2010). t-statistic based correlation and heterogeneity robust inference. Journal of Business & Economic Statistics, 28(4), 453-468. https://doi.org/10.1198/jbes.2009.08046
Imai, K., Keele, L., & Tingley, D. (2010). A general approach to causal mediation analysis. Statistical Science, 25(1), 51-71. https://doi.org/10.1214/10-STS321
Imbens, G. W., & Kolesar, M. (2016). Robust standard errors in small samples: Some practical advice. Review of Economics and Statistics, 98(4), 701-712. https://doi.org/10.1162/REST_a_00552
Imbens, G. W., & Wooldridge, J. M. (2009). Recent developments in the econometrics of program evaluation. Journal of Economic Literature, 47(1), 5-86. https://doi.org/10.1257/jel.47.1.5
Jiang, X., Lim, L.-H., Yao, Y., & Ye, Y. (2011). Statistical ranking and combinatorial Hodge theory. Mathematical Programming, 127, 203-244. https://doi.org/10.1007/s10107-010-0419-x
Johnson, R. C., & Noguera, G. (2012). Accounting for intermediates: Production sharing and trade in value added. Journal of International Economics, 86(2), 224-236. https://doi.org/10.1016/j.jinteco.2011.10.003
Kivela, M., Arenas, A., Barthelemy, M., Gleeson, J. P., Moreno, Y., & Porter, M. A. (2014). Multilayer networks. Journal of Complex Networks, 2(3), 203-271. https://doi.org/10.1093/comnet/cnu016
Kleinberg, J. M. (2000). Navigation in a small world. Nature, 406, 845. https://doi.org/10.1038/35022643
Koopman, R., Wang, Z., & Wei, S.-J. (2014). Tracing value-added and double counting in gross exports. American Economic Review, 104(2), 459-494. https://doi.org/10.1257/aer.104.2.459
Krugman, P. (1991). Increasing returns and economic geography. Journal of Political Economy, 99(3), 483-499. https://doi.org/10.1086/261763
Lenstra, H. W. (1987). Factoring integers with elliptic curves. Annals of Mathematics, 126(3), 649-673. https://doi.org/10.2307/1971363
Limao, N., & Venables, A. J. (2001). Infrastructure, geographical disadvantage, transport costs, and trade. World Bank Economic Review, 15(3), 451-479. https://doi.org/10.1093/wber/15.3.451
Lin, L. I.-K. (1989). A concordance correlation coefficient to evaluate reproducibility. Biometrics, 45(1), 255-268. https://doi.org/10.2307/2532051
Lipsitch, M., Tchetgen Tchetgen, E., & Cohen, T. (2010). Negative controls: A tool for detecting confounding and bias in observational studies. Epidemiology, 21(3), 383-388. https://doi.org/10.1097/EDE.0b013e3181d61eeb
Lucas, R. E. (1988). On the mechanics of economic development. Journal of Monetary Economics, 22(1), 3-42. https://doi.org/10.1016/0304-3932(88)90168-7
MacKinnon, J. G., & White, H. (1985). Some heteroskedasticity-consistent covariance matrix estimators with improved finite sample properties. Journal of Econometrics, 29(3), 305-325. https://doi.org/10.1016/0304-4076(85)90158-7
Mankiw, N. G., Romer, D., & Weil, D. N. (1992). A contribution to the empirics of economic growth. Quarterly Journal of Economics, 107(2), 407-437. https://doi.org/10.2307/2118477
Manski, C. F. (1993). Identification of endogenous social effects: The reflection problem. Review of Economic Studies, 60(3), 531-542. https://doi.org/10.2307/2298123
Martincus, C. V., Carballo, J., & Cusolito, A. (2017). Roads, exports and employment: Evidence from a developing country. Journal of International Economics, 105, 101-121. https://doi.org/10.1016/j.jinteco.2016.10.001
May, R. M., Levin, S. A., & Sugihara, G. (2008). Complex systems: Ecology for bankers. Nature, 451, 893-895. https://doi.org/10.1038/451893a

Melitz, M. J. (2003). The impact of trade on intra-industry reallocations and aggregate industry productivity. Econometrica, 71(6), 1695-1725. https://doi.org/10.1111/1468-0262.00467
Mucha, P. J., Richardson, T., Macon, K., Porter, M. A., & Onnela, J.-P. (2010). Community structure in time-dependent, multiscale, and multiplex networks. Science, 328(5980), 876-878. https://doi.org/10.1126/science.1184819
Mundlak, Y. (1978). On the pooling of time series and cross section data. Econometrica, 46(1), 69-85. https://doi.org/10.2307/1913646
Newey, W. K., & West, K. D. (1987). A simple, positive semi-definite, heteroskedasticity and autocorrelation consistent covariance matrix. Econometrica, 55(3), 703-708. https://doi.org/10.2307/1913610
Newman, M. E. J. (2003). The structure and function of complex networks. SIAM Review, 45(2), 167-256. https://doi.org/10.1137/S003614450342480
Newman, M. E. J. (2003). Assortative mixing in networks. Physical Review E, 67(2), 026126. https://doi.org/10.1103/PhysRevE.67.026126
Newman, M. E. J. (2006). Modularity and community structure in networks. Proceedings of the National Academy of Sciences, 103(23), 8577-8582. https://doi.org/10.1073/pnas.0601602103
Newman, M. E. J., & Girvan, M. (2004). Finding and evaluating community structure in networks. Physical Review E, 69(2), 026113. https://doi.org/10.1103/PhysRevE.69.026113
Nickell, S. (1981). Biases in dynamic models with fixed effects. Econometrica, 49(6), 1417-1426. https://doi.org/10.2307/1911408
Nier, E., Yang, J., Yorulmazer, T., & Alentorn, A. (2007). Network models and financial stability. Journal of Economic Dynamics and Control, 31(6), 2033-2060. https://doi.org/10.1016/j.jedc.2007.01.014
Nunn, N. (2007). Relationship-specificity, incomplete contracts, and the pattern of trade. Quarterly Journal of Economics, 122(2), 569-600. https://doi.org/10.1162/qjec.122.2.569
Onnela, J.-P., Saramaki, J., Kertesz, J., & Kaski, K. (2005). Intensity and coherence of motifs in weighted complex networks. Physical Review E, 71(6), 065103. https://doi.org/10.1103/PhysRevE.71.065103
Opsahl, T., Agneessens, F., & Skvoretz, J. (2010). Node centrality in weighted networks: Generalizing degree and shortest paths. Social Networks, 32(3), 245-251. https://doi.org/10.1016/j.socnet.2010.03.006
Otter, N., Porter, M. A., Tillmann, U., Grindrod, P., & Harrington, H. A. (2017). A roadmap for the computation of persistent homology. EPJ Data Science, 6, 17. https://doi.org/10.1140/epjds/s13688-017-0109-5
Pearl, J. (1995). Causal diagrams for empirical research. Biometrika, 82(4), 669-688. https://doi.org/10.1093/biomet/82.4.669
Pesaran, M. H. (2006). Estimation and inference in large heterogeneous panels with a multifactor error structure. Econometrica, 74(4), 967-1012. https://doi.org/10.1111/j.1468-0262.2006.00692.x
Pesaran, M. H. (2015). Testing weak cross-sectional dependence in large panels. Econometric Reviews, 34(6-10), 1089-1117. https://doi.org/10.1080/07474938.2014.956623
Portugal-Perez, A., & Wilson, J. S. (2012). Export performance and trade facilitation reform: Hard and soft infrastructure. World Bank Economic Review, 26(1), 129-150. https://doi.org/10.1093/wber/lhr039
Radicchi, F., Castellano, C., Cecconi, F., Loreto, V., & Parisi, D. (2004). Defining and identifying communities in networks. Proceedings of the National Academy of Sciences, 101(9), 2658-2663. https://doi.org/10.1073/pnas.0400054101
Rauch, J. E. (1999). Networks versus markets in international trade. Journal of International Economics, 48(1), 7-35. https://doi.org/10.1016/S0022-1996(98)00009-9
Redding, S. J., & Sturm, D. M. (2008). The costs of remoteness: Evidence from German division and reunification. American Economic Review, 98(5), 1766-1797. https://doi.org/10.1257/aer.98.5.1766
Rodrik, D., Subramanian, A., & Trebbi, F. (2004). Institutions rule: The primacy of institutions over geography and integration in economic development. Journal of Economic Growth, 9, 131-165. https://doi.org/10.1023/B:JOEG.0000031425.72248.85
Rogers, L. C. G., & Veraart, L. A. M. (2013). Failure and rescue in an interbank network. Management Science, 59(4), 882-898. https://doi.org/10.1287/mnsc.1120.1569
Romer, P. M. (1986). Increasing returns and long-run growth. Journal of Political Economy, 94(5), 1002-1037. https://doi.org/10.1086/261420
Roodman, D. (2009). A note on the theme of too many instruments. Oxford Bulletin of Economics and Statistics, 71(1), 135-158. https://doi.org/10.1111/j.1468-0084.2008.00542.x
Rosenbaum, P. R. (1987). Sensitivity analysis for certain permutation inferences in matched observational studies. Biometrika, 74(1), 13-26. https://doi.org/10.1093/biomet/74.1.13

Rosvall, M., & Bergstrom, C. T. (2008). Maps of random walks on complex networks reveal community structure. Proceedings of the National Academy of Sciences, 105(4), 1118-1123. https://doi.org/10.1073/pnas.0706851105

Rubin, D. B. (1974). Estimating causal effects of treatments in randomized and nonrandomized studies. Journal of Educational Psychology, 66(5), 688-701. https://doi.org/10.1037/h0037350

Schoof, R. (1985). Elliptic curves over finite fields and the computation of square roots mod p. Mathematics of Computation, 44(170), 483-494. https://doi.org/10.1090/S0025-5718-1985-0777280-6

Schuirmann, D. J. (1987). A comparison of the two one-sided tests procedure and the power approach for assessing the equivalence of average bioavailability. Journal of Pharmacokinetics and Biopharmaceutics, 15, 657-680. https://doi.org/10.1007/BF01068419

Solow, R. M. (1956). A contribution to the theory of economic growth. Quarterly Journal of Economics, 70(1), 65-94. https://doi.org/10.2307/1884513

Stock, J. H., & Watson, M. W. (2008). Heteroskedasticity-robust standard errors for fixed-effects panel-data regression. Econometrica, 76(1), 155-174. https://doi.org/10.1111/j.0012-9682.2008.00821.x

Strogatz, S. H. (2001). Exploring complex networks. Nature, 410, 268-276. https://doi.org/10.1038/35065725

Sun, L., & Abraham, S. (2021). Estimating dynamic treatment effects in event studies with heterogeneous treatment effects. Journal of Econometrics, 225(2), 175-199. https://doi.org/10.1016/j.jeconom.2020.09.006

Tacchella, A., Cristelli, M., Caldarelli, G., Gabrielli, A., & Pietronero, L. (2012). A new metrics for countries' fitness and products' complexity. Scientific Reports, 2, 723. https://doi.org/10.1038/srep00723

Taylor, R., & Wiles, A. (1995). Ring-theoretic properties of certain Hecke algebras. Annals of Mathematics, 141(3), 553-572. https://doi.org/10.2307/2118560

Watts, D. J., & Strogatz, S. H. (1998). Collective dynamics of small-world networks. Nature, 393, 440-442. https://doi.org/10.1038/30918

White, H. (1980). A heteroskedasticity-consistent covariance matrix estimator and a direct test for heteroskedasticity. Econometrica, 48(4), 817-838. https://doi.org/10.2307/1912934

Wiles, A. (1995). Modular elliptic curves and Fermat's last theorem. Annals of Mathematics, 141(3), 443-551. https://doi.org/10.2307/2118559

Windmeijer, F. (2005). A finite sample correction for the variance of linear efficient two-step GMM estimators. Journal of Econometrics, 126(1), 25-51. https://doi.org/10.1016/j.jeconom.2004.02.005

Wooldridge, J. M. (2005). Fixed-effects and related estimators for correlated random-coefficient and treatment-effect panel data models. Review of Economics and Statistics, 87(2), 385-390. https://doi.org/10.1162/0034653053970320

Yi, K.-M. (2003). Can vertical specialization explain the growth of world trade? Journal of Political Economy, 111(1), 52-102. https://doi.org/10.1086/344805

Zomorodian, A., & Carlsson, G. (2005). Computing persistent homology. Discrete & Computational Geometry, 33, 249-274. https://doi.org/10.1007/s00454-004-1146-y